Idaho National Engineering and Environmental Laboratory

INEEL/EXT-98-00286
Revision 1

September 1998

SCDAP/RELAP5 Evaluation Of The Potential For Steam Generator Tube Ruptures As A Result Of Severe Accidents In Operating Pressurized Water Reactors

D. L. Knudson
L. S. Ghan
C. A. Dobbe

LOCKHEED MARTIN

INEEL/EXT-98-00286
Revision 1

SCDAP/RELAP5 EVALUATION OF THE POTENTIAL FOR STEAM GENERATOR TUBE RUPTURES AS A RESULT OF SEVERE ACCIDENTS IN OPERATING PRESSURIZED WATER REACTORS

D. L. Knudson
L. S. Ghan
C. A. Dobbe

September 14, 1998

Idaho National Engineering and Environmental Laboratory
Idaho Falls, ID 83415

Prepared for the
U. S. Nuclear Regulatory Commission
Office of Nuclear Reactor Research
Washington, D. C. 20555
Under DOE Idaho Operations Office
Contract DE-AC07-94ID13223
Job Code Number W6242

SUMMARY

Natural circulation flows can develop within a reactor coolant system (RCS) during certain severe reactor accidents, transferring decay energy from the core to other parts of the RCS. The associated heatup of RCS structures can lead to pressure boundary failures; with notable vulnerabilities in the pressurizer surge line, the hot leg nozzles, and the steam generator (SG) tubes. The potential for a steam generator tube rupture (SGTR) is of particular concern because fission products could be released to the environment through such a failure. The Nuclear Regulatory Commission (NRC) developed a program to address SG tube integrity issues in operating pressurized water reactors (PWRs) based on the possibility for environmental release. An extensive effort to evaluate the potential for accident-induced SGTRs using SCDAP/RELAP5 at the Idaho National Engineering and Environmental Laboratory (INEEL) was directed as one part of the NRC program.

All SCDAP/RELAP5 calculations performed during the INEEL evaluation were based on station blackout accidents (and variations thereof) because those accidents are considered to be one of the more likely scenarios leading to natural circulation flows at temperatures and pressures that could threaten SG tube integrity (as well as the integrity of other vulnerable RCS pressure boundaries). Variations that were addressed included consideration of the effects of RCP seal leaks, intentional RCS depressurization through pressurizer PORVs, SG secondary depressurization, DC-HL bypass flows, U-tube SG sludge accumulation, and quenching of upper plenum stainless steel upon relocation to the lower head. Where available, experimental data was used to guide simulation of natural circulation flows. Independent reviews of the applicability of the natural circulation experimental data, the suitability of the code, and the adequacy of the modeling were completed and review recommendations were incorporated into the evaluation within budget and schedule limitations.

SCDAP/RELAP5 results indicate that surge line (or hot leg) failures will be the first failures in the RCS pressure boundary in all calculations as a result of heat transferred by natural circulation flows. Those results held for all operating PWRs that were analyzed in cases with and without RCP seal leaks, cases with and without intentional RCS depressurization through pressurizer PORVs, cases with and without SG secondary depressurization, cases with and without DC-HL bypass flows, cases with and without U-tube SG sludge accumulation, and cases with and without quenching of upper plenum stainless steel upon relocation to the lower head (if that steel was predicted to melt). Results also indicated that secondary failures of the RCS pressure boundary will not occur after RCS depressurization and accumulator injection associated with the first RCS pressure boundary failure. In other words, a SGTR (or any other secondary failure in the RCS pressure boundary) would not be expected after depressurization through the first (surge line or hot leg) failure. Results from sensitivity analyses indicate that uncertainties associated with natural circulation behavior, heat transfer, and variety of other related factors are not large enough to adversely affect those conclusions. In one calculation for one operating PWR, SGTR was found to be imminent at the time of the first RCS pressure boundary failure as a result of large pressure pertubations associated with quenching of molten upper plenum stainless steel. Uncertainties may be large enough to preclude the possibility that SGTR could be the first RCS pressure boundary failure in that case. However, the assumption that stainless steel can candle through the core without refreezing and the subsequent simulation of complete and essentially instantaneous quenching are believed to be overly conservative with respect to the SGTR prediction. Any SGTR concerns in this single case would be expected to significantly decrease if more detailed modeling were applied. Consequently, the potential for SGTR in operating PWRs during TMLB' accidents is low. These conclusions apply if SG tubes (and other RCS piping) are defect free.

CONTENTS

FIGURES

TABLES

SCDAP/RELAP5 EVALUATION OF THE POTENTIAL FOR STEAM GENERATOR TUBE RUPTURES AS A RESULT OF SEVERE ACCIDENTS IN OPERATING PRESSURIZED WATER REACTORS

1. INTRODUCTION

Natural circulation flows can develop within a reactor coolant system (RCS) during certain severe reactor accidents. Those flows are important because they can transfer decay energy from the core to other parts of the RCS. The associated heatup of RCS structures can lead to pressure boundary failures; with notable vulnerabilities in the pressurizer surge line, the hot leg nozzles, and the steam generator (SG) tubes. The potential for a steam generator tube rupture (SGTR) is of particular concern because fission products could be released to the environment through such a failure.

The Nuclear Regulatory Commission (NRC) developed a program to address SG tube integrity issues in operating pressurized water reactors (PWRs) based on the possibility for environmental release. An extensive effort to evaluate the potential for accident-induced SGTRs using SCDAP/RELAP5[1] at the Idaho National Engineering and Environmental Laboratory (INEEL) was directed as one part of the NRC program. This report summarizes the work completed during the course of that INEEL evaluation.

All SCDAP/RELAP5 analyses performed during this evaluation were based on station blackout accidents (and variations thereof) because those accidents are considered to be one of the more likely scenarios leading to natural circulation flows at temperatures and pressures that could threaten SG tube integrity (as well as the integrity of other vulnerable RCS pressure boundaries). Natural circulation flows that can develop in operating PWRs during a station blackout and contribute to RCS structural heating are described in Section 2. That section also includes a summary of the experimental work that was available and used as a basis for the SCDAP/RELAP5 simulation of corresponding natural circulation flows. Section 3 contains descriptions of the SCDAP/RELAP5 code, the operating PWRs that were analyzed at the INEEL, and the associated SCDAP/RELAP5 models. Independent reviews of the applicability of the natural circulation experimental data, the suitability of the code, and the adequacy of the modeling are discussed in Section 4. Section 5 contains descriptions of the analyses that were performed, explanations why each of the analyses were needed, and summaries of the SCDAP/RELAP5 results. Associated uncertainties are discussed in Section 6 and conclusions based on the INEEL work are given in Section 7. Finally, references are listed in Section 8.

2. NATURAL CIRCULATION IN OPERATING PWRS

Three different natural circulation flow patterns can develop in operating PWRs during station blackout accidents including in-vessel, full-loop, and hot leg countercurrent modes. Provisions were made to appropriately simulate those natural circulation modes in all SCDAP/RELAP5 analyses completed in this evaluation. However, operating PWRs use either U-tube or once-through SGs and the SG configuration has some impact on the nature of the flow patterns as explained below.

2.1. Flows in PWRs with U-Tube SGs

In-vessel, full-loop, and hot leg countercurrent natural circulation flow patterns that can develop during station blackout accidents in operating PWRs with U-tube SGs are depicted in Figure 1. In-vessel natural circulation is generally characterized by fluid heating in the center of the core and fluid cooling in the vessel upper plenum as indicated in the figure. In-vessel natural circulation of either liquid or vapor can develop. In-vessel natural circulation of liquid primarily occurs when vessels are liquid solid. In-vessel natural circulation of vapor can develop after the vessel liquid level drops below the top of the core. At that time, the circulation "cell" may be only slightly taller than the upper plenum, although "cell" height can increase if the liquid level continues to drop. Upper plenum internal structures can be heated to the melting point as a result of in-vessel natural circulation of superheated vapor. However, heating of the vessel in the upper plenum to the point of failure is not normally a concern because less massive structures (i.e., the pressurizer surge line, the hot leg nozzles, and the SG tubes) are subject to creep rupture much earlier.

Full-loop natural circulation consists of hot flow from the core with fluid cooling primarily in the SGs. Full-loop natural circulation can normally develop only when a continuous single phase (either liquid or vapor) flow path exists from the bottom of the vessel downcomer skirt, to the vessel outlet, through the RCS hot and cold leg piping, and back through the vessel downcomer (see Figure 1). In station blackout accidents, full-loop natural circulation of liquid generally begins shortly after reactor coolant pump (RCP) coastdown and persists until vapor from in-core boiling begins to accumulate in the top of the SGs. Full-loop circulation of vapor can develop after the vessel liquid level falls below the bottom of the downcomer skirt and liquid in at least one RCP loop seal begins to clear. A potential for significant SG tube heating exists if full-loop circulation of superheated vapor develops.

As indicated in Figure 1, hot leg countercurrent natural circulation in PWRs with U-tube SGs consists of hot flow from the core to the SG outlet plenum through the top of the hot leg pipe and a fraction of the SG U-tubes. Colder flow then returns to the core through the remaining U-tubes and the bottom of the hot leg pipe. Unlike in-vessel and full-loop natural circulation modes, hot leg countercurrent natural circulation develops only with vapor flow. That is because countercurrent flow requires a single phase flow path and a blockage downstream of the SG outlet plenum. When the RCS is liquid solid, the single phase flow path exists but the required flow blockage does not. Consequently, full-loop natural circulation of liquid tends to develop under those conditions. After vapor begins to accumulate in the top of the SGs, full-loop circulation of liquid stops and loop fluids temporarily stagnate. As boiling progresses, loop liquids are gradually depleted until the required single phase vapor flow path is established. At that point, RCP loop seals are normally full of liquid, providing the required blockage of vapor flow downstream of the SGs. Under those conditions, countercurrent natural circulation of vapor can develop. If liquid in a RCP loop seal subsequently begins to clear (and the vessel liquid level is below the bottom of the downcomer skirt), hot leg countercurrent natural circulation of vapor can transition to full-loop natural circulation of vapor. (Note that hot leg countercurrent natural circulation and full-loop natural circulation of vapor can develop simultaneously in multi-loop plants depending on the vessel liquid level and conditions in the various RCP loop seals.)

Experimental investigations of hot leg countercurrent natural circulation were conducted by Westinghouse because that flow pattern can be a primary mechanism for RCS structural heating during station blackout accidents.[2,3] A one-seventh scale model of a Westinghouse four-loop PWR was used in the experiments. The model represented a half section of the PWR and therefore included a vessel to simulate an equivalent portion of the reactor, two hot legs, and two SGs. The vessel contained structures to repre-

sent the upper plenum internals and one half of the core fuel assemblies with radial and axial flow resistance similar to the prototype. Core power was supplied through electrical heaters.

Initial experiments were conducted at low (atmospheric) pressure using water and sulfur hexafluoride (SF_6) as working fluids. Subsequent experiments were conducted at high pressure (1.4 to 3.4 MPa) using SF_6. (Experimental pressures of 1.4 to 3.4 MPa with SF_6 are reported to be equivalent to 15.2 to 16.5 MPa with steam in the prototype.) Both steady state and transient tests were completed with variations in core power. In all cases, experimental results verified that relatively-stable hot leg countercurrent natural circulation flow patterns will develop. In this context, stability is used as a descriptor because countercurrent flows developed over a wide range of experimental conditions, stratified flow patterns in the hot leg pipe existed without interaction between the hot and cold streams, and natural circulation flows were robust in that they quickly re-established following major pertubations (like that introduced by pressurizer relief valve cycling).

Evaluation of experiment data indicated that hot leg countercurrent natural circulation in PWRs with U-tube SGs can be characterized by mixing fractions, a recirculation ratio, and the fraction of SG U-tubes that carry hot flow in the forward direction. The mixing fraction refers to experimentally-observed interactions between hot and cold streams in the SG inlet plenum as depicted in Figure 1. The hot mixing fraction was defined as the fraction of hot flow discharged from the top of the hot leg pipe that mixes with vapor in the SG inlet plenum before entering the SG U-tubes. Similarly, the cold mixing fraction was defined as the fraction of the cold flow returning from the SG U-tubes that mixes with the SG inlet plenum vapor before entering the bottom of the hot leg pipe. The recirculation ratio refers to the relative magnitude of flow within the SG and was defined as the SG U-tube flow divided by the hot leg flow. Recirculation ratios greater than one indicate that SG tube-to-plenum-to-SG tube flow is larger than the flow entering the SG inlet plenum from the hot leg. The fraction of SG U-tubes that carry hot flow in the forward direction and the other characteristic parameters from Westinghouse high pressure steady state and transient tests are summarized in Table 1. Hot leg countercurrent modeling for plants with U-tube SGs considered in this evaluation was based on benchmarks derived from the high pressure tests because those tests were assumed to be closest to the conditions that would be expected during station blackout accidents.

2.2. Flows in PWRs with Once-Through SGs

In-vessel, full-loop, and hot leg countercurrent natural circulation flow patterns that can develop during station blackout accidents in operating PWRs with once-through SGs are depicted in Figure 2. In-vessel and full-loop natural circulation flows (as previously described) behave similarly in PWRs with either U-tube or once-through SGs. However, the SG configuration substantially affects hot leg countercurrent flow patterns, which can be seen by comparing Figures 1 and 2.

Results from experiments conducted at the University of Maryland at College Park indicate that countercurrent natural circulation in PWRs with once-through SGs includes the flow of hot vapor through the top of the horizontal part of the hot leg pipe.[4] Complex mixing and heat transfer occurs in the vertical part of the hot leg, with a net flow of cooler vapor that moves downward and returns to the vessel through the bottom of the horizontal part of the hot leg pipe as shown in Figure 2. Like countercurrent flow in PWRs with U-tube SGs, the described pattern will only develop with a single phase vapor flow path and a flow blockage downstream of the SG. If the flow blockage is not maintained (i.e., if liquid in a RCP loop seal begins to clear and the vessel liquid level falls below the bottom of the downcomer skirt), hot leg counter-

current natural circulation of vapor can transition to full-loop natural circulation of vapor. (Note that hot leg countercurrent natural circulation and full-loop natural circulation of vapor can develop simultaneously in multi-loop plants depending on the vessel liquid level and conditions in the various RCP loop seals.)

The University of Maryland experiments were conducted in a comprehensive scaled representation of a Babcock & Wilcox PWR. The model included a reactor vessel with an internal downcomer and reactor vessel vent valves, two hot legs, two once-through SGs, four cold legs, and a pressurizer with a surge line and a power-operated relief valve (PORV). Experimental data indicated that hot leg countercurrent natural circulation in PWRs with once-through SGs can be characterized by changes in structural temperatures. Results typical of data collected during the University of Maryland experiments are summarized in Table 2. Hot leg countercurrent modeling for plants with once-through SGs considered in this evaluation was based on benchmarks derived from those data, which were assumed to be close to conditions that could be expected during station blackout accidents.

3. SCDAP/RELAP5 MODELING

A substantial number of SCDAP/RELAP5 analyses were completed during the course of this study in order to evaluate the potential for SGTRs as a result of severe reactor accidents in operating PWRs. Descriptions of the code, the operating PWRs that were analyzed, and the associated SCDAP/RELAP5 models are provided in the sections that follow.

3.1. SCDAP/RELAP5

SCDAP/RELAP5 is a light water reactor (LWR) transient analysis computer code that is currently being developed at the INEEL. It can be used to simulate a very wide variety of system transients of interest in LWR safety. The core, RCS, secondary systems (including feedwater and steam turbine trains), auxiliary systems, pumps, valves, and all system controls can be simulated.

SCDAP/RELAP5 development includes incorporation of models from the SCDAP,[5] TRAP-MELT,[6] and COUPLE[7] codes into the RELAP5[8] code. SCDAP models provide coding for simulation of the reactor core. TRAP-MELT models serve as the basis for simulation of fission product release, transport, and deposition. COUPLE models provide coding to allow detailed two-dimensional, finite-element heat transfer calculations at user-specified locations. (Detailed thermal simulation is typically used to represent lower head regions where molten core materials may collect.) And finally, RELAP5 models allow simulation of fluid thermal-hydraulic behavior throughout the LWR system, as well as the thermal behavior of structures outside the core. Feedbacks between the various parts of the code are developed to provide an integral analysis capability. For example, changes in coolant flow area associated with ballooning of fuel rod cladding are taken into consideration in core thermal-hydraulics.

RELAP5 uses a one-dimensional, two-fluid, nonequilibrium, six-equation thermal-hydraulic model with a simplified capability to treat multidimensional flows. This model provides continuity, momentum, and energy equations for both liquid and vapor phases within a control volume. The energy equation contains source terms that link the thermal-hydraulic model to the heat structure conduction model by a convective heat transfer formulation. The code contains special process models for critical flow, abrupt area changes, branching, crossflow junctions, pumps, accumulators, valves, core neutronics, and control sys-

tems. A generalized creep rupture model, which accounts for the cumulative effects of pressure and temperature induced stresses, is also included for prediction of pressure boundary failures. The creep rupture model can be applied to any RELAP5 heat structure or to any part of any structure represented by a finite-element COUPLE mesh. The creep rupture model, which provides critical insight into the potential for SGTR, uses a Larsen-Miller formulation to estimate when the combined pressure/temperature effects will lead to failure of each identified component.

SCDAP components simulate core disruption by modeling heatup, geometry changes, and material relocation. Detailed modeling of cylindrical and slab heat structures is allowed. Thus, fuel rods, control rods and blades, instrument tubes, and flow shrouds can be represented. Models in SCDAP calculate fuel and cladding temperatures, zircaloy oxidation, hydrogen generation, cladding ballooning and rupture, fuel and cladding liquefaction, flow and freezing of the liquefied materials, and release of fission products. Fragmentation of fuel rods during reflood is also calculated. Oxidation of the inside surface of the fuel rod cladding is calculated for ballooned and ruptured cladding. Interactions between molten core material and any surrounding fluid are explicitly modeled. Debris formation and behavior in the reactor vessel lower head and the resultant thermal attack on the lower head structure by the relocated material are also treated.

Version 8dl of SCDAP/RELAP5, with updates, was used to complete all analyses described in this report. The updates included error corrections that have been added to subsequent versions and model changes to improve the predictive capabilities of the code. The most significant model changes included logic to refine the calculation of molten debris/lower head interaction and the addition of code updates to treat the combined effects of forced and free (mixed) convection. (It should be noted, however, that the mixed convection coding was not in place for some of the earliest analyses completed in this evaluation as discussed in Section 5.)

3.2. Analyzed PWRs and Associated SCDAP/RELAP5 Models

Operating PWRs include plants designed by Westinghouse, Combustion Engineering, and Babcock & Wilcox. All operating PWRs use either U-tube or once-through SGs. PWRs with U-tube SGs include plants designed by Westinghouse and Combustion Engineering while all operating PWRs with once-through SGs were designed by Babcock & Wilcox. Westinghouse PWRs have either two, three, or four primary coolant loops. All Combustion Engineering and Babcock & Wilcox PWRs have a “2x4” design, where two hot legs carry primary flows from the reactor vessel (to two SGs) and four cold legs return those flows to the vessel. In this evaluation, Surry and Zion PWRs were used to represent Westinghouse three and four loop plants, respectively. Calvert Cliffs and Arkansas Nuclear One Unit 2 (ANO2) PWRs were used to represent Combustion Engineering plants with and without pressurizer PORVs, respectively. Finally, Babcock & Wilcox plants were represented by the Oconee PWR. SCDAP/RELAP5 models for those plants are described in sections that follow.

3.2.1. Surry PWR

The Surry PWR was used to represent Westinghouse three-loop plants in this evaluation. Surry is rated at 2441 MW_t based on a core of 157 15x15 assemblies with an active fuel height of approximately 3.66 m. Each of the three primary coolant loops contain a hot leg, a U-tube SG, a RCP, and a cold leg. A single pressurizer is attached to the hot leg piping in one of the loops. The pressurizer surge line and the hot/cold leg piping are made of stainless steel. The SG U-tubes are made of inconel. Two PORVs, with a combined

capacity of 45.1 kg/s, are used to relieve excess RCS pressure from the top of the pressurizer. Pressurizer safety relief valves (SRVs) are also available to handle excursions exceeding PORV capacity. One accumulator, with 29.4 m^3 (29,100 kg) of borated water at 322 K, is attached to each cold leg. The accumulators, which are initially pressurized to 4.24 MPa by a nitrogen cover gas, are the only operational part of the ECCS (emergency core cooling system) during a station blackout. A large, dry, subatmospheric containment building surrounds the reactor systems.

SCDAP/RELAP5 nodalizations representing those features of the Surry PWR, including pertinent portions of the secondary systems, are shown in Figures 3 and 4. (The two non-pressurizer loops are not shown but they were modeled separately with nodalizations similar to that shown in Figure 4.) Shaded areas represent core structures, cross-hatched areas represent all other pipe/vessel structures, and the remaining regions represent the hydrodynamic volume within the plant.

Nodalizations shown in Figures 3 and 4 were used from station blackout initiation until the time hot leg piping was drained. That approach was adequate for simulation of both in-vessel and full-loop natural circulation flows that could potentially develop during that period. Thereafter, the nodalization shown in Figure 5 was used in place of the Figure 4 nodalization. That substitution provided the additional flow paths needed to simulate hot leg countercurrent natural circulation, which can develop only after the hot legs are voided.

The nodalization shown in Figure 5 was developed to accommodate both full-loop and hot leg countercurrent natural circulation in case RCP loop seals clear. That was accomplished using RELAP5 servo valves to connect (a) the split hot leg to the split SG inlet plenum, (b) the split SG inlet plenum to the split SG tube bundle, and (c) the split SG tube bundle to the SG outlet plenum; for a total of ten locations in each primary coolant loop. The valves were configured with two sets of loss coefficients; one set consistent with those used to model normal plant operation and one set necessary for appropriate simulation of hot leg countercurrent natural circulation based on Westinghouse experimental data. All other losses in the loop network were unaltered relative to those used for normal plant operation (i.e., equivalent to those used in the nodalization shown in Figure 4). If the horizontal portion of the RCP loop seal in a given loop is full of liquid, control logic directs the use of countercurrent loss coefficients in all servo valves in that loop. Alternately, if voids begin to form in the horizontal portion of the RCP loop seal, control logic directs a loss coefficient transition to values used for normal plant operation. As a result, both full-loop and countercurrent natural circulation flows should be appropriately calculated in each loop if/when transient loop conditions change. (Since it may have been a possibility, it should be noted that the nodalization shown in Figure 5 was not used to simulate the entire transient because requirements for computation and output would be significantly increased and because the simplistic control logic, as described above, was assumed to be inadequate.)

A horizontal section of the surge line in the Surry PWR connects to the centerline of the horizontal hot leg pipe. That orientation required a surge line split, as indicated in Figure 6, to represent potential countercurrent surge line flow in a fashion similar to the rest of the loop piping. The associated valves (numbered 463 and 465 in Figure 6) were configured to open and close with the pressurizer PORV. As a result, the valves prevent hot to cold (top to bottom) hot leg communication when the PORV is closed and they allow both hot and cold hot leg flow streams to be drawn into both halves of the surge line when the PORV is opened. Preventing hot to cold communication when the valves are closed is consistent with experimental results indicating that interaction between hot leg flows is minimal during countercurrent natural circulation. Furthermore, countercurrent natural circulation is interrupted as fluid from the core tends to flow in both halves of the split hot leg toward the split surge line when the PORV opens. It is reasonable to expect

a high degree of mixing as the flow streams reach the entrance to the surge line and respond to the large pressure differential generated by the open PORV. Valves 463 and 465 were opened with the PORV as a way to approximate conditions that would result from that mixing. Input was also needed in the model to calculate creep rupture of the stainless steel surge line (numbered 455-2 in Figure 5), all three stainless steel hot legs (numbered 400-1 in Figure 5 and at 200-1 and 300-1 in non-pressurizer loops that are not shown), and the hottest inconel SG U-tubes (numbered 408-1 in Figure 5 and at 208-1 and 308-1 in non-pressurizer loops that are not shown).

The Surry PWR model included only a simple two volume representation of containment (numbered 449-1 and 449-2 in Figures 4 and 5), which was not expected to adequately calculate condensation of primary effluent. Consequently, reasonable prediction of containment pressure was not expected. To resolve that problem, containment pressure was not allowed to increase above 0.2 MPa, based on results from containment scoping calculations.

The SCDAP/RELAP5 modeling approach outlined in the foregoing was originally developed using results from the Westinghouse low pressure experiments.[9] However, all Surry analyses completed in this evaluation were based on benchmarks derived from the high pressure results (listed in Table 1) because those results were assumed to be more applicable to conditions that would be expected during station blackout accidents. With the exception of the servo valve refinement, additional details regarding the natural circulation modeling approach and its evolution are outlined in Reference 10. Servo valves were added in this evaluation only after Surry analyses were identified that appeared to have a high probability for sustained RCP loop seal clearing. It then became important to be able to simulate transition from hot leg countercurrent to full-loop natural circulation. Consequently, the earliest Surry analyses completed in this evaluation did not include the servo valves while subsequent analyses incorporated that refinement. Surry analyses with and without the servo valve modeling refinement are identified in Section 5.

3.2.2. Zion PWR

The Zion PWR was used to represent Westinghouse four-loop plants in this evaluation. Zion is rated at 3250 MW_t based on a core of 193 15x15 assemblies with an active fuel height of approximately 3.66 m. Each of the four primary coolant loops contain a hot leg, a U-tube SG, a RCP, and a cold leg. A single pressurizer is attached to the hot leg piping in one of the loops. The pressurizer surge line and the hot/cold leg piping are made of stainless steel. The SG U-tubes are made of inconel. Two PORVs, with a combined capacity of 52.9 kg/s, are used to relieve excess RCS pressure from the top of the pressurizer. Pressurizer SRVs are also available to handle excursions exceeding PORV capacity. One accumulator, with 25.4 m^3 (25,100 kg) of borated water at 325 K, is attached to each cold leg. The accumulators, which are initially pressurized to 4.24 MPa by a nitrogen cover gas, are the only operational part of the ECCS during a station blackout. A large, dry containment building surrounds the reactor systems.

SCDAP/RELAP5 nodalizations representing those features of the Zion PWR, including pertinent portions of the secondary systems, are shown in Figures 7 and 8. (The three non-pressurizer loops are not shown but they were modeled separately with nodalizations similar to that shown in Figure 8.) Shaded areas represent core structures, cross-hatched areas represent all other pipe/vessel structures, and the remaining regions represent the hydrodynamic volume within the plant.

The approach used to model Zion was similar to the modeling of Surry (as outlined in Section 3.2.1). Specifically, nodalizations shown in Figures 7 and 8 were used from station blackout initiation until the

time hot leg piping was drained in order to accommodate the potential for both in-vessel and full-loop natural circulation. Thereafter, the nodalization shown in Figure 9 was used in place of the Figure 8 nodalization to provide the additional flow paths needed if hot leg countercurrent natural circulation develops. In addition, the nodalization shown in Figure 9 utilized the RELAP5 servo valve refinement as described for Surry to accommodate full-loop natural circulation if RCP loop seals clear. That refinement was used in all Zion analyses completed in this evaluation. (Like Surry modeling, the nodalization shown in Figure 9 was not used to simulate the entire transient because requirements for computation and output would be significantly increased and because the associated simplistic control logic was assumed to be inadequate.)

The Zion surge line is angled upward from its connection to the upper half of the horizontal hot leg, which is different than the Surry surge line connection. A split is not required for the Zion orientation because any potential for surge line countercurrent natural circulation is eliminated since the surge line generally sees only the hottest vapor in the top of the hot leg. However, valves numbered 155 and 156 in Figure 9 were needed to accommodate pressurizer draining and the mixing that would be expected when the pressurizer PORV opens. Specifically, while the pressurizer drained and the PORV was closed, control logic kept Valve 156 open and Valve 155 closed. Consequently, all liquid draining from the pressurizer appropriately flowed into the bottom half of the split hot leg. After pressurizer dryout, Valve 155 opened and Valve 156 closed whenever the PORV was closed. The surge line was appropriately exposed to the hottest flow stream under those conditions. And finally, control logic opened both valves whenever the PORV was opened. Countercurrent natural circulation is interrupted as fluid from the core tends to flow in both halves of the split hot leg toward the surge line when the PORV opens. It is reasonable to expect a high degree of mixing as the flow streams reach the entrance to the surge line and respond to the large pressure differential generated by the open PORV. Valves 155 and 156 were opened with the PORV as a way to approximate conditions that would result from that mixing. Model input was also needed to calculate creep rupture of the stainless steel surge line (numbered 153-3 in Figure 9), all four stainless steel hot legs (numbered 100-1 in Figure 9 and at 200-1, 300-1, and 400-1 in non-pressurizer loops that are not shown), and the hottest inconel SG U-tubes (numbered 110-1 in Figure 9 and at 210-1, 310-1, and 410-1 in non-pressurizer loops that are not shown).

Like Surry, containment pressure was not allowed to increase above 0.2 MPa because the Zion model included only a simple single volume representation of containment (numbered 160 in Figures 8 and 9). In addition, all Zion countercurrent natural circulation modeling in analyses completed in this evaluation was based on benchmarks derived from Westinghouse high pressure results as listed in Table 1.

3.2.3. Calvert Cliffs PWR

The Calvert Cliffs PWR was used to represent Combustion Engineering "2x4" plants with pressurizer PORVs in this evaluation. Calvert Cliffs is rated at 2700 MW_t based on a core of 217 14x14 assemblies with an active fuel height of approximately 3.47 m. Both primary coolant loops contain a hot leg, a U-tube SG, two RCPs, and two cold legs. A single pressurizer is attached to the hot leg piping in one of the loops. The pressurizer surge line is made of stainless steel, the hot/cold leg piping is made of carbon steel with a stainless steel lining, and the SG U-tubes are made of inconel. Two PORVs, with a combined capacity of 38.6 kg/s, are used to relieve excess RCS pressure from the top of the pressurizer. Pressurizer SRVs are also available to handle excursions exceeding PORV capacity. One accumulator, with 32.9 m^3 (32,800 kg) of borated water at 300 K, is attached to each cold leg. The accumulators, which are initially pressurized to 1.48 MPa by a nitrogen cover gas, are the only operational part of the ECCS during a station blackout. A large, dry containment building surrounds the reactor systems.

SCDAP/RELAP5 nodalizations representing those features of the Calvert Cliffs PWR, including pertinent portions of the secondary systems, are shown in Figures 10 and 11. Shaded areas represent core structures, cross-hatched areas represent all other pipe/vessel structures, and the remaining regions represent the hydrodynamic volume within the plant.

The approach used to model Calvert Cliffs was similar to the modeling of Surry (as outlined in Section 3.2.1). Specifically, nodalizations shown in Figures 10 and 11 were used from station blackout initiation until the time hot leg piping was drained in order to accommodate the potential for both in-vessel and full-loop natural circulation. Thereafter, the nodalization shown in Figure 12 was used in place of the Figure 11 nodalization to provide the additional flow paths needed if hot leg countercurrent natural circulation develops. In addition, the nodalization shown in Figure 12 utilized the RELAP5 servo valve refinement as described for Surry to accommodate full-loop natural circulation if RCP loop seals clear. That refinement was used in all Calvert Cliffs analyses completed in this evaluation. (Like Surry modeling, the nodalization shown in Figure 12 was not used to simulate the entire transient because requirements for computation and output would be significantly increased and because the associated simplistic control logic was assumed to be inadequate.)

Like Zion, the Calvert Cliffs surge line is angled upward from its connection to the upper half of the horizontal hot leg. A split is not required for that orientation because any potential for surge line countercurrent natural circulation is eliminated since the surge line generally sees only the hottest vapor in the top of the hot leg. However, valves numbered 601 and 603 in Figure 12 were needed to accommodate pressurizer draining and the mixing that would be expected when the pressurizer PORV opens. Specifically, while the pressurizer drained and the PORV was closed, control logic kept Valve 603 open and Valve 601 closed. Consequently, all liquid draining from the pressurizer appropriately flowed into the bottom half of the split hot leg. After pressurizer dryout, Valve 601 opened and Valve 603 closed whenever the PORV was closed. The surge line was appropriately exposed to the hottest flow stream under those conditions. And finally, control logic opened both valves whenever the PORV was opened. Countercurrent natural circulation is interrupted as fluid from the core tends to flow in both halves of the split hot leg toward the surge line when the PORV opens. It is reasonable to expect a high degree of mixing as the flow streams reach the entrance to the surge line and respond to the large pressure differential generated by the open PORV. Valves 601 and 603 were opened with the PORV as a way to approximate conditions that would result from that mixing. Model input was also needed to calculate creep rupture of the stainless steel surge line (numbered 600-3 in Figure 12), both carbon steel hot legs (numbered 105-1 and 205-1 in Figure 12), and the hottest inconel SG U-tubes (numbered 125-1 and 225-1 in Figure 12).

Like Surry, containment pressure was not allowed to increase above 0.2 MPa because the Calvert Cliffs model included only a simple single volume representation of containment (numbered 890 in Figures 11 and 12). In addition, all Calvert Cliffs countercurrent natural circulation modeling in analyses completed in this evaluation was based on benchmarks derived from Westinghouse high pressure results as listed in Table 1.

3.2.4. ANO2 PWR

The ANO2 PWR was used to represent Combustion Engineering “2x4” plants without pressurizer PORVs in this evaluation. Although Calvert Cliffs was selected as representative of Combustion Engineering plants, ANO2 was also included because it has a relatively high power density and because it is one of seven Combustion Engineering plants without pressurizer PORVs. Both factors may contribute to the

potential for SGTR. Specifically, a high power density may accelerate core damage progression and the corresponding heatup. In addition, SG tubes (and other RCS pressure boundaries) may be exposed to higher pressures in the absence of PORVs because pressure is controlled via pressurizer SRVs, which operate with relatively high set points.

ANO2 is rated at 2815 MW_t based on a core of 177 16x16 assemblies with an active fuel height of approximately 3.81 m. Both primary coolant loops contain a hot leg, a U-tube SG, two RCPs, and two cold legs. A single pressurizer is attached to the hot leg piping in one of the loops. The pressurizer surge line is made of stainless steel, the hot/cold leg piping is made of carbon steel with a stainless steel lining, and the SG U-tubes are made of inconel. ANO2 has no PORVs, but it does have two SRVs for relief of excess RCS pressure from the top of the pressurizer. The SRVs have a combined capacity of 99.5 kg/s. One accumulator, with 44.7 m^3 (44,200 kg) of borated water at 322 K, is attached to each cold leg. The accumulators, which are initially pressurized to 4.31 MPa by a nitrogen cover gas, are the only operational part of the ECCS during a station blackout. A large, dry containment building surrounds the reactor systems.

SCDAP/RELAP5 nodalizations representing those features of the ANO2 PWR, including pertinent portions of the secondary systems, are shown in Figures 13 and 14. Shaded areas represent core structures, cross-hatched areas represent all other pipe/vessel structures, and the remaining regions represent the hydrodynamic volume within the plant.

The approach used to model ANO2 was similar to the modeling of Surry (as outlined in Section 3.2.1). Specifically, nodalizations shown in Figures 13 and 14 were used from station blackout initiation until the time hot leg piping was drained in order to accommodate the potential for both in-vessel and full-loop natural circulation. Thereafter, the nodalization shown in Figure 15 was used in place of the Figure 14 nodalization to provide the additional flow paths needed if hot leg countercurrent natural circulation develops. However, all ANO2 analyses were completed during the early phase of this evaluation. Consequently, the RELAP5 servo valve refinement as described for Surry was not included in the ANO2 model. As a result, some loss of fidelity is expected if full loop natural circulation happens to develop after the nodalization shown in Figure 15 is introduced.

Like Zion, the ANO2 surge line is angled upward from its connection to the upper half of the horizontal hot leg. A split is not required for that orientation because any potential for surge line countercurrent natural circulation is eliminated since the surge line generally sees only the hottest vapor in the top of the hot leg. However, valves numbered 157 and 159 in Figure 15 were needed to accommodate pressurizer draining and the mixing that would be expected when the pressurizer PORV opens. Specifically, while the pressurizer drained and the PORV was closed, control logic kept Valve 159 open and Valve 157 closed. Consequently, all liquid draining from the pressurizer appropriately flowed into the bottom half of the split hot leg. After pressurizer dryout, Valve 157 opened and Valve 159 closed whenever the PORV was closed. The surge line was appropriately exposed to the hottest flow stream under those conditions. And finally, control logic opened both valves whenever the PORV was opened. Countercurrent natural circulation is interrupted as fluid from the core tends to flow in both halves of the split hot leg toward the surge line when the PORV opens. It is reasonable to expect a high degree of mixing as the flow streams reach the entrance to the surge line and respond to the large pressure differential generated by the open PORV. Valves 157 and 159 were opened with the PORV as a way to approximate conditions that would result from that mixing. Model input was also needed to calculate creep rupture of the stainless steel surge line (numbered 155-5 in Figure 15), both carbon steel hot legs (numbered 210-1 and 220-1 in Figure 15), and the hottest inconel SG U-tubes (numbered 301-1 and 331-1 in Figure 15).

Like Surry, containment pressure was not allowed to increase above 0.2 MPa because the ANO2 model included only a simple single volume representation of containment (numbered 890 in Figures 14 and 15). In addition, all ANO2 countercurrent natural circulation modeling in analyses completed in this evaluation was based on benchmarks derived from Westinghouse high pressure results as listed in Table 1.

3.2.5. Oconee PWR

The Oconee PWR was used to represent Babcock & Wilcox "2x4" plants in this evaluation. Oconee is rated at 2568 MW_t based on a core of 177 15x15 assemblies with an active fuel height of approximately 3.57 m. Both primary coolant loops contain a hot leg, a once-through SG, two RCPs, and two cold legs. A single pressurizer is attached to the hot leg piping in one of the loops. The pressurizer surge line is made of stainless steel, the hot/cold leg piping is made of carbon steel with a stainless steel lining, and the SG tubes are made of inconel. One PORV, with a capacity of 13.5 kg/s, can be used to relieve excess RCS pressure from the top of the pressurizer. Pressurizer SRVs are also available to handle excursions exceeding PORV capacity. A core flood tank, with 60.9 m^3 (60,800 kg) of borated water at 300 K, is attached near the top of the reactor vessel downcomer. The core flood tank, which is initially pressurized to 4.08 MPa by a nitrogen cover gas, is the only operational part of the ECCS during a station blackout. A large, dry containment building surrounds the reactor systems.

SCDAP/RELAP5 nodalizations representing those features of the Oconee PWR, including pertinent portions of the secondary systems, are shown in Figures 16 and 17. Shaded areas represent core structures, cross-hatched areas represent all other pipe/vessel structures, and the remaining regions represent the hydrodynamic volume within the plant.

Nodalizations shown in Figures 16 and 17 were used from station blackout initiation until the time hot leg piping was drained. That approach was adequate for simulation of both in-vessel and full-loop natural circulation flows that could potentially develop during that period. Thereafter, the nodalization shown in Figure 18 was used in place of the Figure 17 nodalization. That substitution provided the additional flow paths needed to simulate hot leg countercurrent natural circulation, which can develop only after the hot legs are voided.

The nodalization shown in Figure 18 was developed to accommodate both full-loop and hot leg countercurrent natural circulation in case RCP loop seals clear. That was accomplished using RELAP5 servo valves to connect (a) the hot leg crossover (from pipe 107 to pipe 108 and from pipe 207 to pipe 208), (b) the hot leg return (from pipe 113 to pipe 110-1 and from pipe 213 to pipe 210-1), and (c) the surge line return (from pipe 598 to pipe 106); for a total of five locations. The valves were configured with two sets of loss coefficients; one set consistent with those used to model normal plant operation and one set necessary for appropriate simulation of hot leg countercurrent natural circulation based on University of Maryland data. All other losses in the loop network were unaltered relative to those used for normal plant operation (i.e., equivalent to those used in the nodalization shown in Figure 17). If the horizontal portion of the RCP loop seal in a given loop is full of liquid, control logic directs the use of countercurrent loss coefficients in all servo valves in that loop. Alternately, if voids begin to form in the horizontal portion of the RCP loop seal, control logic directs a loss coefficient transition to values used for normal plant operation. As a result, both full-loop and countercurrent natural circulation flows should be calculated appropriately in each loop if/when transient loop conditions change. (Since it may have been a possibility, it should be noted that the nodalization shown in Figure 18 was not used to simulate the entire transient because

requirements for computation and output would be significantly increased and because the simplistic control logic, as described above, was assumed to be inadequate.)

A short horizontal section of the surge line in the Oconee PWR connects to the vertical section of the hot leg pipe. It was acceptable to lump that horizontal section into the pipe numbered 600-1 (as shown in Figure 17) prior to the onset of countercurrent natural circulation. However, experimental data indicated that a surge line split, as depicted in Figure 18, was needed to represent potential countercurrent flow. The crossover connection between pipes numbered 107 and 108 in Figure 18 was expected to help mix hot and cold hot leg vapor streams relative to the top of the surge line whenever the pressurizer PORV opens. Therefore, hot leg-to-surge line cross connections as shown for Surry in Figure 6 (and as discussed for all other models) did not appear to be necessary. However, model input was needed to calculate creep rupture of the stainless steel surge line (numbered 596 in Figure 18), both carbon steel hot legs (numbered 101 and 201 in Figure 18), and the hottest inconel SG tubes (numbered 120-1 and 220-1 in Figure 18).

Like Surry, containment pressure was not allowed to increase above 0.2 MPa because the Oconee model included only a simple three volume representation of containment (numbered 949-1, 949-2, and 949-3 in Figures 17 and 18). Countercurrent natural circulation modeling in all Oconee analyses completed in this evaluation was based on benchmarks derived from University of Maryland results as listed in Table 2. Reference 11 contains additional details regarding the Oconee natural circulation modeling.

4. INDEPENDENT REVIEWS OF THE EVALUATION APPROACH

Independent review committee meetings were held in August 1996 to address the applicability of the Westinghouse natural circulation experimental data, the suitability of the SCDAP/RELAP5 code, and the adequacy of SCDAP/RELAP5 natural circulation modeling with respect to this evaluation. Review committee members included Dr. P. Griffith, a private consultant and former professor at Massachusetts Institute of Technology, Dr. M. Ishii, a professor at Purdue University, and Dr. R. Viskanta, a professor at Purdue University. Dr. I. Catton, a member of Advisory Committee on Reactor Safeguards (ACRS), also attended the meetings as an observer. Findings and recommendations associated with review committee activities[12,13,14] and conclusions subsequently offered by the ACRS[15] are summarized below.

4.1. Applicability of Westinghouse Natural Circulation Data

The independent review committee concluded that the Westinghouse experiments were well designed and executed based on reports and presentations by the NRC, INEEL, and Fauske and Associates, Inc. (who provided design details of the experiments). Similar remarks were separately made by the ACRS. However, the reviewers indicated that uncertainties in the experimental parameters used to characterize hot leg countercurrent natural circulation had to be considered. In addition, the absence of radiation heat transfer in the experiments and other shortcomings in experimental scaling were noted.

Experimental parameters used to characterize hot leg countercurrent natural circulation in PWRs with U-tube SGs include mixing fractions, a recirculation ratio, and the fraction of SG U-tubes that carry hot flow in the forward direction (see Table 1). As discussed in Section 5, analyses were performed to evaluate the impact of variations in individual parameters and the impact of simultaneous variations (or the syner-

gistic effects) of those parameters. It was assumed that the completed sensitivity analyses adequately addressed uncertainties in the characteristic parameters with respect to the potential for SGTR.

The Westinghouse experiments were conducted at relatively low temperatures where radiation heat transfer was unimportant. That raised reviewer concerns about prototypicality and scalability because radiation may not be negligible at the temperatures expected during severe accidents in operating PWRs. However, scaling of the experiments is an issue that has been studied extensively. The first scaling analyses were conducted by Westinghouse during both low pressure and high pressure experimental programs.[2,3] The NRC subsequently sponsored an independent scaling review of the low pressure experiments by Wassel.[16] The Wassel analysis was limited to evaluation of the low pressure tests without consideration of radiation issues. Consequently, the NRC directed an additional review by Tung to evaluate the high pressure experiments including the treatment of radiation effects.[17] The Tung evaluation was subject to an independent review, where one review finding indicated the need for a more detailed analysis of radiation heat transfer. Accordingly, O'Brien completed a separate scaling report to examine radiation effects more closely.[17] Several additional radiation and scaling-related issues were also raised and addressed in conjunction with the subject evaluation.[18,19,20]

Results from the varied scaling reviews indicated that the absence of radiation introduced some scaling distortions in terms of low experimental core and SG heat transfer (compared to heat transfer expected in the prototype). Radiation-related scaling distortions were not found relative to transient heat transfer to unheated core structures or relative to heat transfer to the hot leg pipe. A separate assessment of the potential impact of radiation heat transfer between hot leg countercurrent vapor streams was addressed through SCDAP/RELAP5 analyses as outlined in Section 5. Results from those analyses indicated that vapor-to-vapor radiation was not significant because heat transfer in the hot leg was dominated by convection from vapor to the pipe wall.

Other scaling distortions were introduced by the configuration of the experimental apparatus. For example, the experimental SG tube diameter (of 0.305 in) was larger than the one-seventh scale would have dictated (~0.775/7 = 0.111 in), flow resistance in the experimental core was somewhat low, and upper plenum heat sinks in the experimental vessel were somewhat large. The concession on experimental SG tube size was presumably driven by practical problems associated with the fabrication of relatively-long small-diameter tubes and the assembly of such tubes into a U-tube geometry. However, Westinghouse did ensure the appropriate scaling of experimental SG flow and SG heat capacity. Natural circulation flow rates in the core of an operating PWR would be smaller than predicted from direct scaling of the Westinghouse data because experimental core resistances were somewhat low and experimental upper plenum heat sinks were somewhat large, although reasons for that discrepancy is unknown.

In spite of scaling discrepancies, the Westinghouse experiments are quite useful in two major respects. First, the experiments clearly demonstrated the robustness of the natural circulation flow patterns including flows upward through the center of the core and downward through the core periphery, the countercurrent flows in the hot legs, and the participation of the SG tubes for U-tube designs. Those flow patterns were demonstrated to persist over a broad range of conditions in tests using water, low pressure SF_6, and high pressure SF_6. Furthermore, after completion of all of the varied reviews, there is no evidence to indicate that the basic phenomenology of hot leg countercurrent natural circulation was altered by scaling discrepancies. It is therefore reasonable to expect that similar natural circulation flow patterns would develop during a severe accident in an operating PWR with U-tube SGs. And second, the experimental results, while not representative of the scaled natural circulation flows and heat transfer rates of an operating PWR in every detail, do provide a data base for code validation. In fact, RELAP5 simulations of selected experi-

ments were completed and the code results were found to be in reasonable agreement with the data. Confidence is therefore gained in code simulation of similar natural circulation patterns in operating PWRs.

It is also worth noting that the original SCDAP/RELAP5 model was developed without reliance on scaling of experimental results. Instead, Westinghouse experiments were used as a means for validation of the COMMIX code results. Once confidence was established in COMMIX capabilities, SCDAP/RELAP5 models were developed by direct comparison to COMMIX results as outlined in Reference 10.

4.2. Suitability of SCDAP/RELAP5

The independent review committee concluded that SCDAP/RELAP5 is capable of modeling natural circulation in PWRs under severe accident conditions for the purpose of calculating the relative timing of RCS component failures in order to assess the SGTR potential. After consideration of the independent review committee findings, the ACRS concurred that "it [SCDAP/RELAP5] can be used for the analyses required to support the development of the steam generator integrity rule". Those conclusions were at least partially based on the fact that SCDAP/RELAP5 was shown to be capable of reproducing major trends in the Westinghouse experiments and that agreement between data and code predictions was satisfactory. Furthermore, code predictions from transient initiation through core oxidation and the onset of core degradation were acknowledged to be reliable, which generally covers the period of interest in this evaluation. However, reviewers indicated that refinement was warranted in the calculation of convection heat transfer.

SCDAP/RELAP5 normally calculates forced and free convection heat transfer coefficients for either laminar or turbulent flow (as appropriate) and then uses the larger value. Results from some of the earliest analyses performed in this evaluation indicated that natural circulation flows through the SGs were generally turbulent. The largest coefficients for that flow regime were found to be those generated using the Dittus-Boelter correlation. The reviewers argued that a correlation for fully-developed turbulent forced convection inside pipes may not provide the best heat transfer simulation for natural circulation in the SGs. Accordingly, the code was modified by the addition of a mixed convection heat transfer capability, which combines the effects of both forced and free convection. A comparison of results for the ANO2 PWR with and without the mixed convection update indicated that ex-vessel temperatures were relatively insensitive to the modification because the predicted contribution from free convection effects was relatively small.[21] The code modification was retained, however, because it extended code applicability and that added capability could be more important in other transients. As a result, all but the earliest analyses performed in this evaluation were completed with the mixed convection update. Analyses completed prior to the addition of the update are identified in Section 5.

4.3. Adequacy of SCDAP/RELAP5 Modeling

The independent review committee acknowledged the completion of a significant number of SCDAP/RELAP5 calculations along with an indication that the code had been applied correctly in this evaluation. However, the committee also recommended non-dimensionalization so that results from Westinghouse experiments and results from SCDAP/RELAP5 analyses could be directly compared; sensitivity studies to evaluate uncertainties associated with heat transfer coefficients and the other parameters that characterize hot leg countercurrent natural circulation in PWRs with U-tube SGs, including the synergistic effects associated with varying several parameters at a time; and analyses to evaluate conjugate heat trans-

fer effects in the split hot leg model (consisting of the combination of fluid-to-wall heat transfer, fluid-to-fluid heat transfer, and circumferential conduction around the hot leg pipe wall).

The committee was concerned that conclusions were not clear and definitive based on the results available at the time of the review meetings. Non-dimensionalization (in terms of some convenient temperature difference, temperature ramp, or other suitable basis) was recommended as a way to compare code results and experimental data so that more definitive conclusions could be developed. However, non-dimensionalization was not performed. Instead, a broader series of sensitivity analyses for a broader spectrum of operating PWRs was completed. Among other issues, uncertainties in heat transfer coefficients, the parameters that characterize hot leg countercurrent natural circulation, and conjugate heat transfer effects in the split hot leg model were considered in the SCDAP/RELAP5 analyses as discussed in the following section.

5. SCDAP/RELAP5 ANALYSES

All SCDAP/RELAP5 analyses performed during this evaluation were based on station blackout accidents (and variations thereof) because those accidents are considered to be one of the more likely scenarios leading to natural circulation at temperatures and pressures that could threaten SG tube integrity (as well as the integrity of other vulnerable RCS pressure boundaries). The particular station blackout accident considered is generally designated TMLB', which includes an immediate loss of all alternating current (AC) power and all feedwater. An additional assumption of accident progression without recovery allows the potential for development of natural circulation flows (including in-vessel, full-loop, and hot leg countercurrent modes as discussed in Section 2). All SCDAP/RELAP5 models used in this evaluation appropriately accounted for the potential development of all natural circulation flows (as discussed in Section 3).

A TMLB' accident is initiated by the loss of off-site power. On-site AC power is unavailable because diesel generators fail to start or fail to supply power. Decay heat removal cannot be maintained because there is no power for electrical feedwater pumps and steam driven auxiliary feedwater pumps fail to supply water. As the transient begins, control rod drives lose power, the reactor scrams, and the main feedwater pumps and RCPs begin to coastdown. The flow of feedwater is reduced to zero before pump coastdown is complete because the main feedwater valves close quickly. The turbine stop valves then close, effectively isolating the SG secondaries. After isolation, SG pressures increase as a result of boiling associated with decay heat transfer until relief valves open. SG pressures are normally maintained between the opening and closing pressures of the relief valves thereafter. Decay heat transfer to the SGs is significantly reduced after secondary inventories are boiled away. RCS temperatures and pressures increase when decay heat removal is reduced until the pressurizer PORVs open. The RCS pressure is normally controlled by cyclic operation of the PORVs thereafter. However, the RCS pressure can be influenced by RCP seal leaks, which can develop following the loss of AC power and the associated loss of seal cooling water. After the RCS is heated to saturation, a high pressure boiloff begins, ultimately leading to core uncovery and heatup. Without recovery of power or equipment, the transient proceeds to severe core damage and melting.

A substantial number of SCDAP/RELAP5 analyses were performed to evaluate the potential for SGTR that could develop in operating PWRs as a result of natural circulation heating during TMLB' accidents (and variations thereof). Those analyses included "stand alone" loop simulations to evaluate uncertainties associated with Westinghouse countercurrent natural circulation data and a large number of analyses for operating PWRs to determine if conditions associated with TMLB' accidents could threaten SG tube integrity (and the integrity of other vulnerable RCS pressure boundaries). Operating PWRs were

represented by Surry, Zion, Calvert Cliffs, ANO2, and Oconee plants, thereby covering all existing PWR designs. All RCS pressure boundaries, including the SG tubes, were assumed to be defect free with respect to the prediction of RCS pressure boundary failures in all analyses. The remainder of this section contains descriptions of the specific analyses that were performed, explanations why each of the analyses were needed, and summaries of the associated SCDAP/RELAP5 results.

5.1. Stand Alone Loop Analyses

In this evaluation, all hot leg countercurrent natural circulation modeling for operating PWRs with U-tube SGs was based on Westinghouse experimental data. However, there is some variability in the data that characterize countercurrent natural circulation as indicated in Table 1. An understanding of the corresponding tube heatup sensitivity was an important part of evaluating uncertainties relative to the potential for SGTR. Analyses were therefore needed to determine how SG U-tube heatup might be affected as a result of the experimental variability.

The needed analyses were based on a "stand alone" version of the Surry pressurizer loop (shown in Figure 5). The Surry loop was simplified through the use of time dependent junctions to represent the pressurizer PORVs, to connect the split hot legs to the reactor vessel, and to connect the top of the split hot leg to the hot side of the SG inlet plenum. Time dependent volumes were used to represent the reactor vessel and the RCP suction. The resulting nodalization, which allows the loop to "stand alone", is shown in Figure 19. This approach provided a fast-running model that could be readily modified.

Time dependent junctions and volumes in the stand alone loop model were configured to use SCDAP/RELAP5 results derived from benchmarking a base case from the onset of hot leg countercurrent natural circulation (9200 s) through the time of surge line failure (15,350 s). The Base Case benchmark included 35% of the SG U-tubes participating in hot (forward) flow (or a hot/cold SG U-tube split of 35%/65%), mixing fractions of 0.87, and a recirculation ratio of 1.9. Variations in the natural circulation parameters were then evaluated individually, while all other parameters (and the time dependent results derived from the Base Case benchmark) were held constant, as indicated by the matrix provided in Table 3. That calculation matrix was designed to cover the full range of experimental variability indicated in Table 1. (Although a recirculation ratio of 2.39 was needed to cover the experimental range and a maximum of only 2.25 was actually reached [in Case 7]. Reasons for that discrepancy will be explained below.)

5.1.1. SG U-Tube Split Sensitivity

As indicated in Table 3, the number of tubes allowed to participate in hot (forward) flow in the SG U-tube split sensitivity analyses (Cases 1, 2, and 3) ranged from 29 to 61% (while all other conditions were held constant). That range covered the experimental variation listed in Table 1. A comparison of temperatures for the hottest tubes in the Base Case and the SG U-tube split sensitivity analyses is provided in Figure 20. Results shown in the figure indicate that SG U-tube temperatures increase as the number of tubes participating in hot (forward) flow decreases. That occurs because tube temperatures must increase as the tube area decreases when decay heat transfer is constant. However, by 15,000 s (which was the end of all stand alone loop sensitivity analyses), the maximum temperature difference (between minimum and maximum tube splits) was no more than ~26 K. That is an insignificant difference considering all other uncertainties involved in the simulation of severe reactor accidents. Furthermore, the calculated temperature increases did not significantly increase tube creep damage, indicating that any potential for SGTR

would not develop until long after surge line failure (at 15,350 s) for the range of SG U-tube splits considered. Effects on SG U-tubes as a result of individual variations in the tube split are minimal based on those results.

5.1.2. Mixing Fraction Sensitivity

Sensitivity analyses with mixing fractions of 0.76 and 0.89 were completed as outlined in Table 3 to cover the experimental variation listed in Table 1. A comparison of temperatures for the hottest tubes in the Base Case and the mixing fraction sensitivity analyses (Cases 4 and 5) is provided in Figure 21. Results shown in the figure indicate that SG U-tube temperatures increase as the mixing fraction decreases. That occurs because vapor temperatures entering the hot portion of the SG U-tube bundle increase as mixing in the SG inlet plenum is reduced. However, at the end of the sensitivity analyses (15,000 s), the maximum temperature difference (between minimum and maximum mixing fractions) was ~24 K. Again, that is an insignificant difference considering all other uncertainties involved in the simulation of severe reactor accidents, indicating that the effect on SG U-tubes as a result of individual variations in the mixing fraction is minimal.

5.1.3. Recirculation Ratio Sensitivity

Sensitivity analyses with recirculation ratios of 1.69 and 2.25 were completed (while all other conditions were held constant) as outlined in Table 3; although a recirculation ratio of 2.39 was needed to cover the experimental variation listed in Table 1. A ratio of 2.39 was not achieved because vapor temperatures entering the SG U-tubes were too low. Those temperatures, which affect the magnitude of the buoyancy driven flow, are functions of the mixing fraction (and other related parameters). A lower mixing fraction, which could have increased the vapor temperatures and the recirculation ratio, was not an option because all parameters, other than the variable being evaluated, were held constant by design. Given that discrepancy, a comparison of temperatures for the hottest tubes in the Base Case and the recirculation ratio sensitivity analyses (Cases 6 and 7) is provided in Figure 22. Results shown in the figure indicate that SG U-tube temperatures increase as the recirculation ratio increases. That occurs because heat transfer coefficients in the tubes increase as velocities increase. However, at the end of the sensitivity analyses (15,000 s), the maximum temperature difference (between minimum and maximum recirculation ratios considered) was no more that ~10 K. Based on trends in those results, it would appear that a recirculation ratio of 2.39 could result in SG U-tube temperatures that could be ~5 K higher, which would increase the maximum temperature difference over the full range to ~15 K. In either case, however, those are insignificant differences. Furthermore, those differences would not significantly increase tube creep damage, indicating that any potential for SGTR would not develop until long after surge line failure (at 15,350 s) for the range of recirculation ratios considered. Based on those results, effects on SG U-tubes as a result of individual variations in the recirculation ratio are minimal.

All of the foregoing stand alone loop analyses were completed before SCDAP/RELAP5 updates to treat mixed convection were developed. However, results from ANO2 scoping calculations indicate that those updates should not have any significant impact on SG tube heating.[21] Furthermore, differences in SG U-tube temperatures are the results of interest, and similar differences would be expected as long as all analyses were completed either with or without use of the mixed convection updates. The servo valve refinement, as discussed in Section 3.2, was not needed because the time dependent results used in the analyses did not include RCP loop seal clearing. Since those conditions were fixed, loop seal clearing

could not occur in any of the stand alone loop analyses, which means that servo valve loss coefficient transitions (to full-loop flow values) were unnecessary. Additional information regarding the stand alone loop analyses is available for further reference in a previously issued document.[22]

5.2. Initial Plant Analyses

Nine analyses for the Surry PWR (with Case SUR-01 through Case SUR-09 designations) and four analyses for the ANO2 PWR (with Case ANO2-01 through Case ANO2-04 designations) were completed in the initial stages of this evaluation. All of factors that could affect the potential for SGTR were not identified or completely understood at the time that these analyses were initiated. Consequently, these analyses were used to explore SGTR response in two different PWRs for a variety of different factors. It was assumed that this approach would provide results that could be used to guide additional analyses in terms of those factors with the largest impact on the potential for SGTR.

RCP seal leaks were among the factors that were considered. The following sections have been organized to discuss the initial Surry and ANO2 analyses in terms of those with and without RCP seal leaks because those leaks significantly alter plant response, the potential for loop seal clearing, and therefore, the potential for increased SG tube heating associated with full loop natural circulation. Other factors that were considered include SG secondary depressurization, RCS depressurization following predicted pressure boundary failures, the hot/cold SG tube split, and the treatment of upper plenum steel if it is predicted to melt. A summary description for each of the initial plant analyses is provided in Table 4. The table also identifies references to supporting documentation, if available.

It should be noted that there are a number of similarities between the Surry and ANO2 analyses, which will become apparent through the following discussions. Those similarities were intentional, thereby providing a way to explore the potential for SGTR relative to some basic design differences. Specifically, ANO2 has a higher core power density than Surry (at 97 versus 92 MW/m^3, respectively) and ANO2 has a lower RCP loop seal depth than Surry (at 1.2 versus 1.7 m, respectively). In addition, ANO2 RCS pressure is normally controlled via pressurizer SRVs operating between 16.7 and 17.2 MPa while pressurizer PORVs operating between 15.7 and 16.2 MPa control the Surry RCS pressure.

5.2.1. Surry Analyses without RCP Seal Leaks

Surry Case SUR-01 was the first plant analysis completed in this evaluation. As such, this particular analysis will be described in some detail in order to provide a foundation for the general conduct of this evaluation and the general nature of the plant response during a TMLB' transient. Furthermore, all plant analyses share a number of similarities. By providing details for Surry Case SUR-01, it was assumed that descriptions of all other analyses can be summarized to emphasize only those highlights that are important relative to the potential for SGTR without any significant loss of understanding.

As indicated in Table 4, Case SUR-01 was performed without accident recovery and without operator actions, which basically means that feedwater is never restored and that no action is taken to try to mitigate accident progression. If upper plenum steel was predicted to melt, it was assumed that the molten steel would relocate into the lower head and quench to the lower head liquid temperature, given an adequate liquid inventory. Hot leg countercurrent natural circulation was benchmarked at average values derived from Westinghouse steady state experiments (as specified in the table) before the analysis began. After the anal-

ysis was completed, it was recognized that the process used to benchmark natural circulation biased heat transfer so that SG energy deposition levels were somewhat higher than levels established in previous analyses[9], which could lead to some increase in SG tube temperatures. An adjustment was not made because differences were small and conservative relative to the potential for SGTR. Break initiation and the associated depressurization was not simulated following any predicted RCS pressure boundary failure. Instead, the calculation was allowed to proceed without a break in order to conservatively determine the timing associated with other potential RCS pressure boundary failures. That approach is conservative because the RCS pressure will remain high without break simulation, thereby providing the potential for subsequent failures at the earliest possible times. In addition, the potential for subsequent failures is increased because natural circulation heating will continue without the disruption that would otherwise be associated with an RCS pressure boundary failure.

In Surry Case SUR-01, the loss of AC power resulted in reactor scram and RCP trips at transient initiation (at 0 s). In addition, SG isolation valves closed and feed water pumps tripped, effectively isolating the SG secondaries. The RCS pressure initially decreased from (the steady state value of) 15.9 MPa to about 14.5 MPa because core power dropped rapidly after scram while RCP coastdown was relatively gradual. A pressure increase (to about 15.7 MPa) then occurred as indicated in Figure 23 while full-loop natural circulation of primary liquid was established. Thereafter, the RCS pressure gradually decreased to about 14.8 MPa because full-loop natural circulation was effective in cooling the core by rejecting decay heat to SG secondary fluids.

SG secondary pressures in Surry Case SUR-01 increased (from initial values of about 5.4 MPa) as a result of heat transferred by full-loop natural circulation. Consequently, relief valves (RVs) in all three SGs were challenged by ~20 s when secondary pressures increased to opening pressures of 7.2 MPa. SG RVs in all loops were assumed to cycle normally to control secondary pressures between 6.9 and 7.2 MPa as indicated in Figure 24. Note that a large number of valve cycles are required, particularly while SGs are in the process of drying out. The RCS pressure gradually increased as SG secondary liquids were boiled away. By 4980 s, the RCS pressure had increased to the pressurizer PORV opening set point of 16.2 MPa as shown in Figure 23. All secondary inventories were depleted shortly thereafter (by 5040 s).

The (steady state) RCS subcooled margin in Surry Case SUR-01 was basically maintained as long as some liquid remained in the SG secondaries. However, heat transfer from the RCS was substantially reduced after SG secondary dry out. With reduced heat transfer to the SGs and the continuous addition of core decay energy, the RCS inventory was ultimately heated to a saturated state. Addition of decay heat thereafter resulted in boiling of the RCS liquid in the core. By that time, vapor in the pressurizer dome had been vented and liquid was being discharged through the pressurizer PORV. Consequently, the volume expansion associated with boiling caused the RCS pressure to increase substantially above the pressurizer PORV set point as indicated in Figure 23. (It should be noted, however, that the pressurizer SRV was not challenged.) As boiling progressed, vapor collected in the top of the SG U-tubes, ending full-loop natural circulation of primary liquid by about 7760 s. Some vapor also made its way to the pressurizer PORV. The energy relieved by venting two-phase flow led to an RCS pressure reduction back to the range of 15.7 to 16.2 MPa, as controlled by the pressurizer PORV.

Boiling in the core and venting through the pressurizer PORV led to depletion of the RCS inventory in Surry Case SUR-01. As indicated in Figure 25, the collapsed liquid level fell below the top of the fuel rods by 9030 s. Shortly thereafter, the hot legs voided and vapor in the core exit began to superheat, presenting conditions that could support development of hot leg countercurrent natural circulation. Accordingly, the calculation was stopped at 9205 s for loop renodalization needed for countercurrent simulation (i.e., the

nodalization used in each primary coolant loop, similar to that shown in Figure 4, was replaced with nodalization similar to that shown in Figure 5). As indicated in Figure 25, core uncovery was complete by 10,670 s. Oxidation of the uncovered core began by about 11,460 s.

Temperatures in the RCS piping in Surry Case SUR-01 increased as shown in Figure 26 as a result of heat transfer associated with natural circulation flows. Creep rupture of the pressurizer surge line at 14,050 s, due to natural circulation heating, was predicted to be the first failure of the RCS pressure boundary. Terms representing the cumulative creep damage of the surge line and other vulnerable RCS boundaries are shown in Figure 27. Surge line failure corresponds with the time when the associated creep damage term reached unity.

A break was not simulated at the time of surge line failure in Surry Case SUR-01. Instead, the calculation was allowed to proceed without a break in order to conservatively determine the timing associated with other potential RCS pressure boundary failures. Pressurizer loop hot leg creep rupture was accordingly predicted at 15,110 s as indicated in Figures 26 and 27. Both non-pressurizer loop hot leg nozzles were predicted to fail shortly thereafter (at 15,670 s). However, SGTR was not predicted, even though simulation of surge line rupture was ignored, because the tubes remained relatively cool. The calculation was terminated at 18,900 s because surge line failure had already occurred (some 4850 s earlier) and creep damage of the SG tubes was essentially zero (as indicated in Figure 27). The potential for SGTR is low in this case based on those results. The timing of all ex-vessel failures in this analysis (and all other initial plant analyses) are summarized in Table 5 for easier reference. The sequence of key events for Surry Case SUR-01 is listed in Table 6. Those events, as just described, are typical of TMLB' transients without RCS or SG secondary depressurization.

Surry Case SUR-02 was identical to Case SUR-01 except that a break was introduced in Case SUR-02 when the first RCS pressure boundary was predicted to fail. Comparing results from the two analyses was expected to provide insights into the modifications in natural circulation heating that could occur when the RCS is depressurized through a break.

Transient progression in Surry Case SUR-02 was identical to the progression of Case SUR-01 until surge line failure (at 14,050 s). At that time, a surge line break was introduced in Case SUR-02, resulting in rapid depressurization of the RCS and the end of pressurizer PORV cycling as shown in Figure 28. Accumulator injection followed, providing water sufficient to reflood the active core by 14,350 s as shown in Figure 29. The reflood effectively arrested the heatup of the core and cooled the RCS piping as indicated in Figure 30. Core reheating did occur after the accumulator water was boiled away. However, energy associated with core reheating was primarily directed out the surge line break, which prevented any significant reheating of the RCS piping. A decision was made to terminate Case SUR-02 at 21,000 s because it was clear that additional RCS pressure boundary failures would be very unlikely. In fact, SGTR cannot occur if the surge line fails as predicted in this case because the SG tubes are subjected to compression loading as a result of RCS depressurization. SG tube collapse is possible under those conditions, but relatively high temperatures in conjunction with the compression loads would be required to generate that type of failure.

Results from Surry Cases SUR-01 and SUR-02 indicated that SGTR will not develop if normal pressures are maintained in the SG secondaries. In Case SUR-01, SG tube differential pressures were limited to 9.3 MPa because both RCS and SG secondary pressures were maintained, despite predictions that the surge line and hot leg nozzles would fail. SG tube heating was not severe enough to induce SGTR for that differential pressure. In Case SUR-02, the RCS was depressurized through a surge line break while SG secondary pressures were maintained. In that case, the SG tubes were subjected to compression loading,

which effectively eliminated the potential for SGTR. Based on those results, two changes were made in Surry Case SUR-03 relative to Case SUR-01.

The first change made in Surry Case SUR-03 involved the treatment of the SG secondaries. In Case SUR-01, it was assumed that all SG secondary relief valves (RVs) cycled as necessary to control secondary pressures (between 6.9 and 7.2 MPa). In Case SUR-03, it was assumed that the first SG secondary RV challenged would open and fail to close, resulting in secondary depressurization and an increased potential for SGTR in the affected SG.[a] Failure of a SG RV does not appear to be a unreasonable assumption given the number of RV cycles required to maintain SG secondary pressures (see Figure 24). SG secondary pressures in Case SUR-03 consistent with failure of the first RV challenged are shown in Figure 31.

The second change made in Surry Case SUR-03 relative to Case SUR-01 affected the treatment of upper plenum steel if melting of that steel was predicted. In Case SUR-01, it was assumed that all upper plenum steel that was predicted to melt would relocate into the lower head and quench, given an adequate liquid inventory. In Case SUR-03, it was assumed that molten upper plenum steel would candle through the core and refreeze at some relatively cool location before reaching the lower head. Core temperatures conducive to refreezing could exist at locations above the vessel liquid level.

Temperatures of the RCS piping in Surry Case SUR-03 are shown in Figure 32. Heating associated with natural circulation flows led to creep rupture of the pressurizer surge line at 13,640 s, which was predicted to be the first failure of the RCS pressure boundary. SGTR in the pressurizer loop SG was predicted 1010 s later (at 14,650 s). SG tube temperatures in Case SUR-03 were not substantially hotter than tube temperatures in Case SUR-01 as indicated through comparison of Figures 26 and 32. However, SGTR was predicted in Case SUR-03, but not in Case SUR-01, because the SG tube differential pressure increased from 9.3 to 16.2 MPa in Case SUR-03 as a result of the assumed SG secondary depressurization. The potential for SGTR is low in this case however, given that surge line failure was predicted 1010 s before tube failure.[b]

Surry Case SUR-04 was identical to Case SUR-02 except that SG secondary RV failure with the associated secondary depressurization was considered in Case SUR-04. Comparing results from the two analyses was expected to provide insights into the modifications in natural circulation heating that could occur with both RCS and SG secondary depressurization. Like Surry Case SUR-02, rapid RCS depressurization was followed by accumulator injection as a result of the break that was introduced in Surry Case SUR-04

a. It is worth noting that the secondary RV associated with the SG attached to the pressurizer loop was always the first SG secondary RV challenged in this evaluation. That is because pressurizer PORV flows tend to keep vapor temperatures in the pressurizer loop somewhat hotter than vapor temperatures in the non-pressurizer loops. Heat transfer to the pressurizer loop SG secondary is somewhat higher because of the hotter vapor temperatures. Consequently, the pressurizer loop SG secondary is heated to the RV set point somewhat quicker than the non-pressurizer loop secondaries.

b. Surry Case SUR-03, and Surry Case SUR-06, were originally completed without code updates to treat mixed convection heat transfer.[23] Both analyses were ultimately revised using a version of the code with mixed convection updates.[24] The code was modified to treat mixed convection based on peer reviewer recommendations (see Section 4.2) and the modified code was used in all analyses performed after the recommendations were made. Revisions of Cases SUR-03, and SUR-06, were completed so that comparisons with subsequent analyses could be made without concern that observed differences were related to the updates. All results presented here were taken from the revised analyses.

at the time of surge line failure. Accumulator reflood effectively arrested the heatup of the core and cooled the RCS piping. Case SUR-04 results indicate that cooling was sufficient to prevent additional RCS pressure boundary failures even though the secondary side of the pressurizer loop SG was depressurized. Therefore, results from Cases SUR-04 and SUR-02 indicate that additional RCS pressure boundary failures will not develop after the RCS is depressurized through an initial pressure boundary failure, with or without SG secondary depressurization.

Surry Case SUR-05 was identical to Case SUR-01 except that a hot/cold SG tube split of 53%/47% was simulated in Case SUR-05 as outlined in Table 4. (A tube split of 53%/47% is the average observed during Westinghouse high pressure transient tests.) SG U-tube temperatures for the two cases are compared in Figure 33. As shown, SG tubes in Case SUR-05 were somewhat cooler than tubes in Case SUR-01, which is consistent with results from the stand alone loop analyses. Specifically, SG U-tube temperatures were found to decrease as the number of tubes participating in hot (forward) flow was increased. A close examination indicates that differences between Cases SUR-05 and SUR-01 are on the order of 10 to 20 K, which is approximately equivalent to differences observed in the stand alone loop analyses. Results from Cases SUR-05 and SUR-01 were essentially identical otherwise, indicating that changes in the SG tube split do not significantly affect general accident progression in cases without SG secondary depressurization.

As outlined in Table 4, the assumed hot/cold SG tube split was also the only difference between Surry Cases SUR-06 and SUR-03. Specifically, a hot/cold SG tube split of 53%/47% was simulated in Case SUR-06. RCS piping temperatures in Case SUR-06 were somewhat cooler than the corresponding piping temperatures in Case SUR-03, which was expected based on results from the stand alone loop analyses and Surry Case SUR-05. Because RCS piping temperatures were somewhat cooler, surge line failure in Case SUR-06 at 13,730 s (as shown in Figure 34) was slightly delayed compared to surge line failure in Case SUR-03 at 13,640 s (as shown in Figure 32). Furthermore, SGTR in Case SUR-06 at 14,960 s was slightly delayed compared to SGTR in Case SUR-03 at 14,650 s (as indicated in the same figures and Table 5). Based on those results, SGTR could be delayed 220 s relative surge line failure if the fraction of SG tubes participating in forward (hot) flow during countercurrent natural circulation is increased from 35 to 53% (and the surge line failure is not simulated when predicted). All other results were essentially identical, indicating that the SG tube split does not affect the general accident progression or adversely affect the potential for SGTR even if SG secondaries are depressurized. The sequence of key events for Surry Case SUR-06 is listed in Table 7. Those events are typical of TMLB' transients with SG secondary depressurization.

Surry Case SUR-07 was identical to Case SUR-01 except that all three SG secondaries were assumed to depressurize through failed RVs. Multiple RV failures would be unlikely, but results should provide some indication how depressurization of multiple SG secondaries could affect the potential for SGTR. Decay heat transfer from the RCS to the SG secondaries was reduced in Case SUR-07 relative to Case SUR-01 because secondary inventories were depleted more rapidly with all SG RVs open. RCS piping temperatures heated more rapidly and creep ruptures of that piping were accelerated in Case SUR-07 because heat transfer to the secondaries was reduced. However, surge line failure was still predicted to be the first failure of the RCS pressure boundary as indicated in Table 5. Furthermore, surge line failure could be expected 1340 s before SGTR if the surge line failure is not simulated when predicted. Those results indicate that the potential for SGTR in this case is not adversely affected even if all SG secondaries are depressurized.

5.2.2. Surry Analyses with RCP Seal Leaks

RCP seal leaks were simulated in Surry Cases SUR-08 and SUR-09. The leak simulation was based on the expected behavior of Westinghouse RCP seals, which are used in the Surry plant.[25] Specifically, Westinghouse seals are expected to leak 21 gpm of subcooled water per RCP at nominal operating conditions if seal cooling water is lost.[26] Subsequent seal degradation and failure is expected as a TMLB' accident progresses because the seals are not designed for exposure to high temperature steam. The seals are particularly vulnerable to failure when fluid in the RCP reaches a saturated condition because seal faces tend to pop open as a result of two-phase flow instabilities. Although a specific leak rate is difficult to predict given possible variations in seal failure, a panel of experts concluded that 250 gpm per RCP is the most likely leak rate from Westinghouse pumps during a TMLB' accident.[27] Based on that information, a seal leak area equivalent to 21 gpm per RCP was introduced in Cases SUR-08 and SUR-09 at TMLB' accident initiation since seal cooling water is lost when AC power is lost. The appropriate leak area was established for flow of saturated liquid at nominal conditions. Seal leak areas were subsequently increased from the equivalent of 21 gpm per RCP to the equivalent of 250 gpm per RCP at the time saturated conditions were reached at any of the pumps. Seal leaks of 250 gpm per RCP were assumed in both cases because the rate was considered likely and because the rate seemed large enough to potentially influence RCP loop seal clearing. The appropriate leak area was established for flow of saturated liquid at 16.0 MPa, corresponding with the average of the opening and closing set points of the pressurizer PORVs.

Surry Cases SUR-08 and SUR-09 differed only with respect to the treatment of upper plenum steel if melting of that steel was predicted. In Case SUR-08, it was assumed that all upper plenum steel that was predicted to melt would relocate into the lower head and quench, given an adequate liquid inventory. In Case SUR-09, it was assumed that molten upper plenum steel would candle through the core and refreeze at some relatively cool core location without quenching.

The first RCS pressure boundary failures in Surry Cases SUR-08 and SUR-09 were predicted to be hot leg failures, instead of the surge line failures that developed in all previous Surry cases, and SGTRs did not develop (see Table 5). Hot leg failures, rather than surge line failures, were predicted in Cases SUR-08 and SUR-09 because pressurizer PORV flow and therefore, surge line heating, was reduced as a result of flows through RCP seal leaks. SGTRs did not develop because the RCS was depressurized by the RCP seal leaks. Tube differential pressures were reduced to zero in pressurizer loop SGs and tube differential pressures were transformed into compressive loads in non-pressurizer loop SGs as a result of RCS depressurization, which effectively eliminated the potential for SGTR in Cases SUR-08 and SUR-09. Differences due to the treatment of upper plenum steel were insignificant. Additional information regarding all initial Surry analyses (Cases SUR-01 through SUR-09) is available for further reference in previously issued documents.[23,24,28]

5.2.3. ANO2 Analyses without RCP Seal Leaks

As indicated in Table 4, ANO2 Case ANO2-01 was similar to Surry Case SUR-01 except that SG secondary depressurization was simulated in Case ANO2-01. SG secondary depressurization was simulated in all ANO2 analyses completed during the course of this evaluation based on the initial Surry results, which indicated that a potential for SGTR will not develop if normal SG secondary pressures are maintained. Like other TMLB' accidents, decay heat transfer from the core led to SG secondary dry out and the subsequent boiling of primary inventory in Case ANO2-01. Natural circulation of vapor was ultimately established, leading to ex-vessel heating as shown in Figure 35. As indicated in the figure and in Table 5, the

first failure in the RCS pressure boundary developed when the surge line was heated to the point of creep rupture at 11,330 s. The calculation was allowed to proceed without introduction of a break at the time of surge line failure in order to conservatively determine the timing associated with other potential RCS pressure boundary failures. Accordingly, failure of both hot legs (at 12,150 and 12,510 s) and a SGTR at 13,750 s were predicted. (Event timing for this analysis, and all other initial plant analyses, has been summarized in Table 5 for reference.) Those results are similar to previously discussed Surry result in that the potential for SGTR is low because surge line failure was predicted 2420 s earlier than tube failure. Consequently, the potential for SGTR was not adversely affected by the Combustion Engineering design of the ANO2 plant relative to the Westinghouse design of the Surry PWR in this case.

ANO2 Case ANO2-02 was identical to Case ANO2-01 except that a break was introduced in Case ANO2-02 when the first RCS pressure boundary was predicted to fail. Accordingly, a surge line break was introduced in Case ANO2-02 at 11,330 s, resulting in rapid depressurization of the RCS and the end of pressurizer PORV cycling. Accumulator injection followed, providing water sufficient to reflood the active core. The reflood effectively arrested the heatup of the core and cooled the RCS piping as shown in Figure 36. Core reheating did occur after the accumulator water was boiled away. However, energy associated with core reheating was primarily directed out the surge line break, which prevented any significant reheating of the RCS piping. A decision was made to terminate Case ANO2-02 at 21,550 s because it was clear that additional RCS pressure boundary failures would be very unlikely. Those results are similar to results for Surry Case SUR-02. Specifically, SGTR cannot occur if the surge line fails as predicted in either ANO2 or Surry for these conditions because the SG tubes are subjected to compression loading as a result of RCS depressurization. SG tube collapse is possible, but relatively high temperatures in conjunction with the compression loads would be required to generate that type of failure. Those results also confirm that the potential for SGTR is not adversely affected by design differences between ANO2 and Surry PWRs.

5.2.4. ANO2 Analyses with RCP Seal Leaks

RCP seal leaks were simulated in ANO2 Cases ANO2-03 and ANO2-04. The simulation was based on the expected behavior of Byron Jackson RCP seals, which are used in the ANO2 plant.[25] Specifically, Byron Jackson pump seals are expected to leak 1.5 gpm of subcooled water per RCP at nominal operating conditions if seal cooling water is lost and an estimated maximum of 220 gpm per RCP.[29] Based on that information, a seal leak area equivalent to 1.5 gpm per RCP was introduced in Cases ANO2-03 and ANO2-04 at TMLB' accident initiation since seal cooling water is lost when AC power is lost. The appropriate leak area was established for flow of saturated liquid at nominal conditions. Seal leak areas were subsequently increased from the equivalent of 1.5 gpm per RCP to the equivalent of 220 gpm per RCP at the time saturated conditions were reached at any of the pumps, similar to the approach used in Surry RCP seal leak cases. Seal leaks of 220 gpm per RCP were assumed in both cases because the rate was the maximum that would be expected and because the rate seemed large enough to potentially influence RCP loop seal clearing. The appropriate leak area was established for flow of saturated liquid at 16.4 MPa, corresponding with the average of the opening and closing set points of the pressurizer PORVs.

ANO2 Cases ANO2-03 and ANO2-04 differed only with respect to the treatment of upper plenum steel if melting of that steel was predicted. In Case ANO2-03, it was assumed that all upper plenum steel that was predicted to melt would relocate into the lower head and quench, given an adequate liquid inventory. In Case ANO2-04, it was assumed that molten upper plenum steel would candle through the core and refreeze at some relatively cool core location without quenching.

The first RCS pressure boundary failures in ANO2 Cases ANO2-03 and ANO2-04 were predicted to be hot leg failures, instead of the surge line failures that developed in all previous ANO2 cases (see Table 5). Hot leg failures, rather than surge line failures, were predicted in Cases ANO2-03 and ANO2-04 because pressurizer PORV flow and therefore, surge line heating, was reduced as a result of flows through RCP seal leaks. Those results are similar to previously discussed results for Surry RCP seal leak analyses. However, there were some important differences between ANO2 and Surry results relative to the potential for SGTR.

SGTRs did not develop in Surry Cases SUR-08 and SUR-09 because the RCS was depressurized by RCP seal leaks. Tube differential pressures were reduced to zero in pressurizer loop SGs and tube differential pressures were transformed into compressive loads in non-pressurizer loop SGs as a result of RCS depressurization, which effectively eliminated the potential for SGTR in those cases. Similar depressurization of the RCS was predicted in ANO2 Cases ANO2-03 and ANO2-04 as a result of RCP seal leaks. However, quenching of upper plenum stainless steel and the associated pressure pertubations had a relatively large affect on the integrity of RCS piping in the ANO2 analyses. Specifically, the first RCS pressure boundary failure in Case ANO2-03 was predicted to be a hot leg failure at 18,330 s. SGTR was predicted in that case at 18,400 s, only 70 s later. That timing difference is insignificant, indicating a potential for SGTR before any other RCS pressure boundary failure for the Case ANO2-03 conditions that were analyzed. In Case ANO2-04, the absence of pressure pertubations associated with stainless steel quenching delayed hot leg failure by 3070 s. More importantly, SGTR was not predicted in Case ANO2-04 as indicated in Table 5.

Reasons for differences between ANO2 and Surry relative to stainless steel quenching and the affects of the associated pressure pertubations were not investigated. However, one possibility could be that larger quantities of steel melt in ANO2 because of upper plenum design differences relative to the Surry PWR. Larger quantities of molten steel could be expected to generate larger pressure pertubations, with a larger affect on RCS piping integrity. In any case, assuming that upper plenum stainless steel is quenched during relocation into the lower head, if melting of that steel is predicted, could be overly conservative with respect to the potential for SGTR. That is because the code conservatively assumes that all relocated material will be completely cooled to the saturation temperature of the lower head coolant during a single time step when the quenching option is activated. Heat rejected from the molten material during that process is added directly to the lower head coolant during the same time step. Furthermore, the stainless steel must candle through a tortuous path from the upper plenum all the way to the lower head without refreezing if quenching is to occur. Results indicate that temperatures near the bottom of the active fuel region (and above the lower head) can be cooler than the stainless steel melting temperature, particularly in cases with RCS depressurization that activates the accumulators, like Case ANO2-03. In such cases, the stainless steel could refreeze before reaching the lower head and thereby eliminate the potential for quenching. If quenching does occur, the results indicate a potential for SGTR in the ANO2 PWR.

It should be noted that all of the foregoing initial plant analyses were originally completed without the servo valve modeling refinement (discussed in Section 3.2) and the mixed convection code updates (discussed in Section 4.2). (Although Surry Cases SUR-03 and SUR-06 were ultimately revised using a version of SCDAP/RELAP5 with mixed convection updates as mentioned above.) Omission of the mixed convection updates is not expected to be critical because a comparison of results for the ANO2 PWR with and without the updates indicated that ex-vessel temperatures were relatively insensitive to the modification. Analyses with RCP loop seal clearing could potentially benefit by the use of the servo valve modeling refinement, which was developed after the initial plant analyses were complete. RCP loop seal clearing

was generally limited to analyses with RCP seal leaks (including two of nine Surry analyses and two of four ANO2 analyses). However, analyses with RCP loop seal clearing were not repeated using the modeling refinement to determine how results might change. Additional information regarding all initial ANO2 analyses (Cases ANO2-01 through ANO2-04) is available for further reference in a previously issued document.[30]

5.3. Plant Sensitivity Analyses

Following completion of the initial plant analyses, six sensitivity analyses for the Surry PWR (with Case SUR-06A through Case SUR-06F designations) were completed to address (1) uncertainties in heat transfer coefficients, (2) the absence of conjugate heat transfer effects in the SCDAP/RELAP5 split hot leg model (consisting of the combination of fluid-to-wall heat transfer, fluid-to-fluid heat transfer, and circumferential conduction around the hot leg pipe wall), and (3) the synergistic effects associated with simultaneous variations in Westinghouse countercurrent natural circulation parameters. These analyses were needed and specifically designed to address comments made by peer reviewers and the ACRS as discussed in Section 4.3. A summary description for each of these analyses is provided in Table 4. The table also identifies references to supporting documentation, if available.

As indicated by their designations, all plant sensitivity analyses were based on Surry Case SUR-06.[a] In fact, the analyses were extended from the onset of hot leg countercurrent natural circulation as predicted in Case SUR-06 (at 9091 s) through the time of SGTR. The period following the onset of countercurrent natural circulation was the only period of interest because there is no threat to any RCS pressure boundary prior to that time. Breaks were not introduced following any predicted pressure boundary failure in any of the calculations in order to conservatively evaluate the potential for other failures.

5.3.1. Sensitivity to Heat Transfer Coefficients

Surry Cases SUR-06A, SUR-06B, SUR-06C, and SUR-06D were designed for evaluation of the potential for a natural-circulation induced SGTR in Surry relative to uncertainties in heat transfer coefficients. In Cases SUR-06A and SUR-06B, heat transfer coefficients that could impact ex-vessel heating were altered to reasonably cover the expected range of uncertainty. Specifically, all code-calculated heat transfer coefficients in the upper plenum, hot legs, surge line, and on the inner and outer surfaces of the SG tubes were increased by 20% in Case SUR-06A and decreased by 20% in Case SUR-06B. Uncertainties in heat transfer that could be associated with entrance effects were addressed in Cases SUR-06C and SUR-06D. In Case SUR-06C, all code-calculated heat transfer coefficients in the hot leg, surge line, and SG tube entrance volumes were increased by 30%. An extreme bias of enhancing only code-calculated heat transfer coefficients in SG tube entrance volumes (by 30%) was assumed in Case SUR-06D.

a. Surry Case SUR-06, and Surry Case SUR-03, were originally completed without code updates to treat mixed convection heat transfer.[23] Both analyses were ultimately revised using a version of the code with mixed convection updates.[24] The code was modified to treat mixed convection based on peer reviewer recommendations (see Section 4.2) and the modified code was used in all analyses performed after the recommendations were made. Revisions of Cases SUR-06, and SUR-03, were completed so that comparisons with subsequent analyses could be made without concern that observed differences were related to the updates. All results presented here were taken from the revised analyses.

As heat transfer coefficients were increased, the temperature of the vapor entering the SGs decreased as shown in Figure 37. Vapor temperatures decreased because more energy was transferred from vapor to structures as heat transfer coefficients increased. As the temperature of the vapor entering the SGs decreased, SG tube temperatures decreased. Lower SG tube temperatures led to delays in predicted SGTRs. Those trends are reflected in the results listed in Table 8. Specifically, the lowest SG tube temperature (at the time of surge line failure) was predicted in Case SUR-06A, which was the transient simulating the largest increase in heat transfer. In addition, the timing difference between surge line failure and SG tube failure was larger in Case SUR-06A than in any other heat transfer coefficient sensitivity calculation. (It is worth noting that the observed vapor temperature differences were relatively small. For that reason, results presented in Figure 37 were limited to only those cases simulating the smallest and largest increases in heat transfer.)

The timing of all ex-vessel failures for Cases SUR-06A through SUR-06D (and all other plant sensitivity analyses considered) are summarized in Table 9 for reference. It is important to note that surge line failure was predicted before SGTR in all analyses. The results also indicate that pressurizer loop SG tube temperatures and differential pressures are consistently more severe than non-pressurizer loop SG tube temperatures and differential pressures. That difference, which is a result of the assumed failure of the pressurizer loop SG RV, minimizes the concern for a non-pressurizer loop SGTR relative to other potential RCS pressure boundary failures.

Results from Cases SUR-06A, SUR-06B, SUR-06C, and SUR-06D indicate that the timing of SGTR could vary by 130 s over the range of heat transfer coefficient uncertainty that was considered. Furthermore, SG tube temperatures at the time of surge line failure could vary from 938 to 964 K, a range of only 26 K. Those results would not be expected to significantly alter the potential for SGTR, indicating that heat transfer coefficient uncertainties are not important factors in this evaluation.

5.3.2. Hot Leg Conjugate Heat Transfer Sensitivity

The absence of fluid-to-fluid heat transfer and circumferential pipe wall conduction in the SCDAP/RELAP5 split hot leg model was addressed in Surry Case SUR-06E. Radiation was assumed to be the primary mechanism for fluid-to-fluid heat transfer since mixing of hot leg countercurrent flow streams was not experimentally observed. Radiation between the hot flow in the top half of the hot leg and the cooler return flow in the bottom half of the hot leg was simulated by placing a very thin heat structure (0.024 m) with a high thermal conductivity (6.23e9 W/m-K) and a low heat capacity (6.71e5 J/m^3-K) between the flow streams in each volume of each hot leg. The inside diameter of the hot leg and the length of each volume were used to establish structure heat transfer surface areas. A high convective heat transfer coefficient (2.04e6 W/m^2-K) was applied to the side of each structure in contact with the hot flow at each time step, which effectively held each structure at the temperature of the associated hot flow stream. A temperature dependent convective heat transfer coefficient equivalent to the black body radiation potential was then calculated for each structure at each time step and applied to the side of the structure in contact with the cooler flow stream. Calculated values ranged from 0 to 245.3 W/m^2-K.

Circumferential pipe wall conduction was simulated in Surry Case SUR-06E by calculating the heat that could be conducted between top and bottom halves of each section of each split hot leg pipe during each time step. The calculations were based on the volume-averaged temperatures of the pipe halves as reported by SCDAP/RELAP5. Specifically, the difference between the volume-averaged temperatures was used as the conduction driving potential and the “average” volume-averaged temperature was used to

determine the thermal conductivity of the stainless steel pipe wall. A conduction path length equal to a quarter of the wall centerline circumference was used since the volume-averaged temperatures were assumed to approximate wall temperatures half way between the top/bottom of the pipe and the intersection of the two pipe halves. Heat transfer surface areas were twice the product of the wall thickness and length of each pipe section, given that conduction will develop symmetrically on both sides of the split hot leg pipe. The calculated conduction of heat for each section of each split hot leg was then added to the bottom half and subtracted from the top half of the pipe during each time step.

The hot leg vapor ΔT (the difference between the temperature of the hot vapor in the top half of the hot leg and the temperature of the cooler vapor in the bottom half of the hot leg) in Case SUR-06E was reduced relative to Case SUR-06 as a result of fluid-to-fluid heat transfer and circumferential pipe wall conduction as indicated in Figure 38. The reduction in hot leg vapor ΔT led to a reduction in hot leg countercurrent flow and an associated reduction in the heat transferred to primary coolant loop structures. With less energy transferred to loop structures, more energy was stored in core and more energy was rejected through PORV cycling. Consequently, creep rupture failure of the pressurizer surge line in Case SUR-06E was predicted 150 s earlier than in Case SUR-06.

Vapor temperatures entering the SG tubes in Surry Case SUR-06E were also reduced as a result of the conjugate heat transfer effects in the split hot leg model. The reduced vapor temperatures entering the SG tubes resulted in lower SG tube temperatures, which delayed SGTR in Case SUR-06E relative to Case SUR-06. Specifically, the results indicate that the addition of fluid-to-fluid heat transfer and circumferential pipe wall conduction could delay SG tube failure by 280 s. Furthermore, SG tube temperatures at the time of surge line failure were 20 K cooler in Case SUR-06E than in Case SUR-06. Those results indicate that conjugate heat transfer effects in the hot leg would tend to decrease the potential for SGTR.

5.3.3. Synergistic Effects Associated with Natural Circulation Parameters

Potential synergistic effects associated with simultaneous variations in Westinghouse natural circulation parameters (i.e., mixing fractions, recirculation ratios, and the fraction of SG tubes that participate in hot [forward] flow during countercurrent natural circulation) were addressed in Surry Case SUR-06F. Specifically, Case SUR-06F was completed using 5% confidence values for the natural circulation parameters, which were calculated assuming a normal distribution of the Westinghouse high pressure transient data and conservatively assuming that the parameters are independent of each other (resulting in mixing fractions of 0.73, a recirculation ratio of 1.8, and 43% of the SG tubes participating in hot [forward] flow). Note that the calculated 5% confidence values, which correspond to parameter values that should be smaller than 95% of all values, are believed to conservatively represent the tail of the assumed distribution because each parameter was calculated independently without any allowance for relationships with the other parameters and all values were lower than any actually observed during the transient experiments.

Results indicate that SG tube temperatures at the time of surge line failure in Case SUR-06F were ~50 K higher than in Case SUR-06. Those results are consistent with the stand alone loop sensitivity analyses where SG tube temperatures were found to increase when mixing fractions are decreased, recirculation is increased, or the fraction of SG tubes participating in hot (forward) flow is decreased. Two of three parameter differences between Cases SUR-06F and SUR-06 support the prediction of higher temperatures in Case SUR-06F. Furthermore, the predicted temperature increase (relative to temperature differences observed in the stand alone loop analyses) indicates that simultaneous variations in natural circulation parameters do not disproportionately impact SG tube heating.

Results listed in Table 9 also indicate that the synergistic effects associated with simultaneous variations in natural circulation parameters could accelerate SGTR by 430 s relative to the timing of SGTR in Surry Case SUR-06. It is important to note, however, that use of the calculated 5% confidence values (which correspond to parameter values that should be smaller than 95% of all values) is believed to conservatively represent the tail of the assumed distribution because each value was calculated independently without any allowance for relationships with the other parameters and all values were lower than any actually observed during the transient experiments. Nevertheless, surge line failure in Case SUR-06F was still predicted some 800 s prior to SGTR. Given that prediction of surge line failure, the potential for SGTR relative to simultaneous variations in natural circulation parameters is still low.

It should be noted that all of the plant sensitivity analyses described above were completed with SCDAP/RELAP5 mixed convection updates, but without the servo valve modeling refinement. Absence of the servo valve refinement did not appear to be critical because the potential for full-loop circulation was expected to be low and the duration of full-loop circulation, if it developed at all, was not expected to be prolonged. Additional information regarding Case SUR-06F and all other plant sensitivity analyses is available for reference in a previously issued document.[24]

5.4. Plant RCS Depressurization Analyses

Results from the initial plant analyses that were completed during the earliest phase of this evaluation indicated that a potential for failure of (defect-free) SG tubes does not exist during TMLB' accidents without SG secondary depressurization (see Section 5.2). That is because SG tube heating is not severe enough to produce SGTR when tube differential pressures are limited by maintenance of secondary pressures. Consequently, all subsequent analyses focused on variations of TMLB' accidents with SG secondary depressurization in order to determine how other conditions could affect the SGTR potential. After a comprehensive set of analyses with SG secondary depressurization were completed (see Section 5.3), RCS depressurization was proposed as an approach that might be used to reduce any SGTR potential by minimizing the tube differential pressure.

The RCS of a PWR can be depressurized if there is a leak in the pressure boundary (i.e., through RCP seals, through pressure boundary failures that initiate an accident, through pressure boundary failures that develop as a result of accident-related natural circulation heating), if the pressurizer PORVs fail open (or partially open), or if plant operators intentionally open the pressurizer PORVs. In this evaluation, it was assumed that operators would open pressurizer PORVs in all RCS depressurization analyses. Although "intentional" RCS depressurization through the PORVs will reduce the tube differential pressure, this part of the evaluation was needed to determine if RCS depressurization will lead to RCP loop seal clearing. If RCP loop seals clear, full-loop natural circulation could be established, which could increase SG tube temperatures and the potential for SGTR, in spite of any differential pressure reduction.

It was assumed that operators would open pressurizer PORVs in all SCDAP/RELAP5 RCS depressurization analyses completed during this evaluation when the core exit temperature reached 922 K. An exit temperature of 922 K indicates that the core is in the process of uncovering and that core damage is imminent. Opening pressurizer PORVs at that temperature is also consistent with the recommendations of an earlier study of intentional RCS depressurization.[31]

Analyses for operating PWRs with pressurizer PORVs (represented by the Surry, Zion, Calvert Cliffs, and Oconee plants) were completed to cover intentional RCS depressurization, intentional RCS depressur-

ization with RCP seal leaks, and intentional RCS depressurization where bypass flow paths from the downcomer to the hot leg were blocked. In addition, analyses for operating PWRs with U-tube SGs (represented by the Surry, Zion, and Calvert Cliffs plants) were completed to cover intentional RCS depressurization with the accumulation of sludge on top of SG tube sheets. (Sludge accumulation in PWRs with once-through SGs was not considered.) As indicated in Table 4, all RCS depressurization analyses were completed using the servo valve modeling refinement and SCDAP/RELAP5 mixed convection updates. Details associated with all RCS depressurization analyses are outlined below.

5.4.1. RCS Depressurization

As indicated in Table 4, analyses designed to address the potential for SGTR in operating PWRs during TMLB' accidents with intentional RCS depressurization include Surry Case SUR-20, Zion Case ZI-01, Calvert Cliffs Case CC-01, and Oconee Case OC-01. Those analyses were also completed to provide a basis for the SGTR potential relative to all other RCS depressurization analyses.

SCDAP/RELAP5 results indicate that RCP loop seal clearing will occur in PWRs with U-tube SGs when the RCS is depressurized through pressurizer PORVs. Furthermore, SG tube temperatures will significantly increase as a result of full-loop natural circulation heating following RCP loop seal clearing. The SG tube temperature increase associated with full-loop circulation shown for Zion Case ZI-01 in Figure 39 is typical. However, SGTR was not predicted for any operating PWR with U-tube SGs and intentional RCS depressurization as indicated in Table 10. SGTR did not occur because SG tube heating was not high enough to result in failure in the absence of any tube differential pressure.

RCP loop seal clearing was not predicted for the Oconee PWR with once-through SGs. Consequently, all SG tube temperatures remained relatively cool because full-loop natural circulation did not develop and once-through SGs tubes do not participate in countercurrent circulation. Basic geometric configurations of the Oconee PWR (i.e., the size, shape, and the relative elevations) appeared to be the most important factors in the retention of RCP loop liquids.

Results listed in Table 10 indicate that the first RCS pressure boundary failure in operating PWRs with intentional RCS depressurization will occur in the surge line. Hot leg failures were also predicted in all analyses, given that breaks were not introduced following predicted surge line failures. The results also indicate that pressurizer loop SG tube temperatures and differential pressures are consistently more severe than non-pressurizer loop SG tube temperatures and differential pressures because of the assumed PORV failure in the pressurizer loop SG. However, SGTR was not predicted in any calculation, indicating that the potential for SGTR is low when the RCS is depressurized through pressurizer PORVs. Additional information regarding analyses with intentional RCS depressurization is available for reference in a previously issued document.[32]

5.4.2. RCS Depressurization with RCP Seal Leaks

Intentional depressurization of the RCS through pressurizer PORVs was augmented by depressurization associated with RCP seal leaks in a second series of analyses for the Surry, Zion, Calvert Cliffs, and Oconee plants. RCP seal leak rates that were considered for those PWRs are discussed below.

Surry and Zion plants, like all other Westinghouse PWRs, use Westinghouse RCPs.[25] Westinghouse pump seals are expected to leak 21 gpm of subcooled water per RCP at nominal operating conditions if

seal cooling water is lost.[26] Since seal cooling water is lost when AC power is lost, a seal leak area equivalent to 21 gpm per RCP was introduced in all Surry and Zion analyses with RCP leaks at TMLB' accident initiation. Subsequent seal degradation and failure is expected as a TMLB' accident progresses because the seals are not designed for exposure to high temperature steam. The seals are particularly vulnerable to failure when fluid in the RCP reaches a saturated condition because seal faces tend to pop open as a result of two-phase flow instabilities. Although a specific leak rate is difficult to predict given possible variations in seal failure, a panel of experts concluded that 250 gpm per RCP is the most likely leak rate from Westinghouse pumps during a TMLB' accident.[27] Based on that information, a decision was made to evaluate seal leaks of 125 and 250 gpm per RCP. That approach encompassed best-estimate leakage and a plausible intermediate value. Areas for both leak rates were established assuming flow of saturated liquid at 16.0 MPa, corresponding with the average of the opening and closing set points of the pressurizer PORVs. Consistent with the foregoing, the seal leak areas were appropriately increased from the equivalent of 21 gpm per RCP to the equivalent of either 125 or 250 gpm per RCP at the time saturated conditions were reached at any of the pumps. As indicated in Table 4, leaks that increase to 125 and 250 gpm per RCP were evaluated in Surry Cases SUR-21 and SUR-22, respectively, and in Zion Cases ZI-02 and ZI-03, respectively.[a]

The Calvert Cliffs plant, like all Combustion Engineering PWRs other than the Palo Verde plants, uses Byron Jackson RCPs.[25] (Klein, Schanzlin, & Becker RCPs are used in Palo Verde 1, 2, and 3.[25]) Byron Jackson pump seals are expected to leak 1.5 gpm of subcooled water per RCP at nominal operating conditions if seal cooling water is lost and an estimated maximum of 220 gpm per RCP.[29] Based on that information, a decision was made to evaluate seal leaks of 110 and 220 gpm per RCP. That approach encompassed the maximum leakage and a plausible intermediate value. Areas for both leak rates were established assuming flow of saturated liquid at 16.4 MPa, corresponding with the average of the opening and closing set points of the pressurizer PORVs. Since seal cooling water is lost when AC power is lost, a seal leak area equivalent to 1.5 gpm per RCP was introduced in all Calvert Cliffs analyses with RCP seal leaks at TMLB' accident initiation. Like the treatment for Surry and Zion, seal leak areas were then appropriately increased from the equivalent of 1.5 gpm per RCP to the equivalent of either 110 or 220 gpm per RCP at the time saturated conditions were reached at any of the pumps. As indicated in Table 4, leaks that increase to 110 and 220 gpm per RCP were evaluated in Calvert Cliffs Cases CC-02 and CC-03, respectively. (Because information was not available, potential seal leaks from Klein, Schanzlin, & Becker RCPs were not specifically considered.)

Three different RCPs are used in Babcock and Wilcox PWRs including Westinghouse RCPs in Oconee 1 and Three Mile Island 1; Byron Jackson RCPs in Arkansas Nuclear One 1, Crystal River 3, and Davis Besse; and Bingham International RCPs in Oconee 2 and 3.[25] Information on Bingham International

a. It should be noted that the need for a modeling improvement in the Zion surge line/hot leg nodalization was identified after Zion Cases ZI-02 and ZI-03 were underway. The need for an improvement became apparent because the surge line was not heating as quickly as expected. It was determined that surge line heatup was delayed because flows into the surge line from the bottom and top halves of the split hot leg were not balanced. The flow imbalance indicated that the flow resistance from the bottom half of the split hot leg to the surge line was not equal to the flow resistance from the top half of the split hot leg to the surge line. After some assessment, it was determined that the flow balance could be improved by moving Valve 156 from the lower half of the split hot leg to the surge line outlet as indicated in Figure 40. Results from scoping calculations performed with that modeling change indicated improvement in the flow balance. Accordingly, Cases ZI-02 and ZI-03, as well as all other remaining Zion analyses, were completed using the improved nodalization.

RCP leakage was not available. Without that information, a decision was made to evaluate the potential for SGTR in the Oconee plant using Westinghouse RCP leaks of 125 and 250 gpm per RCP as discussed above for Surry and Zion. That approach was taken because the Westinghouse leaks encompass the Byron Jackson leaks. As indicated in Table 4, leaks that increase from 21 gpm per RCP to 125 and 250 gpm per RCP were evaluated in Oconee Cases OC-02 and OC-03, respectively.

Results in RCS depressurization analyses with and without RCP seal leaks were quite similar. Most notably, surge line failure was always predicted before any other RCS pressure boundary failure and SGTR did not develop in any calculation as indicated in Tables 10 and 11. The most significant differences that were observed were related to RCP loop seal clearing. Specifically, loop seals cleared in all analyses with RCP seal leaks while loop seal clearing was limited to PWRs with U-tube SGs in analyses without RCP seal leaks. Boiling as steam passed from the SGs to the RCP seal leaks was apparently needed in order to clear RCP loop seals in PWRs with once-through SGs. Although tube temperatures increased in all analyses as a result of RCP loop seal clearing and the associated development of full-loop natural circulation, SGTR did not occur because heating was not severe enough to cause failure in the absence of tube differential pressure. Consequently, the potential for SGTR is low when RCS depressurization is augmented with depressurization through RCP seal leaks. Additional information regarding analyses with intentional RCS depressurization and RCP seal leaks is available for reference in a previously issued document.[33]

5.4.3. RCS Depressurization without Downcomer-Hot Leg Bypass Flows

As indicated in Table 4, analyses designed to address the effects of downcomer-hot leg (DC-HL) bypass flows with respect to the potential for SGTR during TMLB' accidents with intentional RCS depressurization include Surry Case SUR-23, Zion Case ZI-04, Calvert Cliffs Case CC-04, and Oconee Case OC-04. DC-HL bypass flows are associated with small gaps between hot leg nozzles (which are welded to the reactor vessel) and hot leg piping inside the vessel (which is welded to the core barrel). Those gaps are designed to facilitate installation and removal of vessel internals. During normal operation, RCPs drive cold leg flows into the downcomer at pressures greater than pressures in the hot legs. Consequently, some of the downcomer flow can bypass the core by flowing through the gaps directly into the hot legs as shown in Figure 41. (DC-HL bypass flows are normally no more than about 1% of total primary flow.) In this evaluation, it was conservatively assumed that all DC-HL bypass flows were reduced to zero by thermal expansion at the time superheated vapor reaches the core exit in each of the specified analyses. Pertinent results were then compared to results from analyses with unaltered DC-HL bypass flows. That comparison was used to determine the effects of DC-HL bypass flows on natural circulation heating of the SG tubes and the potential for SGTR.

Thermal expansion may reduce DC-HL bypass flows because the core and core barrel could heat up and expand faster than the more massive reactor vessel wall. Reducing all DC-HL bypass flows to zero at the time superheated vapor reaches the core exit provides a uniform criteria for eliminating DC-HL bypass flows and is conservative relative to the potential impact in two respects. First, that approach neglects the possibility for non-symmetric heating. And second, thermal expansion at the time superheated vapor reaches the core exit would probably not be sufficient to completely close the hot leg gaps. Consequently, the effects of DC-HL bypass flows on natural circulation heating of the SG tubes and the potential for SGTR that may develop in operating PWRs should not exceed the effects described here. Specific flows that were eliminated include the Surry DC-HL bypass (connecting Volume 102 to Volume 172 in Figure 3), the Zion DC-HL bypass (connecting Volume 502 to Volume 582 in Figure 7), the Calvert Cliffs

DC-HL bypass (connecting Volume 502 to Volume 535 in Figure 10), and the Oconee DC-HL bypass (connecting Volume 565 to Volume 545 in Figure 16).

SCDAP/RELAP5 results indicate that accumulators will empty quicker and RCP loop seals will clear more readily when DC-HL bypass flow paths are blocked. Accumulators emptied quicker because downcomer pressurization during the steam production phase of accumulator injection was slower without DC-HL bypass flows. Consequently, downcomer (and cold leg) pressures remained below accumulator pressures for longer periods of time, allowing accumulators to empty quicker. Temperatures were cooler overall as a result, which tended to delay RCS pressure boundary failures as indicated in Table 12.

During the initial phase of accumulator injection, cold leg condensation can reduce pressures downstream of the RCP loop seal, which can "pull" water out of the loop seal. In-core boiling near the end of a given injection can increase pressures upstream of the RCP loop seal, which can "push" water out of the loop seal. When DC-HL bypass flow paths are blocked, there is a greater tendency to both "pull" and "push" water out of the RCP loop seals, allowing loop seals to clear more readily. That tendency was not as important for the Oconee PWR because Oconee is the only plant in this evaluation with upper head vent valves. Those valves are large compared to the DC-HL bypass and they can effectively equalize upper plenum pressures with pressures in the downcomer in the absence of DC-HL bypass flows.

Other important results with and without DC-HL bypass flows were similar despite differences in accumulator response and RCP loop seal behavior. Notably, surge line failure was predicted before any other RCS pressure boundary failure with one exception[a], and SGTR did not develop in any calculation as indicated in Table 12. On that basis, it appears that the DC-HL bypass does not adversely impact the potential for SGTR. Additional information regarding the DC-HL bypass evaluation is available for reference in a previously issued document.[34]

5.4.4. RCS Depressurization with SG Sludge Accumulation

Sludge can collect on top of tube sheets on the secondary sides of U-tube SGs. The impact of accumulated sludge on the potential for SGTR in operating PWRs with U-tube SGs was addressed in the final series of RCS depressurization analyses. (Sludge accumulation in once-through SGs was not considered.) The sludge, which primarily consists of a mixture of copper and iron particles, was assumed to be 12 in. deep in all affected analyses. The potential for SGTR could be impacted because relatively high tube temperatures could develop in regions adjacent to the sludge where heat transfer to secondary fluids could be reduced.

The conventional SCDAP/RELAP5 SG nodalization provides only one heat structure representing several feet of tube above the tube sheet as shown in Figure 42(a). Convective boundary conditions for that tube heat structure were defined by single hydrodynamic volumes on either side; one representing RCS fluid and one representing secondary fluid. Direct simulation of tube wall temperatures adjacent to any accumulated sludge is not possible with that nodalization. Refined SG nodalization for operating PWRs

a. The pressure boundary failure exception occurred in Calvert Cliffs Case CC-04, where the hot leg was predicted to fail before the surge line. Although it was not verified, the delay in surge line failure is believed to be an artifact of the surge line/hot leg nodalization. An earlier surge line failure would be expected if the nodalization was modified to balance flows into the surge line from top and bottom halves of the split hot leg as discussed in Section 5.5.

with U-tube SGs (represented by the Surry, Zion, and Calvert Cliffs plants) was therefore necessary as outlined below.

Refined SG nodalization included the addition of a 12 in. sludge layer and division of the single RCS hydraulic volume to provide separate RCS volumes adjacent to the tube sheet, the sludge, and the remaining section of the SG tubes as shown in Figure 42(b). The refined nodalization was applied to inlet and outlet sides of both hot and cold tube bundles in all SGs in each of the representative plants. Specifically, the conventional Surry nodalization for the coolant loop containing the pressurizer is shown in Figure 5. SG hydrodynamic volumes 408-01, 408-08, 409-01, and 409-08 are analogous to the single RCS volume shown in Figure 42(a). Each of those Surry hydrodynamic volumes were divided into three smaller volumes consistent with the refined nodalization shown in Figure 42(b). Thus, eight volumes were added to each Surry SG. Similarly, the conventional Zion nodalization for the pressurizer loop is shown in Figure 9. Hydrodynamic volumes 110-01, 110-08, 111-01, and 111-08 are analogous to the single RCS volume shown in Figure 42(a). Each of the hydrodynamic volumes were divided into three smaller volumes consistent with the refined nodalization shown in Figure 42(b), adding eight volumes to each Zion SG. And finally, the conventional Calvert Cliffs nodalization is shown in Figure 12. Pressurizer loop volumes 125-01, 125-09, 126-01, and 126-09 and non-pressurizer loop volumes 225-01, 225-09, 226-01, and 226-09 are analogous to those shown in Figure 42(a). Each of those volumes were divided into three smaller volumes consistent with the nodalization shown in Figure 42(b).

The refined SG nodalization shown in Figure 42(b) was introduced into Surry, Zion, and Calvert Cliffs models when core exit temperatures reached superheated conditions. (Prior to that time, the presence or absence of sludge was not important because SG tube heating was insignificant.) The corresponding analyses, designated Surry Case SUR-25, Zion Case ZI-06, and Calvert Cliffs Case CC-06 as indicated in Table 4, were then extended with the assumed sludge accumulation. Separate analyses, designated Surry Case SUR-24, Zion Case ZI-05, and Calvert Cliffs Case CC-05, were also completed without sludge using the refined nodalization shown in Figure 42(c). A comparison of results was then possible to determine the effects of sludge on natural circulation heating of the SG tubes and the potential for SGTR in operating PWRs.

Thermal properties of the sludge had to be estimated for use in this evaluation. The estimates were based on samples of sludge that have been collected and analyzed for several different nuclear power plants.[35,36] In all plants, the sludge was found to consist primarily of particles of copper and iron with trace amounts of several other elements. It was assumed that the sludge analysis for Indian Point III was adequate for representing sludge in this evaluation. The corresponding constituents that account for more than one percent, by weight, of the Indian Point III sample are listed in Table 13. That composition was used to estimate sludge thermal properties as outlined below.

Sludge thermal conductivity was calculated assuming that heat transfer occurred through each of the constituents in parallel. Resistance to heat conduction due to imperfect contact between particles was neglected. Density as a function of temperature was not readily available, so room temperature densities were used.[37] (Those densities and the mass fraction data indicate a void fraction of 83 percent, which differs from the reported value of 71 percent.[35] This is a relatively small discrepancy considering that open literature,[38,39] rather than test data, was used to determine the sludge density. It does, however, indicate some level of uncertainty in the estimated thermal properties of the sludge.) Heat capacity of the sludge was assumed to be the mass-weighted average heat capacity of each of the constituents. Sludge samples were collected and analyzed wet. That is, reported mass fractions reflected the presence of water in the sludge. Since the SGs are expected to be dry during the entire period of interest in the current evaluation,

the volume occupied by water was replaced with an equivalent volume of steam and the thermal properties of steam were used when estimating the properties of the sludge. It should be noted that copper, a major constituent of the sludge, melts at the relatively low temperature of 1356 K. The potential for that phase change was neglected. It was assumed that sufficient heat transfer capability was available from the sludge to the tube sheet and the secondary steam that the copper would remain solid throughout most of the sludge (although heat transfer from the sludge to the tube sheet and secondary steam were not actually modeled with SCDAP/RELAP5.) Therefore, for sludge temperatures above 1356 K, the thermal properties of copper were assumed to be those for solid copper at 1356 K. The estimated sludge properties based on the foregoing and used in the SCDAP/RELAP5 analyses are listed in Table 14.

SG tube temperatures in the region just above the tube sheet were hotter with sludge than without. Temperatures with and without accumulated sludge as shown for the Surry PWR in Figure 43 are typical. Higher temperatures occur because sludge retards heat transfer from the SG tube wall. Higher SG tube temperatures led to predictions of SGTRs in both Surry and Zion PWRs. SGTR was not predicted in the Calvert Cliffs calculation, although creep damage with sludge was found to be significantly higher than damage without sludge as indicated in Figure 44. Those results differ from results associated with all other RCS depressurization analyses that were considered in that SGTR was predicted only in cases with sludge. However, the results are also similar to results from all other RCS depressurization analyses in that surge line failure was predicted before any other failure as indicated in Table 15. The table also indicates that the minimum margin between the time of surge line failure and the time of SGTR is ~1 h. Given that margin, the potential for SGTR in PWRs with U-tube SGs as a result of sludge accumulation is low. Additional information regarding analyses with intentional RCS depressurization and SG sludge accumulation is available for reference in a previously issued document.[40]

5.5. Plant Nodalization Sensitivity Analyses

Nodalization sensitivity analyses were needed in the latter stages of this evaluation to address two issues that were identified through a review of results associated with the plant analyses described in Sections 5.2 through 5.4. The first issue arose because relatively large RCS pressure spikes were typically predicted following initial accumulator injections and there was a concern that the magnitude of those spikes could be related to reactor core axial nodalizations. A reasonable prediction of those pressure spikes is of interest because the integrity of RCS pressure boundaries could be affected. The second issue arose because there was an unexpected disparity in the predicted timing of surge line failures in the Calvert Cliffs PWR. There was a concern that the disparity was a function of the nodalization used to connect the surge line to the hot leg. (All of the following sensitivity analyses were completed with the servo valve modeling refinement and SCDAP/RELAP5 mixed convection updates as outlined in Table 4.)

5.5.1. Core Axial Nodalization Sensitivity

With respect to the core axial nodalization issue, some RCS pressure increase is expected as a result of boiling when cold accumulator water is injected into a hot reactor core. Simulation of that process using SCDAP/RELAP5, however, is affected by the fact that the code does not provide a core temperature continuum. Instead, average temperatures are calculated to represent each discrete region, or node, in the core. (Nodal averages are also calculated for all other thermal and thermal-hydraulic conditions.) In this evaluation, each PWR core was normally divided into 5 radial rings with 10 axial elevations, yielding a total of 50 core nodes per plant (see Figures 3, 7, 10, 13, and 16).

When the RCS pressure drops below accumulator pressure, accumulator injection begins and liquid levels start to rise into hot regions of the core. Injection continues until the RCS pressure increases above accumulator pressure as a result of boiling (or until accumulator inventory is depleted). Since boiling and any associated pressure increase calculated by the code is dependent on nodal temperatures, it would appear that refined core nodalization could improve temperature predictions, which could lead to refined pressure predictions. A Calvert Cliffs calculation, designated Case CC-02CN, was completed to evaluate that possibility. As indicated in Table 4, Calvert Cliffs Case CC-02CN was identical to Case CC-02 with the exception of core axial nodalization. Specifically, the 10 axial node configuration used in Case CC-02 was replaced with a 20 axial node configuration in Case CC-02CN as shown in Figure 45. (Current SCDAP dimension statements limit the number of core axial nodes to 20.) The refinement in nodalization focused on the region originally defined by axial nodes 2 through 7 as illustrated. That approach was taken because Case CC-02 results indicated that the bulk of in-core boiling occurred in that region. A comparison of results from the two analyses was expected to provide some indication of how pressure spikes might be affected by core nodalization.

RCS pressures in the Calvert Cliffs PWR using core models with 10 and 20 axial nodes are shown in Figure 46. As indicated, the pressures were quite similar until the first accumulator injections occurred (just after 11,500 s). At that time, large pressure spikes were predicted in both analyses. However, accumulator injection started somewhat earlier, the peak pressure that was reached was somewhat lower, and the duration of spike was somewhat longer in Case CC-02CN (with 20 axial nodes) than in Case CC-02 (with 10 axial nodes).

Accumulator injection started earlier in Calvert Cliffs Case CC-02CN as shown in Figure 47 because the RCS pressure dropped to the initial accumulator pressure relatively quickly. The drop to the initial accumulator pressure was relatively quick because vapor discharged through the pressurizer PORV in Case CC-02CN was hotter than vapor discharged in Case CC-02 as indicated in Figure 48. The depressurization rate is a function of the energy dissipated through the PORV, which is a function of the vapor temperature. Vapor temperatures in Case CC-02CN were hotter than those in Case CC-02 because oxidation began earlier as shown in Figure 49. Oxidation began earlier in Case CC-02CN because the core axial power profile was refined when the core nodalization was refined. The peak to average power density in Case CC-02CN was almost 2% higher than in Case CC-02 as a result of the refinement. Early oxidation in Case CC-02CN was apparently driven by that power difference.

The peak pressure that was reached was somewhat lower and the volume of injected accumulator water was larger in Calvert Cliffs Case CC-02CN than in Case CC-02 because PORV vapor temperatures, and the corresponding rates of energy dissipation, were higher in Case CC-02CN. The duration of the Case CC-02CN pressure spike was relatively long because more water was injected in Case CC-02CN. With more water in the core, depressurization of the RCS in Case CC-02CN was extended by the time required to boil the additional water and vent the additional vapor.

The foregoing results indicate that refined core axial nodalization, as tested, had a relatively minor impact on RCS pressure spikes associated with the initial accumulator injection. When the core axial nodalization was increased, a somewhat lower peak pressure was reached and some extension of the pressure spike was predicted. However, those pressure differences are relatively minor and they would not be expected to significantly alter creep damage of any RCS pressure boundary. Furthermore, the effects that were observed were primarily due to refinement in the core axial power profile that was adopted for consistency with the refined core nodalization. Any effects associated with the refined power profile could have been minimized by retaining a constant (flat) power density for all subdivisions of a given node.

Although that would produce a stepped approximation of the power profile, a better evaluation of the separate effects of axial nodalization might have been achieved. It is believed that differences in RCS pressure spikes, however, would be bounded by the foregoing results if such analyses were completed.

5.5.2. Surge Line/Hot Leg Nodalization Sensitivity

As previously indicated, analyses were also needed to evaluate an unexpected disparity in the predicted timing of surge line failures in the Calvert Cliffs PWR relative to the surge line/hot leg nodalization. Specifically, Calvert Cliffs Cases CC-01 and CC-05 differed only with respect to SG nodalization and surge line/hot leg nodalization as indicated in Table 4. The timing of surge line failure should not have been affected by either difference. However, surge line failures in Cases CC-01 and CC-05 were predicted at 22,000 and 16,230 s, respectively (see Section 5.4). That unexpected disparity required further evaluation of the differences between the analyses.

The difference in SG nodalization introduced in Calvert Cliffs Case CC-05 was needed so that results without sludge accumulation could be directly compared to Case CC-06 results with sludge accumulation as discussed in Section 5.4. The new nodalization basically involved splitting SG inlet and outlet volumes to provide a dedicated region for the potential accumulation of sludge on top of the tube sheet (see Figure 42). Splitting SG volumes for that purpose should not affect the surge line heatup in any way. Scoping calculations verified that the timing of surge line failure was unaffected by that change in SG nodalization.

The difference in surge line/hot leg nodalization was introduced in Calvert Cliffs Case CC-05 only to maintain consistency among plant models. As discussed in Section 5.4, an improvement was needed in modeling the hot leg to surge line connection for the Zion PWR. The improvement involved moving Valve 156 from the lower half of the split hot leg to the surge line outlet as indicated in Figure 40. That change was necessary so that the appropriate flow balance into the surge line could be obtained with application of the abrupt area change option specified in the figure. A flow balance problem did not appear to exist in the Calvert Cliffs model because the smooth area change option was used. Nevertheless, Valve 603 was moved from the lower half of the split hot leg to the surge line outlet as indicated in Figure 50 for consistency. That modification did not seem necessary, but it was assumed to be acceptable because the configurations were expected to be equivalent. However, results from scoping calculations indicated that surge line heating was affected by the surge line/hot leg nodalization. At that point, two formal analyses were performed as described below to complete the evaluation.

The first Calvert Cliffs calculation, designated Case CC-07, was identical to Case CC-05 as indicated in Table 4 except that countercurrent natural circulation behavior was re-benchmarked. Re-benchmarking was completed to eliminate the possibility that surge line heating was affected because natural circulation had been altered by changes in nodalization. Re-benchmarking was performed for the conditions assumed in Case CC-05 (and Case CC-01). Specifically, a hot/cold SG tube split of 53%/47%, a mixing fraction of 0.87, and a recirculation ratio of 1.9 were assumed. The second calculation, designated Case CC-07OSL, was identical to Case CC-07 except that the original surge line/hot leg nodalization (like Case CC-01) was used. A comparison of results from Cases CC-01, CC-05, CC-07, and CC-07OSL was expected to provide some indication of how the timing of surge line failure might be affected by the surge line/hot leg nodalization.

Surge line failure times for Calvert Cliffs Cases CC-01, CC-05, CC-07, and CC-07OSL are listed in Table 16. As indicated, the predicted timing of surge line failure was essentially the same in Cases CC-01 and CC-07OSL (at ~22,000 s) and in Cases CC-05 and CC-07 (at ~16,300 s). Two issues can be resolved based on those results. First, differences in SG nodalization introduced to accommodate sludge accumulation do not affect surge line heatup and failure. That was verified because surge line failures were predicted at the same time in Cases CC-07OSL and CC-01 even though those analyses were completed with and without SG nodalization changes, respectively. Second, differences in surge line/hot leg nodalization were the cause of differences in the timing of surge line failures. That was verified because surge line failure times differed in Cases CC-07 and CC-07OSL, which were completed with and without modified surge line/hot leg nodalizations, respectively. Those results indicate a need for careful attention to the simulation of the surge line/hot leg connection, primarily in cases with intentional RCS depressurization through open pressurizer PORVs.

6. UNCERTAINTIES

Uncertainties can be grouped into those that arise because of current limitations in the simulation of severe reactor accidents, those that arise in relation to the specific sequence being considered, and those introduced through modeling approximations. Uncertainties associated with current limitations in severe accident simulation arise because experimental data addressing all pertinent phenomena are not complete or do not exist and because resources are not always available to develop computer models when data does exist. The prediction of everything from core heatup and oxidation through core degradation, melting, and relocation are affected to varying degrees. In this evaluation, however, such uncertainties are probably not significant because the analyses were generally extended only through the early phase of core damage (covering core heatup and oxidation). It is generally acknowledged within the technical community that severe accident behavior is relatively well characterized by SCDAP/RELAP5 during that phase.

Uncertainties associated with the TMLB' accident are primarily related to the simulation of countercurrent natural circulation. To help evaluate those uncertainties, stand alone loop analyses were completed to determine changes in SG U-tube temperatures that could occur with changes in parameters that characterize countercurrent natural circulation (including the number of tubes participating in hot [forward] flow, mixing fractions, and the recirculation ratio). In those analyses, one parameter was varied over the range of experimentally observed values while other parameters and conditions remained constant. Changes in the hottest tube temperatures near the time of surge line failure were calculated to be ~26 K, or less. A calculation was also completed for the Surry PWR where all parameters characterizing countercurrent natural circulation were simultaneously set at 5% confidence values (corresponding to parameter values that should be smaller than 95% of all values) to determine if synergistic effects were more important. In that calculation, SG tubes were predicted to be ~50 K hotter at the time of surge line failure than they were in base analyses. Those results (covering individual and simultaneous changes in parameters) indicate that uncertainties associated with simulation of countercurrent natural circulation in TMLB' accidents did not significantly affect SG tube temperatures in this evaluation.

Sensitivity analyses were not completed to evaluate uncertainties associated with countercurrent natural circulation behavior in PWRs with once-through SGs. This is not believed to be critical because all once-through SGs analyses included the assumption that pressurizer PORVs would be latched open. Surge line heatup and failure was primarily driven by the resulting high temperature flows through the surge line

to open PORVs, and those conditions would not have been significantly altered by variations in natural circulation behavior.

Uncertainties in the fraction of core decay energy absorbed in each SG as a result of countercurrent natural circulation were not specifically addressed. However, natural circulation flows and/or temperatures would have to increase in order to increase the fraction of energy absorbed. As flows and/or temperatures increase, all RCS piping temperatures, including surge line, hot leg, and SG tube temperatures, would be expected to increase. Therefore, the absolute timing of pressure boundary failures may shift, but a significant difference in the relative timing between surge line and SG tube failures would not be expected. On that basis, further evaluation of the fraction of core decay energy that is absorbed in each SG appears to be unnecessary.

Uncertainties associated with modeling approximations include an under-estimation of the hot leg-to-surge line resistance, potential servo valve logic problems in switching from hot leg countercurrent natural circulation to full-loop circulation, and limitations associated with the lack of natural circulation data for benchmarking models. Underestimation of the hot leg-to-surge line resistance primarily occurred in cases where pressurizer PORVs were latched open. All SCDAP/RELAP5 models used two valves to connect upper and lower halves of the split hot leg to the surge line. The surge line flow area was assigned to each valve. Under most conditions, only one of the two valves would be open at any given time. However, both valves were configured to open when the PORV opened. That approach was judged to be adequate as long the transient involved normal, cyclic PORV operation. However, modeling logic simply opened both valves when the PORV opened without distinguishing between cases with cyclic PORV operation and cases where PORVs were latched open. In cases with sustained PORV flows, the valves should have been opened half way to avoid under-estimation of the hot leg-to-surge line resistance. Since the hot leg-to-surge line resistance was underestimated in cases where PORVs were latched open, flow and heat transfer could have been overestimated, which could lead to a premature prediction of surge line failure. This modeling problem is believed to be a secondary concern, however, because flow from the hot leg to the surge line is generally controlled by choked flow through the open PORV.

The servo valve refinement (discussed in Section 3.2) included logic for switching from hot leg countercurrent natural circulation to full-loop natural circulation based on RCP loop seal liquid levels. That approach appeared to be adequate, given the time available for model development and testing. However, the logic could have been improved if the direction of flows and vessel liquid levels were also checked before allowing transition to full-loop natural circulation loss coefficients. Uncertainties introduced through this modeling simplification are unknown, although the potential for full-loop circulation was basically limited to those analyses where pressurizer PORVs were latched open (the plant RCS depressurization analyses). Significant SG tube heating was predicted in those analyses following the onset of full-loop circulation, although the increased heating did not result in SGTR because SG tube pressure differentials were near zero as a result of RCS and SG secondary depressurization. Improvements in the servo valve switching logic would not be expected to substantially increase the potential for SGTR under those conditions.

Experimental data were used to benchmark hot leg countercurrent natural circulation modeling in PWRs with both U-tube and once-through SGs. Unfortunately, data were not available for benchmarking in-vessel or full-loop natural circulation in either configuration. However, all models were benchmarked against available data at normal, full-power, steady-state conditions, which provides a way to ensure that flows and pressure losses through the vessel and around the RCS piping are appropriate for subcooled liquid flow. The established loss coefficients were subsequently applied, without modification, in the simula-

tion of in-vessel and full-loop natural circulation. (Loss coefficients were only altered during periods of hot leg countercurrent natural circulation based on benchmarking for those particular conditions.) While that approach may not be completely satisfactory, it is a standard modeling procedure when data for specific conditions is not available. Furthermore, the resulting loss coefficients are expected to be reasonable because natural circulation flows are generally turbulent,[21] which minimizes velocity-dependencies that can exist in certain geometries. Therefore, a reasonable simulation of in-vessel and full-loop natural circulation is expected, with the possible exception of surge line modeling.

Surge line flows are generally stagnant during normal, full-power, steady-state operations. As a result, steady-state conditions cannot be used to benchmark surge line modeling. Since no other data were available, engineering judgement was applied. Specifically, standard practices for estimating flows through pipe and fittings were followed to calculate loss coefficients applicable to the surge line and the surge line/hot leg connection. Furthermore, when the surge line had to be connected to the split hot leg, it was assumed that flows into the surge line from top and bottom halves of the split hot leg should be equal. However, a flow imbalance was observed in some analyses with PORVs latched open despite efforts to nodalize with equal resistances between the surge line and the upper and lower halves of the split hot leg. Resistances at split surge line/hot leg connections were not exactly equal apparently because of subtle effects associated with the way flow area changes are treated by the code. In most cases, modifying the surge line/hot leg nodalization to improve the flow balance shortened the time to surge line failure. Those trends were observed for both abrupt and smooth area change modeling options, indicating that the SGTR potential was probably not adversely affected. However, careful attention to simulation of the surge line/hot leg connection would be appropriate if additional analyses are needed.

There was no effort to determine if results for the analyzed plants could be extended to cover all operating PWRs. Based on work that was completed in this evaluation, it would seem reasonable to expect similar trends in other operating plants. However, that expectation is not supported by analysis at this time.

7. CONCLUSIONS

Natural circulation flows can develop during severe reactor accidents and transfer energy from the core to other parts of the RCS. The associated heatup of RCS structures can lead to pressure boundary failures, including a possibility for SGTR. A substantial number of SCDAP/RELAP5 analyses were completed to evaluate the potential for SGTR in operating PWRs as a result of natural circulation heating during TMLB' accidents (and variations thereof). All RCS pressure boundaries, including the SG tubes, were assumed to be defect free with respect to the prediction of pressure boundary failures in all analyses. In this evaluation, Surry and Zion PWRs were used to represent Westinghouse three and four loop plants, respectively; Calvert Cliffs and ANO2 PWRs were used to represent Combustion Engineering plants with and without pressurizer PORVs, respectively; and the Oconee PWR was used to represent Babcock & Wilcox plants; thereby covering all existing PWR designs. In addition, natural circulation sensitivities were evaluated using a stand alone model of the Surry pressurizer coolant loop and selected nodalization sensitivities were considered. Conclusions based on results from the SCDAP/RELAP5 analyses are summarized below.

Within limitations, independent reviewers of this evaluation found Westinghouse experiments characterizing natural circulation during severe accidents to be well designed, SCDAP/RELAP5

to be capable of simulating those natural circulation flows, and SCDAP/RELAP5 modeling to assess the potential for SGTR in this evaluation to be adequate.

Independent review committee meetings were held to address the applicability of Westinghouse natural circulation experimental data, the suitability of the SCDAP/RELAP5 code, and the adequacy of SCDAP/RELAP5 natural circulation modeling with respect to this evaluation of the SGTR potential in operating PWRs. The independent review committee and the ACRS concluded that Westinghouse natural circulation experiments were well designed and executed. The reviewers did indicate that uncertainties in experimental parameters used to characterize hot leg countercurrent natural circulation had to be considered and that scaling could be affected by the absence of radiation heat transfer and other experimental shortcomings. Uncertainties in experimental parameters were addressed through numerous sensitivity analyses completed during the course of this evaluation. Experimental shortcomings were noted, although the experiments are considered valuable despite those problems because they verify the general behavior of natural circulation during severe accidents and provide a means for code validation that yields a level of confidence in similar full plant analyses.

The independent review committee also concluded that SCDAP/RELAP5 is capable of modeling natural circulation in PWRs under severe accident conditions for the purpose of calculating the relative timing of RCS component failures in order to assess the SGTR potential. The ACRS concurred after consideration of the independent review committee findings. Those conclusions were at least partially based on the fact that SCDAP/RELAP5 was shown to be capable of reproducing major trends in the Westinghouse experiments and that agreement between data and code predictions was satisfactory. However, reviewers indicated that code refinement was warranted in the calculation of convection heat transfer. Accordingly, correlations to treat the combination of forced and free (or mixed) convection heat transfer were added to the code and used in all subsequent analyses.

And finally, the independent review committee indicated that SCDAP/RELAP5 had been applied correctly in completing a significant number of analyses. However, the committee recommended non-dimensionalization so that results from Westinghouse experiments and the SCDAP/RELAP5 analyses could be directly compared; sensitivity studies to evaluate uncertainties associated with heat transfer coefficients and the other parameters that characterize hot leg countercurrent natural circulation in PWRs with U-tube SGs, including the synergistic effects associated with varying several parameters at a time; and analyses to evaluate conjugate heat transfer effects in the split hot leg model (consisting of the combination of fluid-to-wall heat transfer, fluid-to-fluid heat transfer, and circumferential conduction around the hot leg pipe wall). A broader series of sensitivity analyses for a broader spectrum of operating PWRs was completed instead of attempts at non-dimensionalization. Among other issues, uncertainties in the parameters that characterize hot leg countercurrent natural circulation, heat transfer coefficients, and conjugate heat transfer effects in the split hot leg model were considered.

SG U-tube temperatures are not significantly affected by changes in any individual parameter that characterizes hot leg countercurrent natural circulation over the range of variation that was experimentally observed.

SCDAP/RELAP5 analyses (using a stand alone version of the Surry pressurizer loop nodalization) were completed to evaluate changes in SG U-tube temperatures that could occur with changes in the parameters that characterize hot leg countercurrent natural circulation. Those parameters include the number of tubes participating in hot (forward) flow, mixing fractions, and the recirculation ratio. Only one parameter was allowed to change in each calculation while all other conditions remained constant. A number of analyses were then completed to cover the range of parameter variation that was experimentally

observed. Temperatures of the hottest SG U-tubes were found to increase (1) as the number of tubes participating in hot (forward) flow decreased, (2) as mixing fractions decreased, and (3) as the recirculation ratio increased. However, changes in the hottest tube temperatures were calculated to be ~26 K, or less, which is insignificant compared to other uncertainties involved in the simulation of severe reactor accidents. Furthermore, those differences did not significantly increase tube creep damage, indicating that any potential for SGTR would not develop until long after surge line failure over the range of parameters considered.

SG U-tube temperature response as a result of the synergistic effects associated simultaneous variations of natural circulation parameters is consistent with the temperature response associated with variations of individual parameters.

Results from stand alone loop sensitivity analyses indicate that SG tube temperatures increase when mixing fractions decrease, recirculation is increased, or the fraction of SG tubes participating in hot (forward) flow is decreased. Results were found to be consistent with those trends in a synergistic sensitivity calculation where all natural circulation parameters were simultaneously adjusted. Specifically, SG U-tube temperatures were predicted to increase when mixing fractions, recirculation, and the fraction of SG tubes participating in hot (forward) flow were simultaneously decreased. Based on the stand alone loop sensitivity analyses, the temperature increase was expected because two of three natural circulation parameter changes supported prediction of the higher temperatures. Those results provide some validation that the stand alone loop analyses reasonably represent the response that could be expected in a full plant simulation.

Simultaneous variations of parameters that characterize natural circulation in PWRs with U-tube SGs to relatively extreme values did not result in a potential for SGTR.

Analyses were completed where all parameters characterizing natural circulation in PWRs with U-tube SGs were simultaneously set to 5% confidence values (which were calculated assuming a normal distribution of the Westinghouse high pressure transient data). SG tube temperatures were predicted to increase and SGTR was accelerated under those conditions as expected. However, use of the 5% confidence values, which correspond to parameter values that should be smaller than 95% of all values, is believed to conservatively represent the tail of the assumed distribution because each value was calculated independently without any allowance for relationships with the other parameters and all values were lower than any actually observed during the transient experiments. Nevertheless, surge line failure was still predicted some 800 s prior to SGTR. Given that prediction of surge line failure, the potential for SGTR relative to simultaneous variations in natural circulation parameters is still low.

Uncertainties in heat transfer coefficients are not important in this evaluation because they do not significantly alter the potential for SGTR.

Uncertainties were considered in all heat transfer coefficients that could impact ex-vessel heating (those in the upper plenum, hot legs, surge line, and on the inner and outer surfaces of the SG U-tubes) and in all heat transfer coefficients in the hot leg, surge line, and SG U-tube entrance volumes, including an extreme case of enhancing only heat transfer coefficients in SG U-tube entrance volumes. Results indicate that the timing of SGTR could vary by 130 s given those uncertainties. Furthermore, SG tube temperatures at the time of surge line failure could vary from 938 to 964 K, a range of only 26 K. Those results would not be expected to significantly alter the potential for SGTR, indicating that heat transfer coefficient uncertainties are not important factors in this evaluation.

Conjugate heat transfer effects in the hot leg during countercurrent natural circulation tend to decrease the potential for SGTR in PWRs with U-tube SGs.

Analyses were completed to address the absence of fluid-to-fluid heat transfer and circumferential pipe wall conduction in the SCDAP/RELAP5 split hot leg model for PWRs with U-tube SGs. Results indicate that conjugate heat transfer effects reduce the difference between the temperature of the hot vapor in the top half of the hot leg and the temperature of the cooler vapor in the bottom half of the hot leg. That differential temperature reduction led to reduced hot leg countercurrent flows and reduced vapor temperatures in the SGs. As a result, SG U-tube temperatures were reduced and SGTR was delayed, indicating that conjugate heat transfer effects in the hot leg decrease the potential for SGTR. Consequently, a degree of conservatism exists in analyses completed during the course of this evaluation due to the absence of conjugate heat transfer effects in hot leg modeling.

RCS pressure spikes associated with boiling that follows accumulator injection were not significantly affected by core axial nodalization, indicating that the core axial nodalization used in this evaluation did not affect SGTR predictions.

Large pressure spikes were predicted following initial accumulator injections with or without refined core axial nodalization. When the core axial nodalization was increased, a somewhat lower peak pressure was reached and some extension of the pressure spike was predicted. However, those pressure differences were relatively minor and they would not be expected to significantly alter creep damage of any RCS pressure boundary. Furthermore, the effects that were observed were primarily due to refinement in the core axial power profile that was adopted for consistency with the refined core nodalization. Effects associated with the refined power profile could have been minimized by retaining a constant (flat) power density for all subdivisions of a given node. Although that would produce a stepped approximation of the power profile, a better evaluation of the separate effects of axial nodalization might have been achieved.

The timing of surge line failure can be affected by the nodalization used to simulate the surge line/hot leg connection, although an adverse impact on the potential for SGTR associated with that nodalization was not indicated in sensitivity analyses that were completed.

Results indicate that the surge line/hot leg nodalization can influence the flow balance between upper and lower halves of the split hot leg into the surge line. If a flow imbalance develops, surge line heating and failure can be affected. In most cases, modifying the surge line/hot leg nodalization to improve the flow balance shortened the time to surge line failure. Those trends were observed for both abrupt and smooth area change modeling options, indicating that the SGTR potential was probably not adversely affected. However, careful attention to simulation of the surge line/hot leg connection would be appropriate if additional analyses are needed.

RCP loop seal clearing can be expected in operating PWRs with U-tube SGs during TMLB' accidents with SG secondary depressurization and intentional RCS depressurization through pressurizer PORVs.

RCP loop seal clearing (sufficient to allow development of full-loop natural circulation of primary vapor) was predicted in all SCDAP/RELAP5 analyses that were completed for PWRs with U-tube SGs and RCS depressurization through pressurizer PORVs. In the analyses that were completed, accumulator injection and RCS depressurization through the pressurizer PORVs appeared to be the most important factors affecting RCP loop seal clearing. Cold leg condensation during the initial phase of accumulator injection can reduce pressures downstream of the RCP loop seal, which can pull water out of the loop seal. In-core

boiling near the end of a given accumulator injection can increase pressures upstream of the RCP loop seal (particularly when water covers the bottom of the downcomer skirt), which can push water out of the loop seal. In addition, RCS depressurization through pressurizer PORVs can lead to flashing of water in the RCP loop seal. Loop seal clearing was predicted with or without RCP seal leaks, with or without DC-HL bypass flows, and with or without SG sludge accumulation.

RCP loop seal clearing in operating PWRs with once-through SGs can develop during TMLB' accidents with SG secondary depressurization and intentional RCS depressurization through pressurizer PORVs only if RCP seals leak.

RCP loop seals in PWRs with once-through SGs cleared in all RCS depressurization analyses with RCP seal leaks but did not clear in analyses without RCP seal leaks. Boiling of liquid in the RCP loop seals as steam passed from the SGs to RCP leaks was apparently needed in order to clear the loop seals in the once-through SG configuration analyzed.

Full-loop natural circulation following RCP loop seal clearing will increase SG tube heating in the affected loop without impact on the potential for SGTR.

Results from SCDAP/RELAP5 analyses clearly indicate that SG tube heating in the affected loop will increase significantly (compared to heating in unaffected loops) after RCP loop seal clearing. The increased tube heating was predicted in U-tube and once-through SG configurations. Those results occurred even though full-loop natural circulation flows remained relatively low because pressurizer PORVs were generally latched open in analyses where RCP loop seal clearing developed. However, increases in SG tube heating were not severe enough to induce SG tube failure prior to the predicted failure of other RCS pressure boundaries. Therefore, full-loop natural circulation was not found to adversely impact the potential for SGTR in this evaluation.

Accumulators empty quicker and RCP loop seals clear more readily without impact on the SGTR potential if the DC-HL bypass is blocked.

Results from SCDAP/RELAP5 RCS depressurization analyses indicate that accumulators will empty quicker because downcomer pressurization during the steam production phase of accumulator injection is slower without DC-HL bypass flows. As a result, downcomer (and cold leg) pressures remain below accumulator pressures for longer periods of time, allowing accumulators to empty quicker. When downcomer pressure response is slowed because DC-HL bypass flow paths are blocked, there is a greater tendency for initial accumulator-related condensation to "pull" and subsequent accumulator-related vaporization to "push" water out of the RCP loop seals, allowing loop seals to clear more readily. Those effects are not as important in plants with upper head vent valves because those valves tend to equalize upper plenum pressures with pressures in the downcomer, with or without DC-HL bypass flows. However, there was no apparent impact on the potential for SGTR as a result of variations in DC-HL bypass flows.

Tube temperatures are higher in SGs with accumulated sludge than in SGs without sludge, although the higher temperatures did not adversely impact the potential for SGTR.

Results from SCDAP/RELAP5 RCS depressurization analyses indicate that tubes in SGs with sludge accumulation are hotter than tubes in clean SGs. Higher temperatures occur because sludge retards heat transfer from the SG tube wall. In some cases, the higher SG tube temperatures associated with sludge accumulation led to SGTR predictions. However, SGTR was always predicted long after failure of another

RCS pressure boundary (i.e., the surge line). Consequently, higher tube temperatures did not adversely impact the potential for SGTR.

A potential for SGTR does not exist without SG secondary depressurization.

Results from SCDAP/RELAP5 analyses for the Surry PWR indicate that SGTR will not occur if normal pressures are maintained the SG secondaries. The maximum pressure SG tube differential pressure is limited to ~9 MPa if normal SG secondary pressures are maintained. SG tube heating was not found to be severe enough to induce SGTR with that limited differential pressure.

Quenching of upper plenum stainless steel, if it is predicted to melt and relocate into the lower head, can contribute to the potential for SGTR in some PWRs.

SCDAP/RELAP5 results for the ANO2 PWR indicate that the integrity of RCS piping can be affected by pressure pertubations associated with boiling following accumulator injection. In one ANO2 calculation, the first failure in the RCS pressure boundary (in the hot leg) was closely followed by a SGTR as a result of the pressure pertubations. However, assuming that upper plenum stainless steel is quenched during molten relocation into the lower head could be overly conservative with respect to the potential for SGTR. That is because the code conservatively assumes that all relocated material will be completely cooled to the saturation temperature of the lower head coolant during a single time step when the quenching option is activated. Heat rejected from the molten material during that process is added directly to the lower head coolant during the same time step, which can lead to large vapor production rates. Furthermore, the stainless steel must candle through a tortuous path from the upper plenum all the way to the lower head without refreezing if quenching is to occur. Results indicate that temperatures near the bottom of the active fuel region (and above the lower head) can be cooler than the stainless steel melting temperature, particularly in cases with RCS depressurization that activates the accumulators. In such cases, the stainless steel could refreeze before reaching the lower head and thereby eliminate the potential for quenching. Although results indicate a potential for SGTR in the ANO2 PWR if quenching does occur under specific conditions, similar results were not predicted for the Surry PWR.

Surge line (or hot leg) failure was predicted to be the first RCS pressure boundary failure in all analyses for all operating PWRs.

Surge line failure was predicted to be the first failure of the RCS pressure boundary in virtually all analyses completed during the course of this evaluation. Those surge line failures developed as a result of natural circulation heating and the flows associated with operation of pressurizer PORVs. The first RCS pressure boundary failures in four analyses with RCP seal leaks (and without intentional RCS depressurization through the pressurizer PORVs) were found to be hot leg failures because surge line flow and therefore, surge line heating, was reduced as a result of flows through the seal leaks. (A hot leg failure was also predicted to be the first RCS pressure boundary failure in one other calculation as the result of a surge line/hot leg nodalization artifact.)

RCS depressurization that occurs following an initial pressure boundary failure effectively eliminates the potential for a second failure at any other location in the RCS pressure boundary.

Rapid depressurization of the RCS will occur if the RCS pressure boundary fails. Accumulator injection will follow, providing water sufficient to arrest the heatup of the core and cool the RCS piping. Core reheating after the accumulator water boils away will primarily be directed out the pressure boundary

break, preventing any significant reheating of the RCS piping that is needed to induce a second failure. Furthermore, SGTR is very unlikely following any other RCS pressure boundary failure because the SG tubes will be subjected to compression loading as a result of RCS depressurization. SG tube collapse is possible, but relatively high temperatures in conjunction with the compression loads would be required to generate that type of failure.

The potential for SGTR in operating PWRs during TMLB' accidents is low.

SCDAP/RELAP5 results indicate that in-vessel, full-loop, and hot leg countercurrent natural circulation flows will develop during TMLB' accidents in operating PWRs. Furthermore, surge line (or hot leg) failures were predicted to be the first failures in the RCS pressure boundary in all analyses as a result of heat transferred by those flows. Those results held for all operating PWRs that were analyzed in cases with and without RCP seal leaks, cases with and without intentional RCS depressurization through pressurizer PORVs, cases with and without SG secondary depressurization, cases with and without DC-HL bypass flows, cases with and without U-tube SG sludge accumulation, and cases with and without quenching of upper plenum stainless steel upon relocation to the lower head (if that steel was predicted to melt). Results also indicated that secondary failures of the RCS pressure boundary will not occur after RCS depressurization, accumulator injection, and disruption of natural circulation heating associated with the first RCS pressure boundary failure. In other words, a SGTR (or any other secondary failure in the RCS pressure boundary) would not be expected after depressurization through the first (surge line or hot leg) failure. Results from sensitivity analyses indicate that uncertainties associated with natural circulation behavior, heat transfer, and variety of other related factors are not large enough to adversely affect those conclusions. In one calculation for one operating PWR, SGTR was found to be imminent at the time of the first RCS pressure boundary failure as a result of large pressure pertubations associated with quenching of molten upper plenum stainless steel. Uncertainties may be large enough to preclude the possibility that SGTR could be the first RCS pressure boundary failure in that case. However, the assumption that stainless steel can candle through the core without refreezing and the subsequent simulation of complete and essentially instantaneous quenching are believed to be overly conservative with respect to the SGTR prediction. Any SGTR concerns in this single case would be expected to significantly to decrease if more detailed modeling were applied. Consequently, the potential for SGTR in operating PWRs during TMLB' accidents is low. The conclusions of this evaluation apply if SG tubes (and other RCS piping) are defect free. Further evaluation would be needed to assess the potential for SGTR given the existence of structural flaws.

8. REFERENCES

1. C. M. Allison et al., *SCDAP/RELAP5/MOD3.1 Code Manuals*, NUREG/CR-6150, Idaho National Engineering and Environmental Laboratory, December 1995.

2. W. A. Stewart et al., *Natural Circulation Experiments for PWR Degraded Core Accidents,* EPRI Report NP-6324-D, Westinghouse Electric Corporation, 1989.

3. W. A. Stewart et al., *Natural Circulation Experiments for PWR High Pressure Accidents*, EPRI Project No. RP2177-5 Final Report, Westinghouse Electric Corporation, July 1992.

4. K. Almenas et al., *Natural Circulation Induced Heating of Primary System Components: Final Report*, University of Maryland at College Park, June 1994.

5. G. A. Berna, C. M. Allison, and L. J. Siefken, *SCDAP/MOD1/V0: A Computer Code for the Analysis of LWR Vessel Behavior During Severe Accident Transients,* IS-SAAM-83-002, Idaho National Engineering and Environmental Laboratory, July 1984.

6. H. Jordan and M. R. Kuhlman, *TRAP-MELT2 User's Manual,* NUREG/CR-4205, Battelle Memorial Institute, May 1985.

7. E. C. Lemmon, *COUPLE/FLUID: A Two-Dimensional Finite Element Thermal Conduction and Advection Code,* EGG-ISD-SCD-80-1, Idaho National Engineering and Environmental Laboratory, February 1980.

8. RELAP5 Development Team, *RELAP5/MOD3.2 User's Guide and Input Requirements,* NUREG/CR-5535 (Volume 2), Idaho National Engineering and Environmental Laboratory, August 1995.

9. P. D. Bayless, *Analyses of Natural Circulation During a Surry Station Blackout Using SCDAP/RELAP5,* NUREG/CR-5214, Idaho National Engineering and Environmental Laboratory, October 1988.

10. D. L. Knudson (Idaho National Engineering and Environmental Laboratory) letter to R. Lee (Nuclear Regulatory Commission), "Hot Leg Countercurrent Natural Circulation Modeling", DLK-7-96, August 14, 1996.

11. C. A. Dobbe (Idaho National Engineering and Environmental Laboratory) letter to D. L. Knudson (Idaho National Engineering and Environmental Laboratory), "Hot Leg Countercurrent Natural Circulation Modeling for PWRs with Once-Through SGs", CXD-01-98, March 6, 1998.

12. P. Griffith (Private Consultant) letter to M. Khatib-Rahbar (Energy Research, Incorporated) regarding the use of Westinghouse hot leg countercurrent natural circulation experimental data and the associated application of SCDAP/RELAP5 in steam generator tube rupture analyses, August 27, 1996.

13. M. Ishii (Professor, Purdue University) letter to R. Lee (Nuclear Regulatory Commission) regarding the use of Westinghouse hot leg countercurrent natural circulation experimental data and the associated application of SCDAP/RELAP5 in steam generator tube rupture analyses, August 30, 1996.

14. R. Viskanta (Professor, Purdue University) letter to M. Khatib-Rahbar (Energy Research, Incorporated) regarding the use of Westinghouse hot leg countercurrent natural circulation experimental data and the associated application of SCDAP/RELAP5 in steam generator tube rupture analyses, September 11, 1996.

15. T. S. Kress (Chairman, Advisory Committee on Reactor Safeguards) letter to S. A. Jackson (Chairman, Nuclear Regulatory Commission), "Capability of the NRC SCDAP/RELAP5 Code to Predict Temperatures and Flows in Steam Generators under Severe Accident Conditions", October 22, 1996.

16. A. T. Wassel et al., *Modeling of Natural Circulation in Reactor Cooling Systems,* FPI R88-05-04, Fluid Physics International, 1988.

17. P. D. Bayless et al., *Severe Accident Natural Circulation Studies at the INEL*, NUREG/CR-6285, Idaho National Engineering and Environmental Laboratory, February 1995.

18. J. E. O'Brien (Idaho National Engineering and Environmental Laboratory) letter to R. Lee (Nuclear Regulatory Commission), "Effect of Radiation Heat Transfer", JEO-01-96, August 14, 1996.

19. D. L. Knudson (Idaho National Engineering and Environmental Laboratory) fax to C. Tinkler (Nuclear Regulatory Commission), October 1, 1996, transmitting J. E. O'Brien (Idaho National Engineering and Environmental Laboratory) response to D. Knudson Memo of 9/17/96 (discussing experimental SG tube diameter, hot leg scaling analyses and associated non-dimensional numbers, and experimental error analysis).

20. D. L. Knudson (Idaho National Engineering and Environmental Laboratory) fax to R. Lee (Nuclear Regulatory Commission), October 29, 1996, transmitting J. O'Brien (Idaho National Engineering and Environmental Laboratory) memo to D. Knudson (Idaho National Engineering and Environmental Laboratory), "Hot Leg Froude Numbers", October 29, 1996.

21. D. L. Knudson (Idaho National Engineering and Environmental Laboratory) fax to R. Lee (Nuclear Regulatory Commission), July 30, 1996, transmitting R. Shumway, "Mixed Convection Wall Heat Transfer in RELAP5/MOD3", Idaho National Engineering and Environmental Laboratory, June 1996.

22. D. L. Knudson (Idaho National Engineering and Environmental Laboratory) letter to R. Lee (Nuclear Regulatory Commission), "Revision 1 of Steam Generator Tube Rupture Analyses under JCN W6242", DLK-4-96, June 6, 1996, transmitting C. A. Dobbe and D. L. Knudson, "SCDAP/RELAP5 Analysis of the Influence of Natural Circulation Parameters on Predicted Steam Generator Tube Temperatures - Revision 1", Idaho National Engineering and Environmental Laboratory, June 1996.

23. D. L. Knudson (Idaho National Engineering and Environmental Laboratory) letter to R. Lee (Nuclear Regulatory Commission), "Revision 1 of Steam Generator Tube Rupture Analyses under JCN W6242", DLK-4-96, June 6, 1996, transmitting K. S. Quick and D. L. Knudson, "A SCDAP/RELAP5 Analysis of the Potential for Steam Generator Tube Rupture in Surry - Revision 1", Idaho National Engineering and Environmental Laboratory, June 1996.

24. D. L. Knudson (Idaho National Engineering and Environmental Laboratory) letter to R. Lee (Nuclear Regulatory Commission), "Revision 1 of Additional Surry SGTR Analyses under JCN W6242", DLK-9-96, December 17, 1996, transmitting D. L. Knudson and C. A. Dobbe, "Additional SCDAP/RELAP5 Calculations Evaluating the Potential for Steam Generator Tube Rupture in Surry - Revision 1", Idaho National Engineering and Environmental Laboratory, December 1996.

25. C. J. Ruger and W. J. Lucas, Jr., *Technical Findings Related to Generic Issue 23: Reactor Coolant Pump Seal Failure*, NUREG/CR-4948, March 1989.

26. T. Boardman et al., *Leak Rate Analysis of the Westinghouse Reactor Coolant Pump*, NUREG/CR-4294, July 1985.

27. T. A. Wheeler et al., *Analysis of Core Damage Frequency from Internal Events: Expert Judgment Elicitation*, NUREG/CR-4550, April 1989.

28. D. L. Knudson (Idaho National Engineering and Environmental Laboratory) letter to R. Lee (Nuclear Regulatory Commission), "Revision 1 of Surry SGTR Analyses with RCP Seal Leaks under JCN W6242", DLK-1-97, February 4, 1997, transmitting K. S. Quick and D. L. Knudson, "A SCDAP/RELAP5 Analysis of the Potential for SGTR in Surry with RCP Seal Leakage - Revision 1", Idaho National Engineering and Environmental Laboratory, February 1997.

29. Baltimore Gas and Electric Co., *Calvert Cliffs Nuclear Power Plant Individual Plant Examination Summary Report*, Volumes 1 and 2, RAN 92-008, Revision 0, December 1993.

30. D. L. Knudson (Idaho National Engineering and Environmental Laboratory) letter to R. Lee (Nuclear Regulatory Commission), "Revision 1 of Steam Generator Tube Rupture Analyses under JCN W6242", DLK-4-96, June 6, 1996, transmitting D. L. Knudson and K. S. Quick, "A SCDAP/RELAP5 Analysis of the Potential for Steam Generator Tube Rupture in Arkansas Nuclear One Unit 2 - Revision 1", Idaho National Engineering and Environmental Laboratory, June 1996.

31. D. A. Brownson et al., *Intentional Depressurization Accident Management Strategy for Pressurized Water Reactors*, NUREG/CR-5937, Idaho National Engineering and Environmental Laboratory, April 1993.

32. D. L. Knudson (Idaho National Engineering and Environmental Laboratory) letter to R. Lee (Nuclear Regulatory Commission), "Transmittal of JCN W6242 Task 6.1 and 6.2 Letter Reports", DLK-4-97, May 23, 1997, transmitting D. L. Knudson and C. A. Dobbe, "SCDAP/RELAP5 Evaluation of the Potential for Steam Generator Tube Rupture when the Reactor Coolant System is Depressurized", Idaho National Engineering and Environmental Laboratory, May 1997

33. D. L. Knudson (Idaho National Engineering and Environmental Laboratory) letter to R. Lee (Nuclear Regulatory Commission), "Transmittal of JCN W6242 Task 6.2 Letter Report", DLK-5-97, June 13, 1997, transmitting D. L. Knudson, L. S. Ghan, and C. A. Dobbe, "SCDAP/RELAP5 Evaluation of the Potential for Steam Generator Tube Rupture with Reactor Coolant System Depressurization and Reactor Coolant Pump Seal Leaks", Idaho National Engineering and Environmental Laboratory, June 1997

34. D. L. Knudson (Idaho National Engineering and Environmental Laboratory) letter to R. Lee (Nuclear Regulatory Commission), "Transmittal of JCN W6242 Task 6.5 Letter Report", DLK-7-97, August 4, 1997, transmitting D. L. Knudson and L. S. Ghan, "SCDAP/RELAP5 Evaluation of Downcomer-Hot Leg Bypass Flows Relative to the Potential for Steam Generator Tube Rupture", Idaho National Engineering and Environmental Laboratory, August 1997

35. A. J. Baum and P. K. Greaney, *Steam Generator Sludge Pile Model Boiler Testing,* NP-1941, Research Project S119-1, Westinghouse Electric Corporation, July 1981.

36. L. F. Becker, Jr. and J. N. Esposito, *Steam Generator Sludge Pile Model Boiler Testing - Sludge Characterization,* NP-2041, Research Project S119-1, Westinghouse Electric Corporation, September 1981.

37. R. E. Bolz and G. L. Tuve, *CRC Handbook of Tables for Applied Engineering Science, Second Edition,* CRC Press, 1977.

38. Y. S. Touloukian et. al., *Thermophysical Properties of Matter, Volume 1, Thermal Conductivity - Metallic Elements and Alloys,* IFI/Plenum Press, 1970.

39. Y. S. Touloukian et. al., *Thermophysical Properties of Matter, Volume 4, Specific Heat - Metallic Elements and Alloys,* IFI/Plenum Press, 1970.

40. D. L. Knudson (Idaho National Engineering and Environmental Laboratory) letter to R. Lee (Nuclear Regulatory Commission), "Transmittal of JCN W6242 Task 6.4 Letter Report", DLK-9-97, September 25, 1997, transmitting D. L. Knudson and L. S. Ghan, "SCDAP/RELAP5 Evaluation of the Effects of Steam Generator Sludge Relative to the Potential for Steam Generator Tube Rupture", Idaho National Engineering and Environmental Laboratory, September 1997

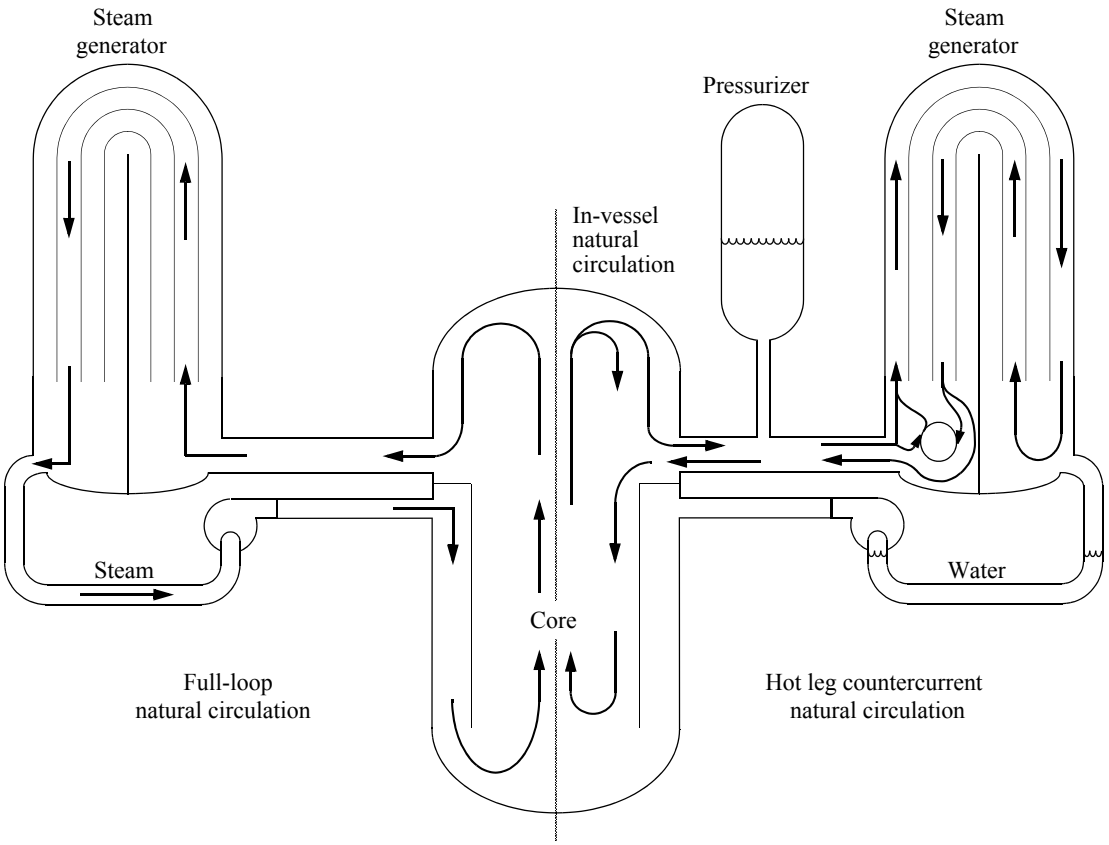

Figure 1. Natural circulation flow patterns that could develop during certain severe accidents in PWRs with U-tube SGs.

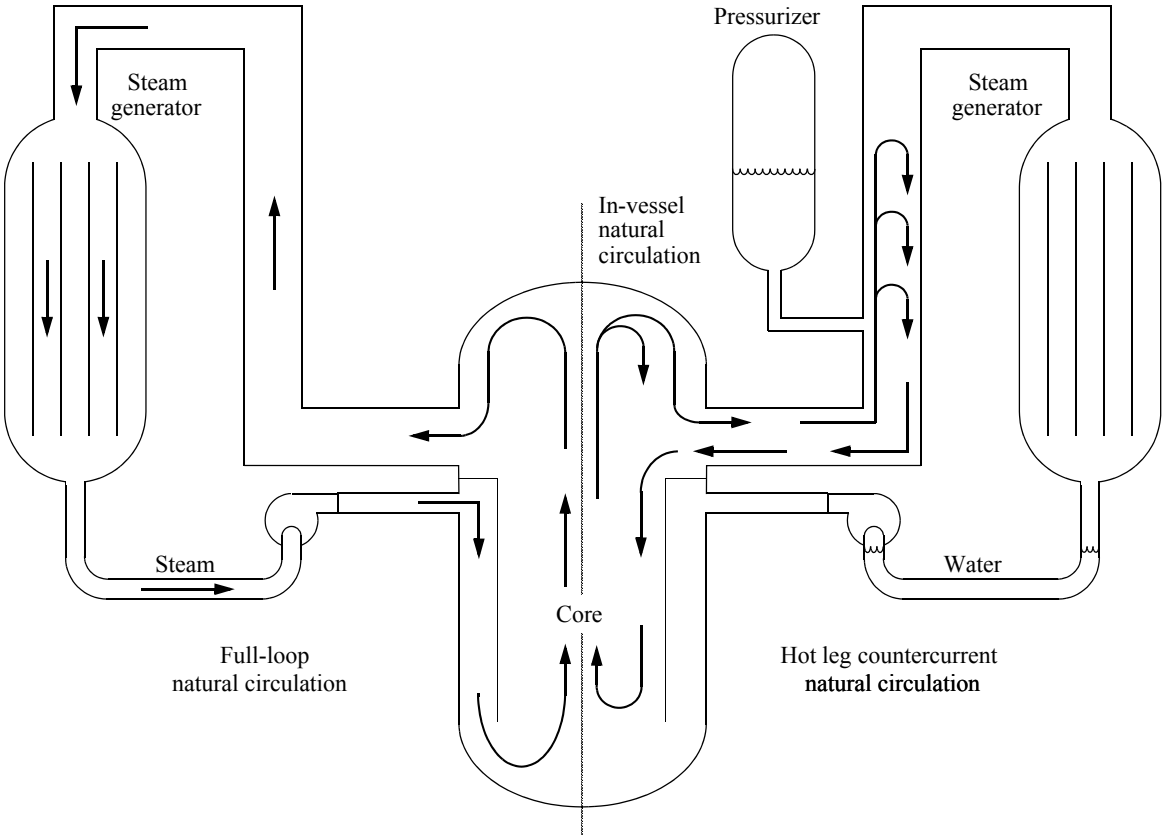

Figure 2. Natural circulation flow patterns that could develop during certain severe accidents in PWRs with once-through SGs.

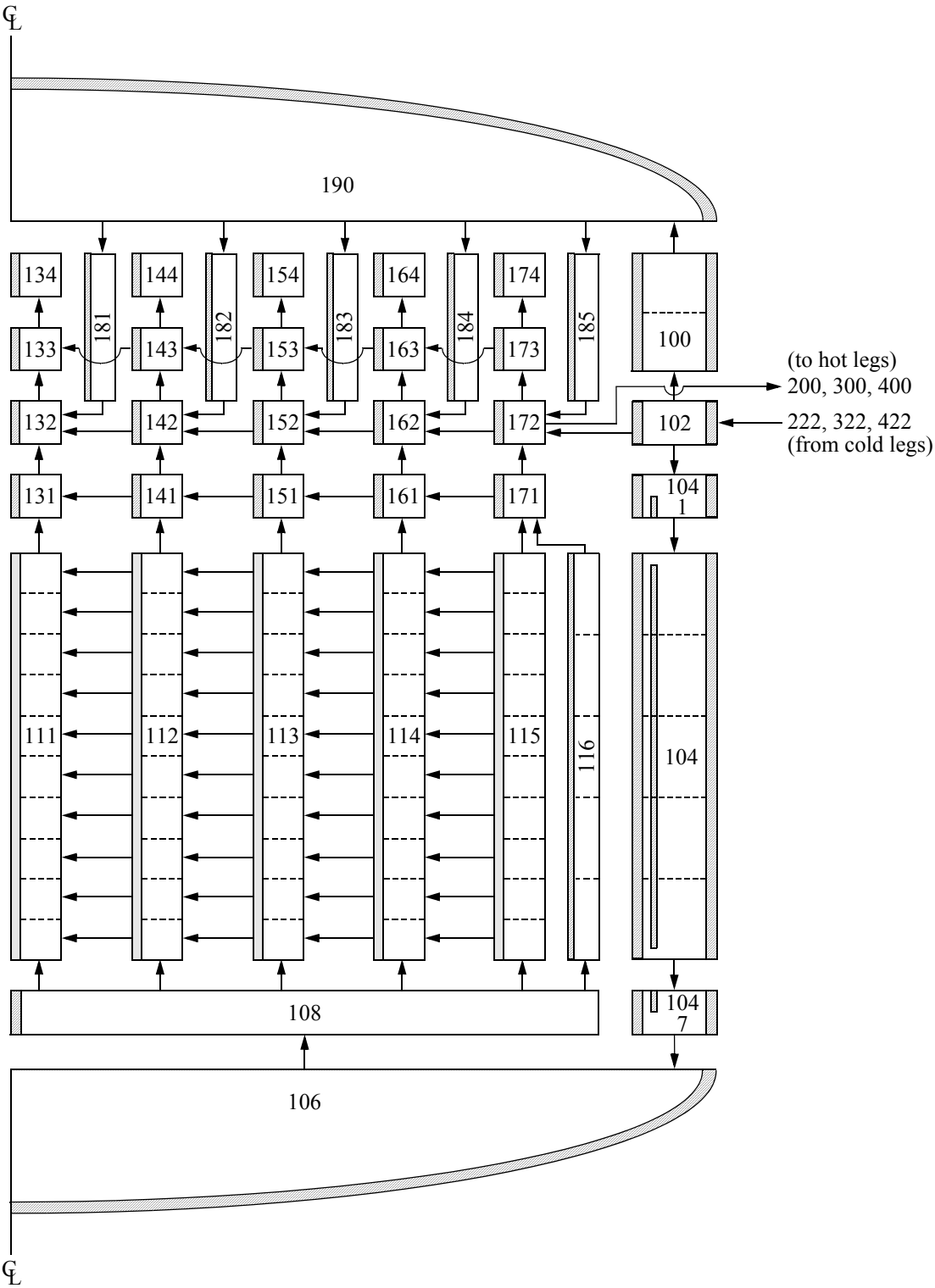

Figure 3. Surry reactor vessel nodalization.

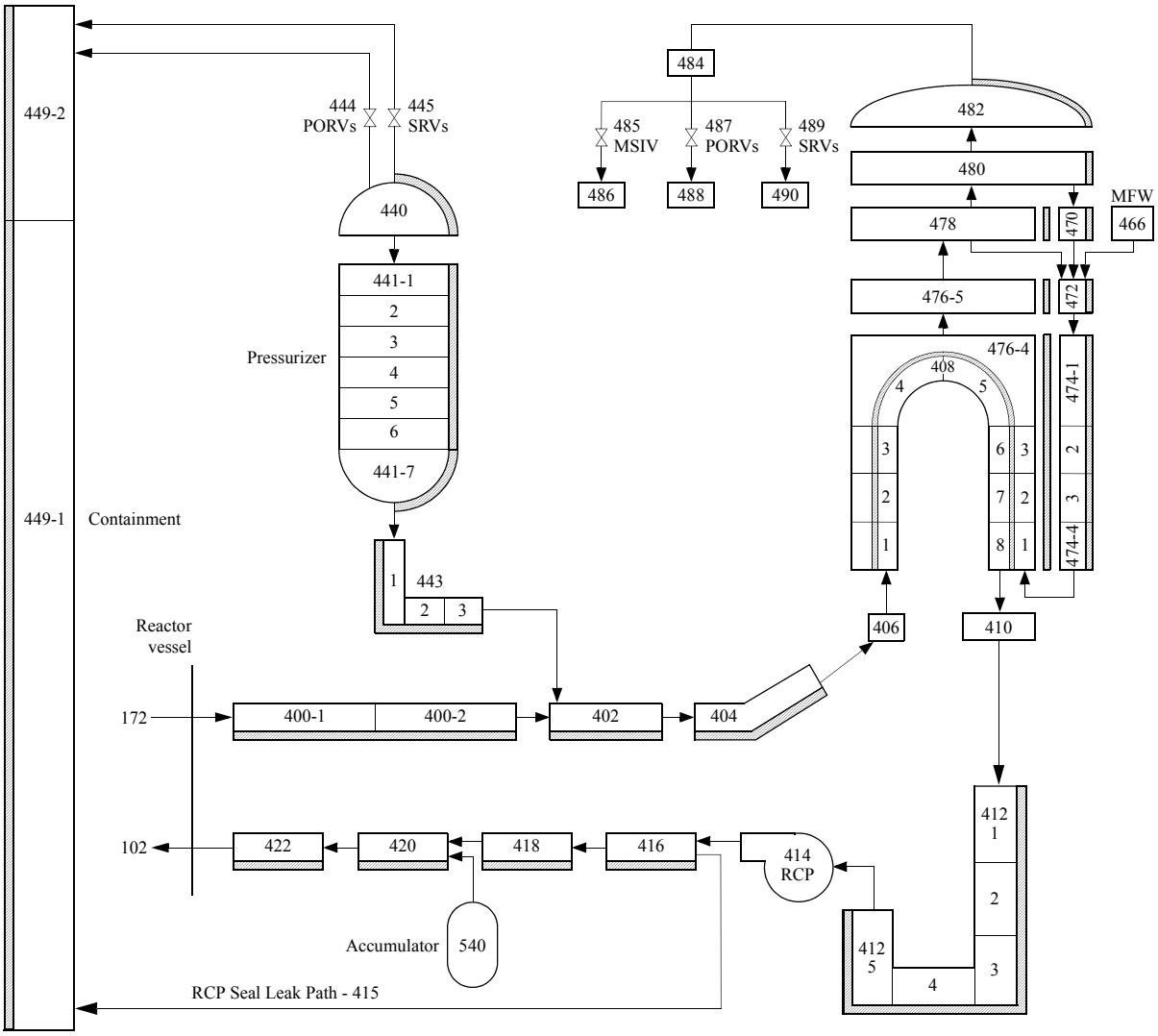

Figure 4. Surry pressurizer loop (Loop C) nodalization without provisions for hot leg countercurrent natural circulation.

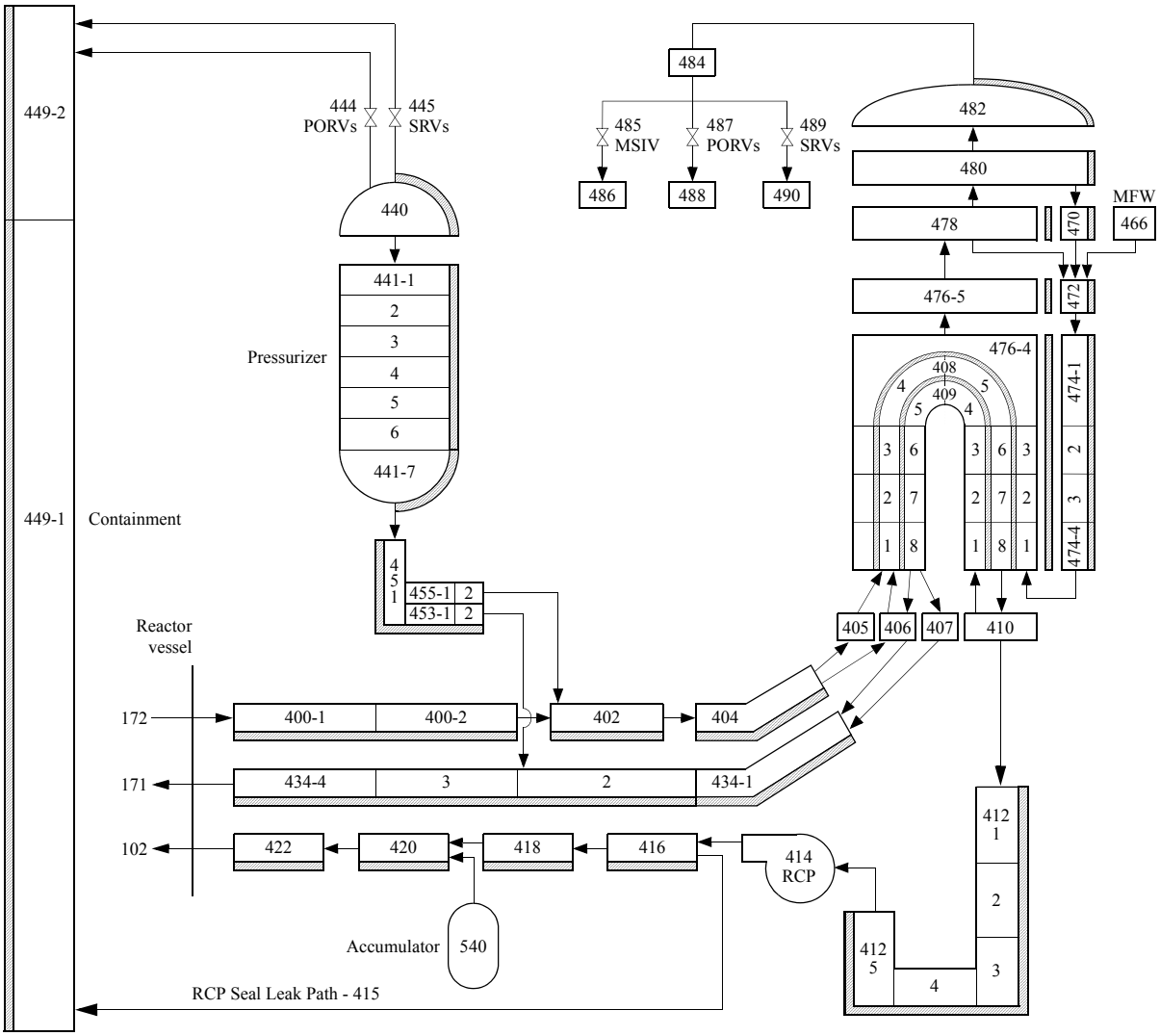

Figure 5. Surry pressurizer loop (Loop C) nodalization with provisions for hot leg countercurrent natural circulation.

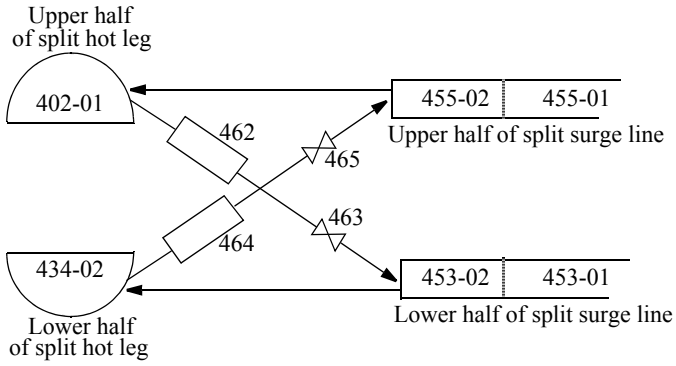

Figure 6. Nodalization detail showing connections between the split hot leg and the split surge line.

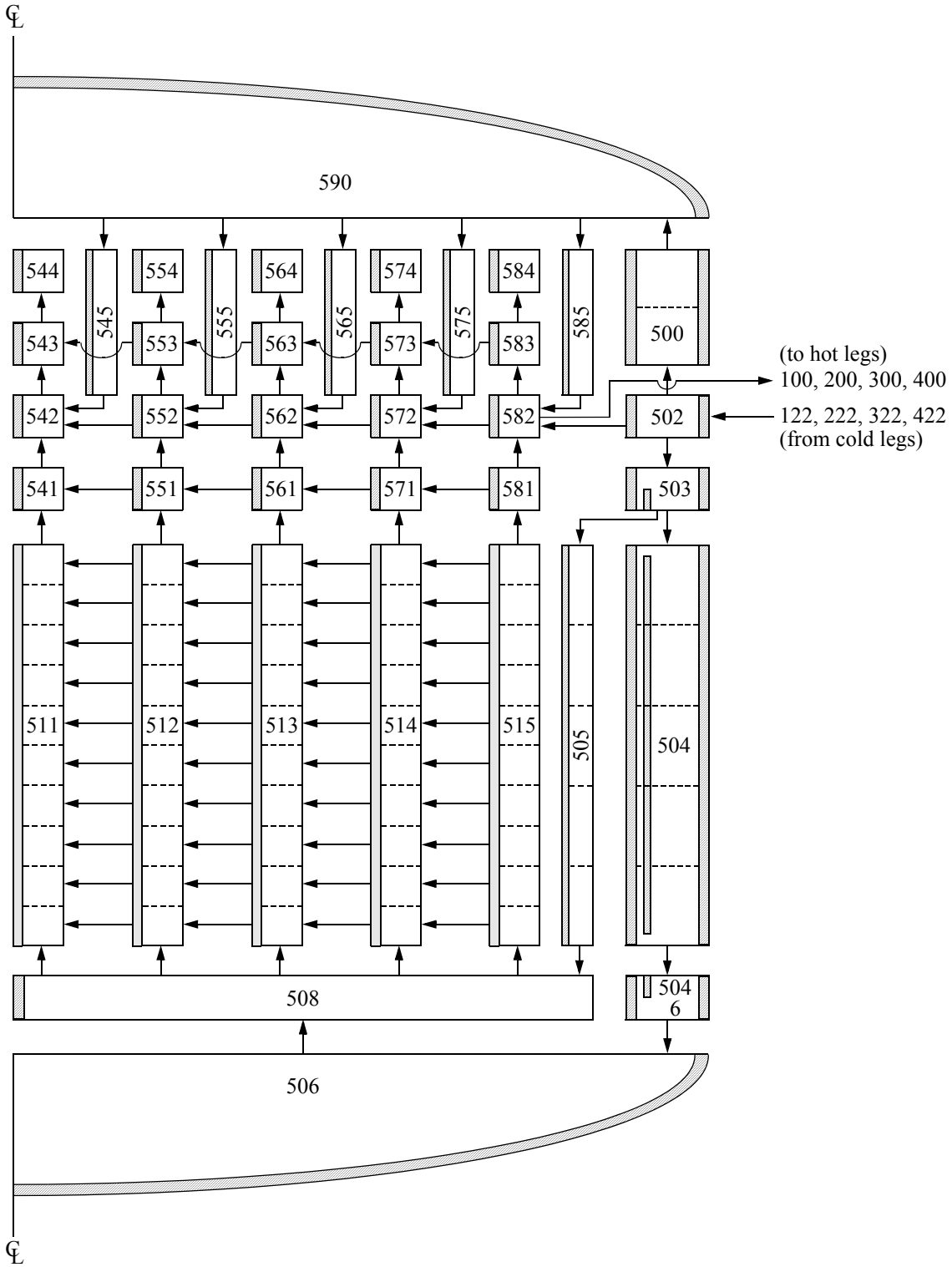

Figure 7. Zion reactor vessel nodalization.

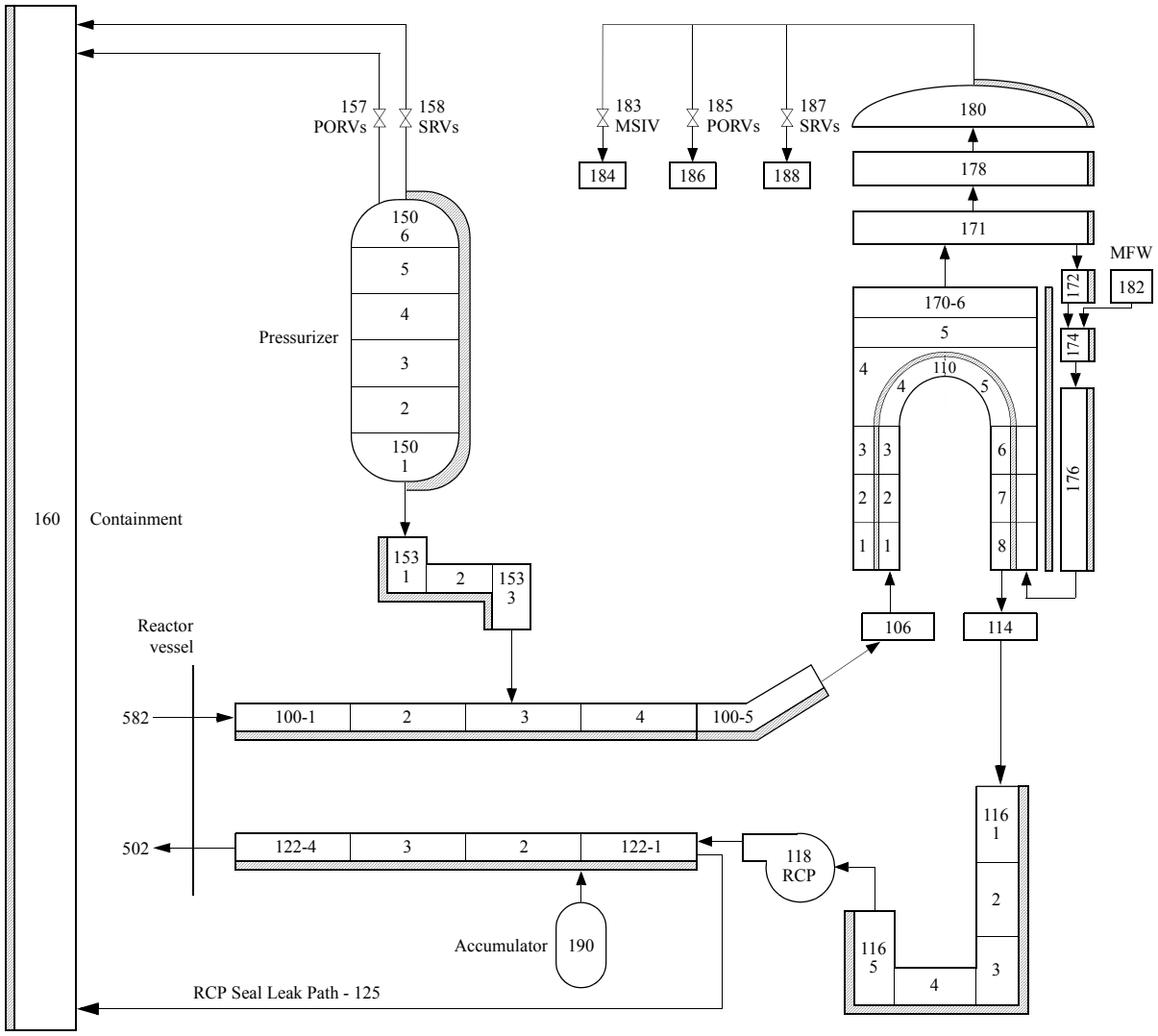

Figure 8. Zion pressurizer loop (Loop A) nodalization without provisions for hot leg countercurrent natural circulation.

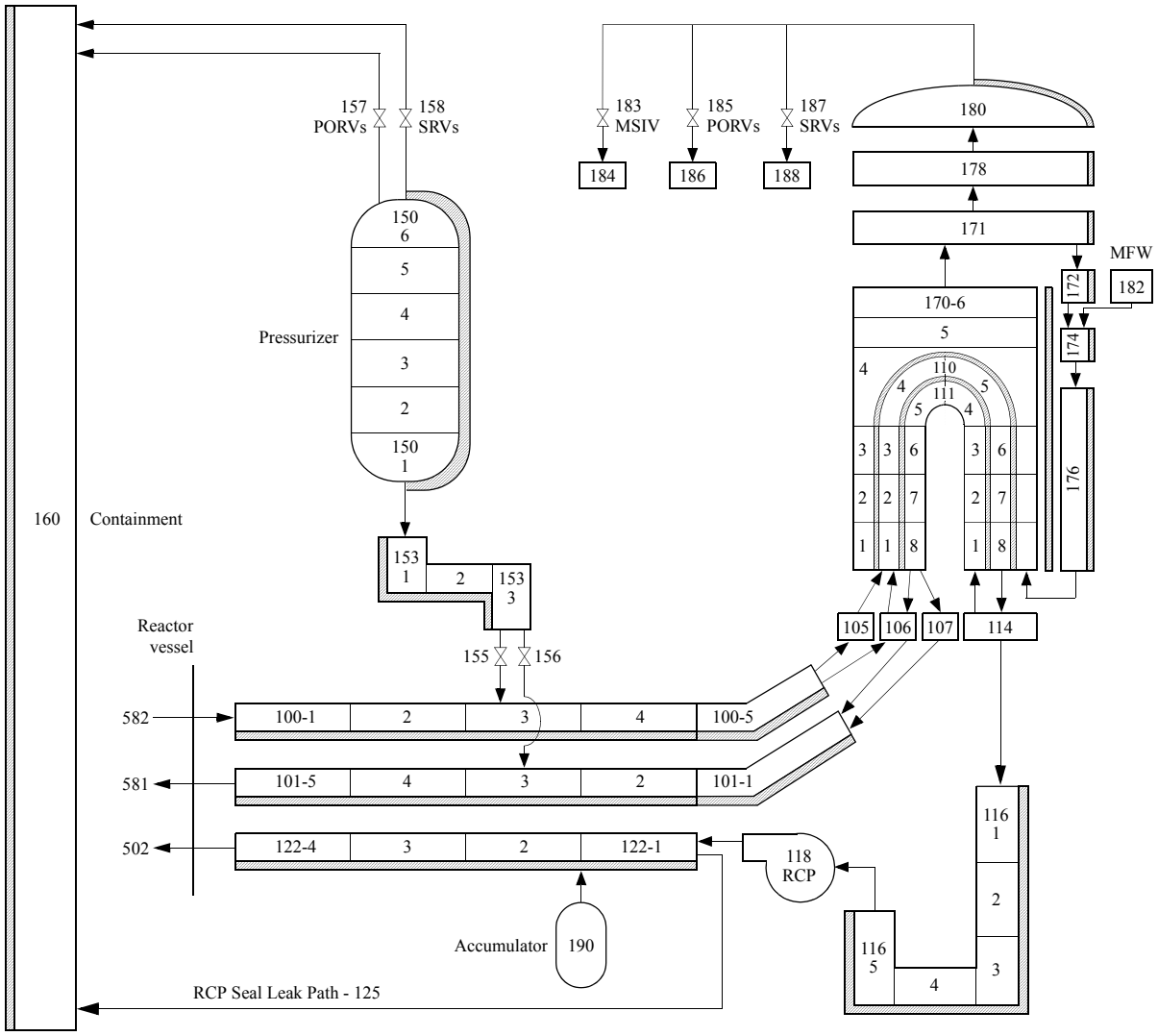

Figure 9. Zion pressurizer loop (Loop A) nodalization with provisions for hot leg countercurrent natural circulation.

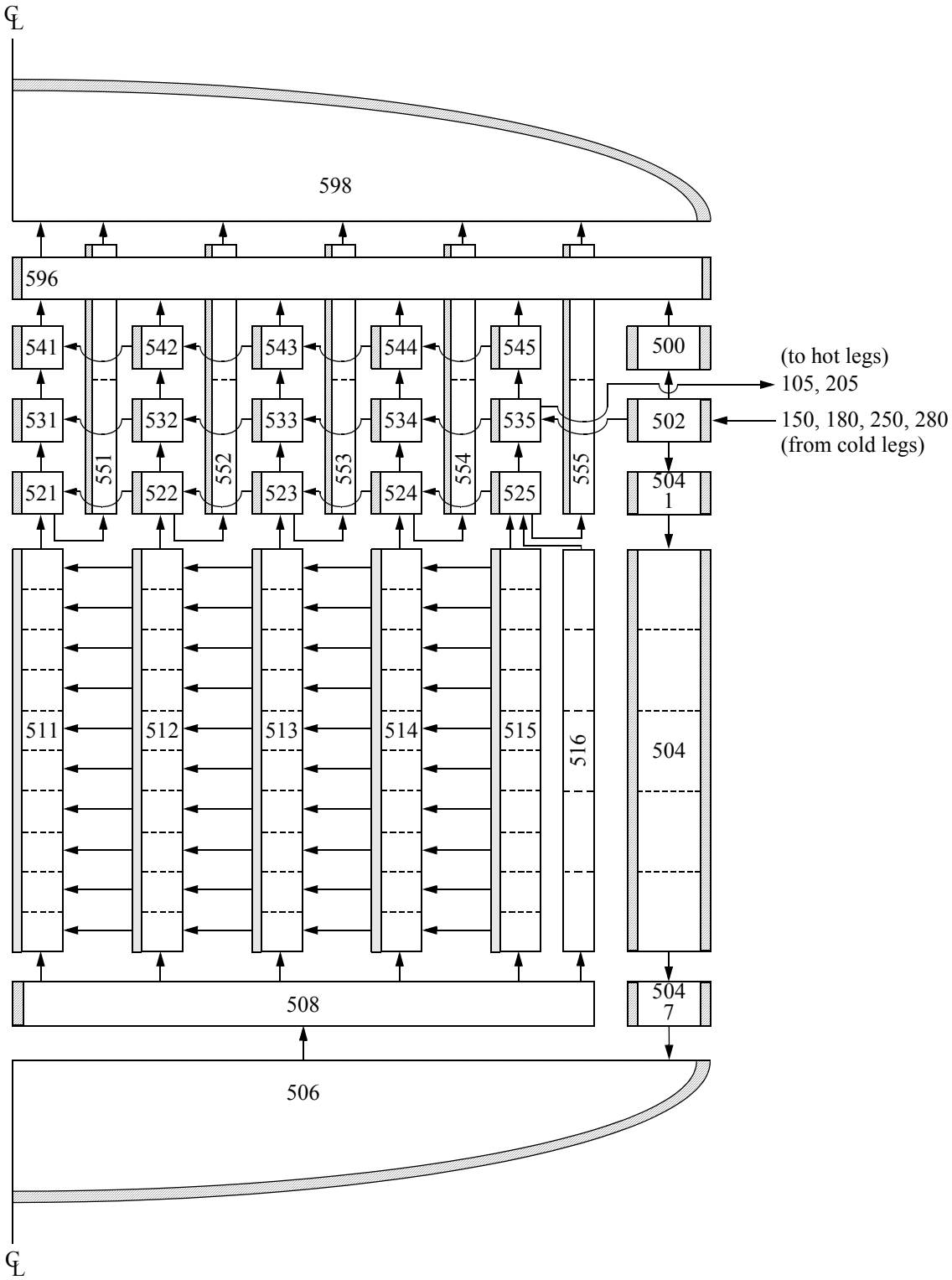

Figure 10. Calvert Cliffs reactor vessel nodalization.

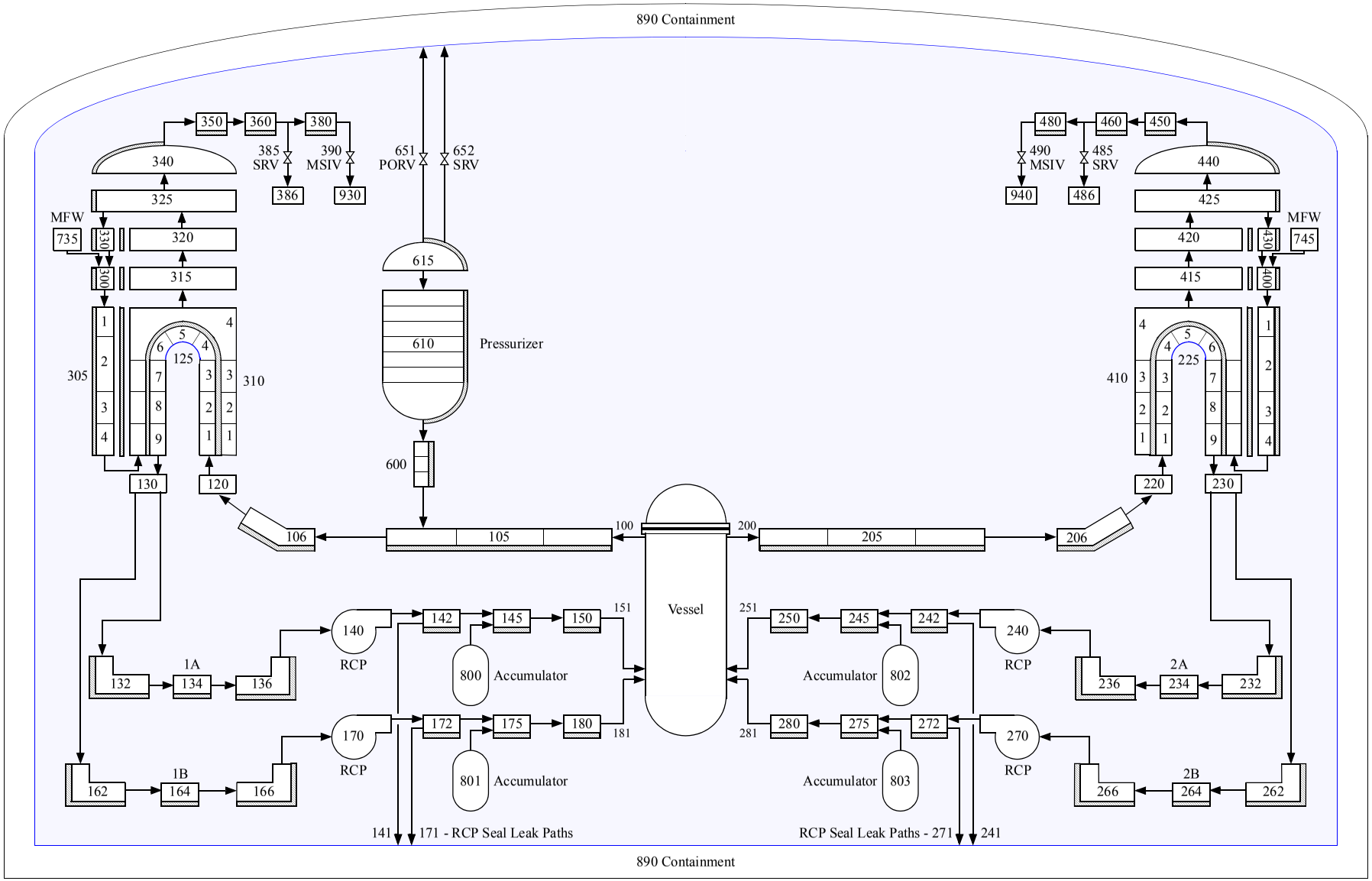

Figure 11. Calvert Cliffs loop nodalization without provisions for hot leg countercurrent natural circulation.

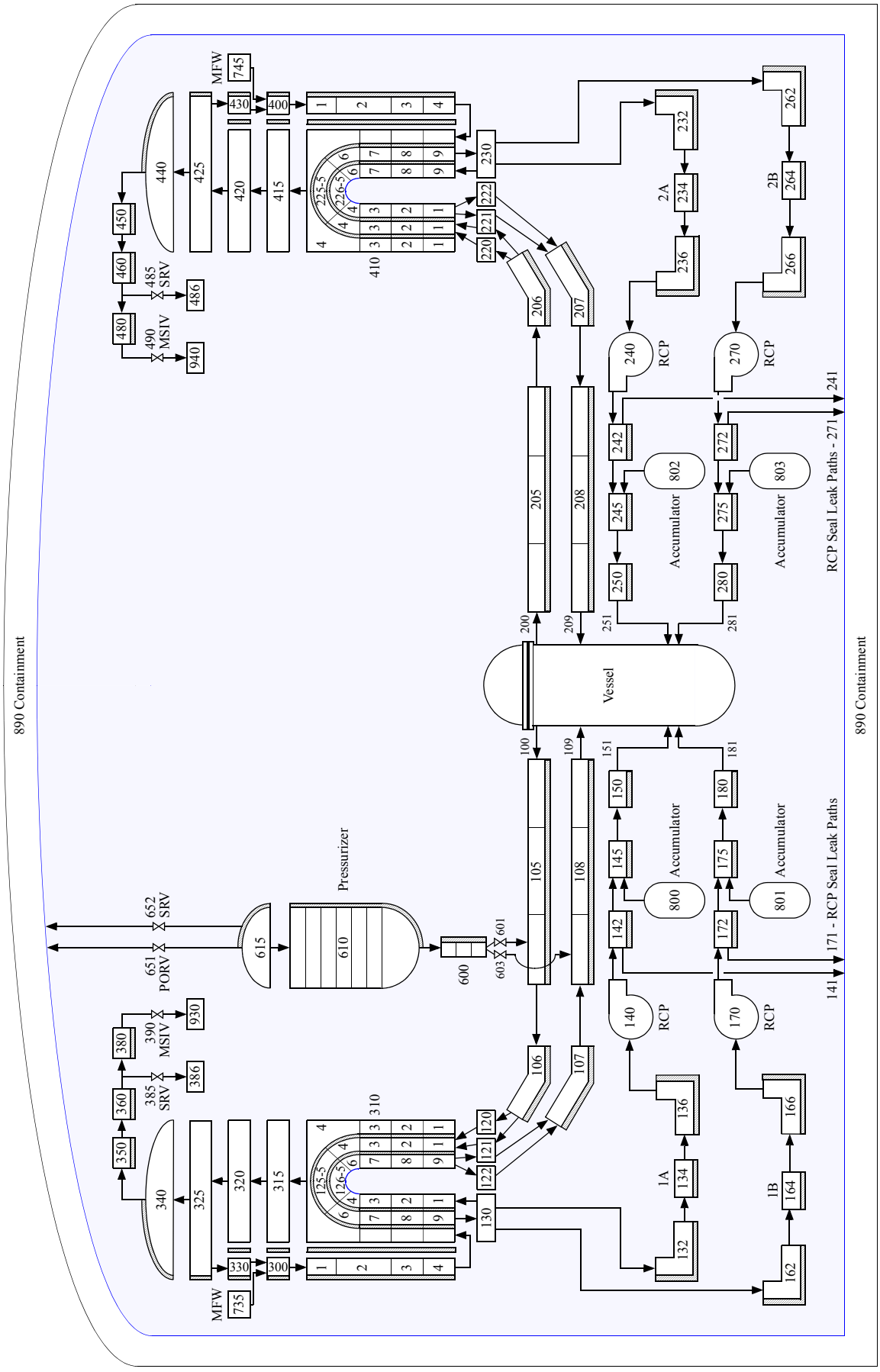

Figure 12. Calvert Cliffs loop nodalization with provisions for hot leg countercurrent natural circulation.

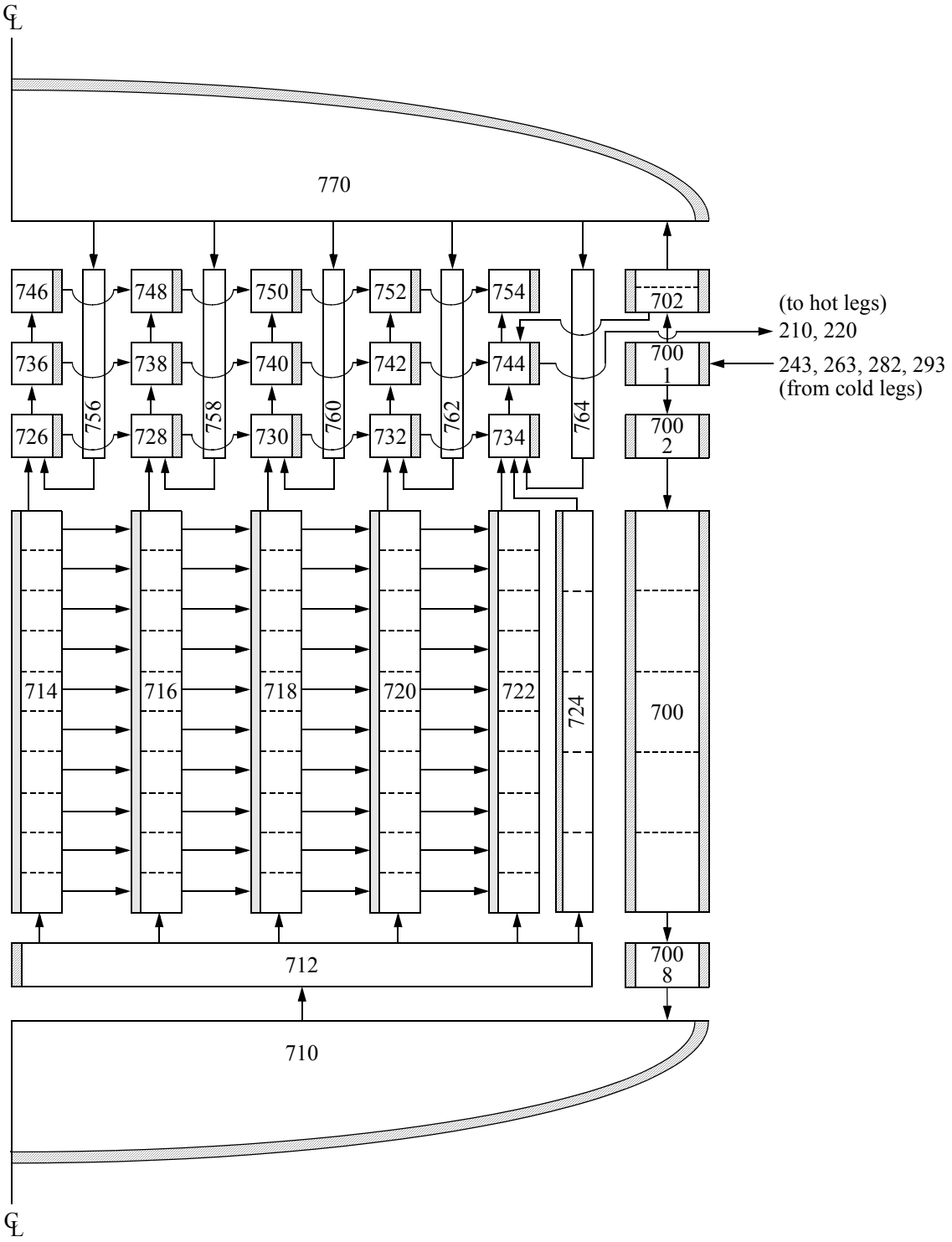

Figure 13. ANO2 reactor vessel nodalization.

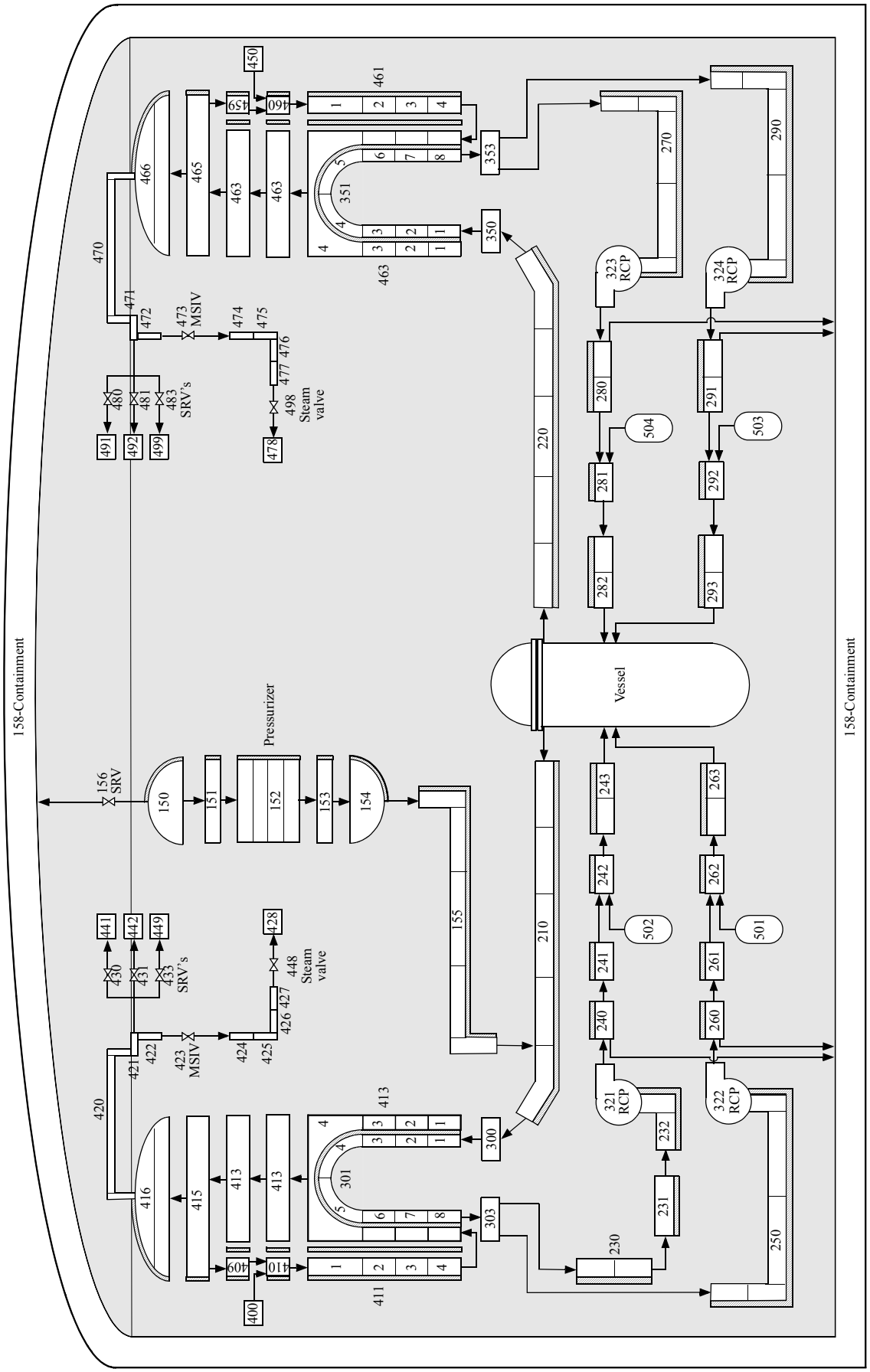

Figure 14. ANO2 loop nodalization without provisions for hot leg countercurrent natural circulation.

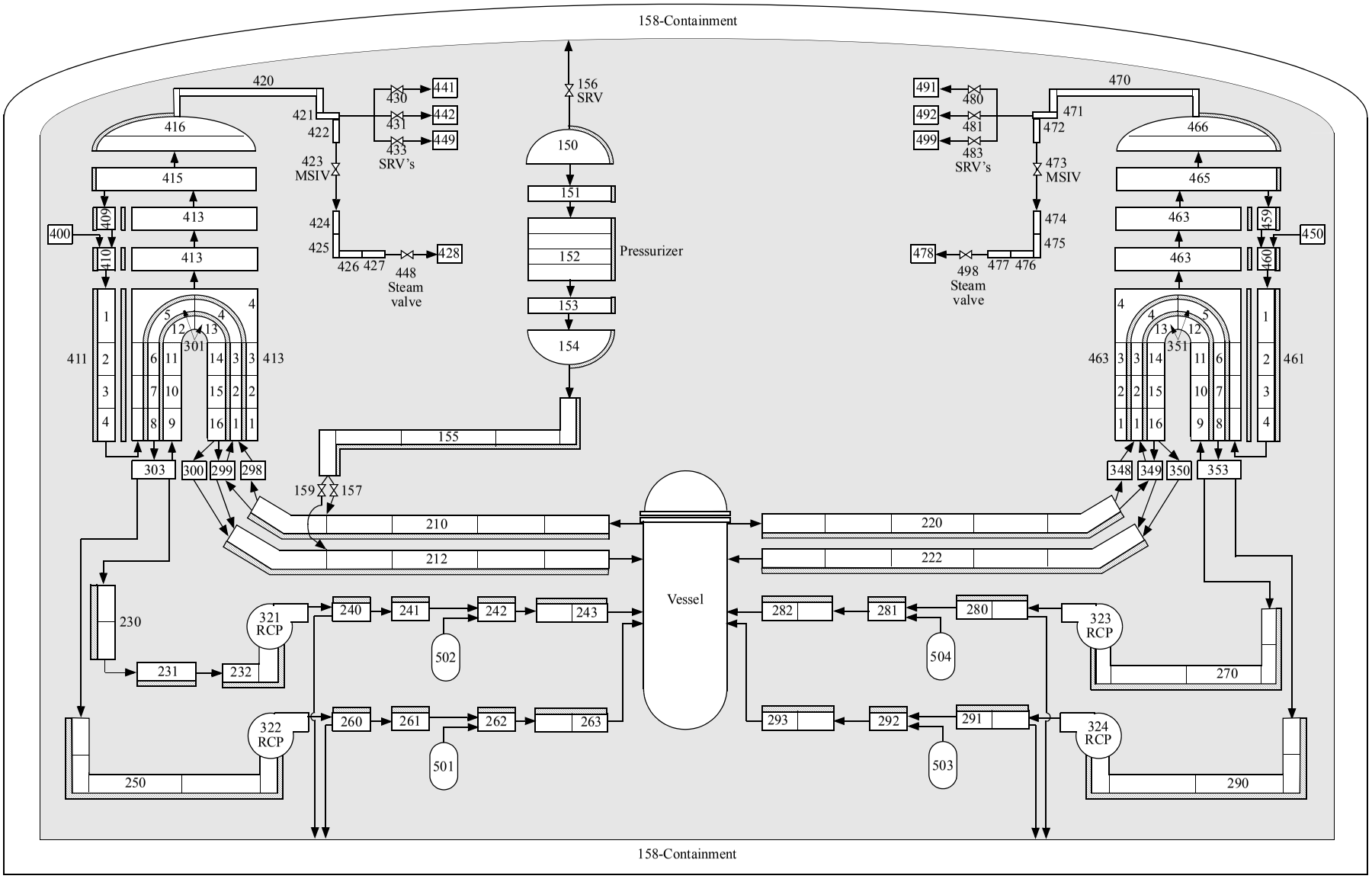

Figure 15. ANO2 loop nodalization with provisions for hot leg countercurrent natural circulation.

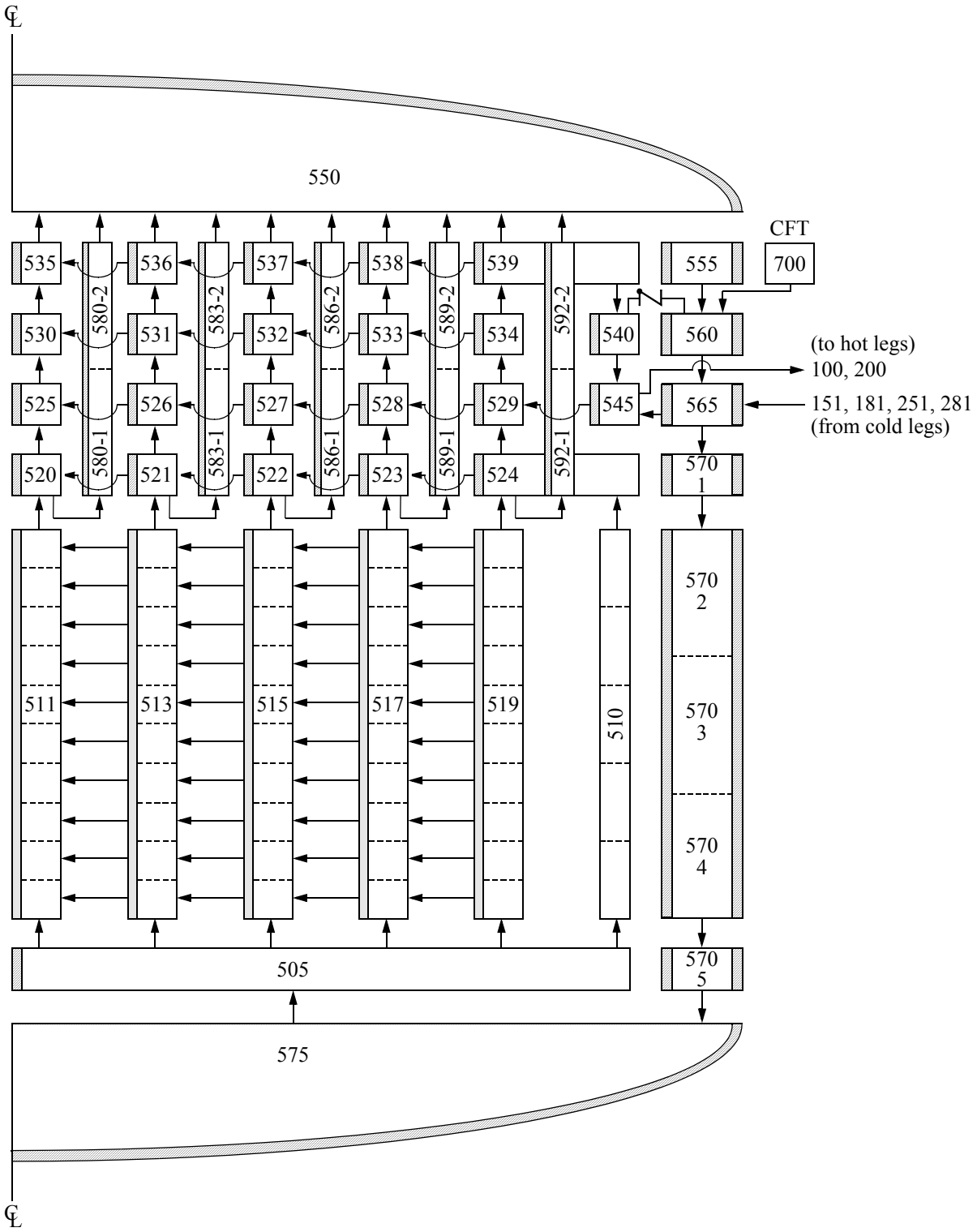

Figure 16. Oconee reactor vessel nodalization.

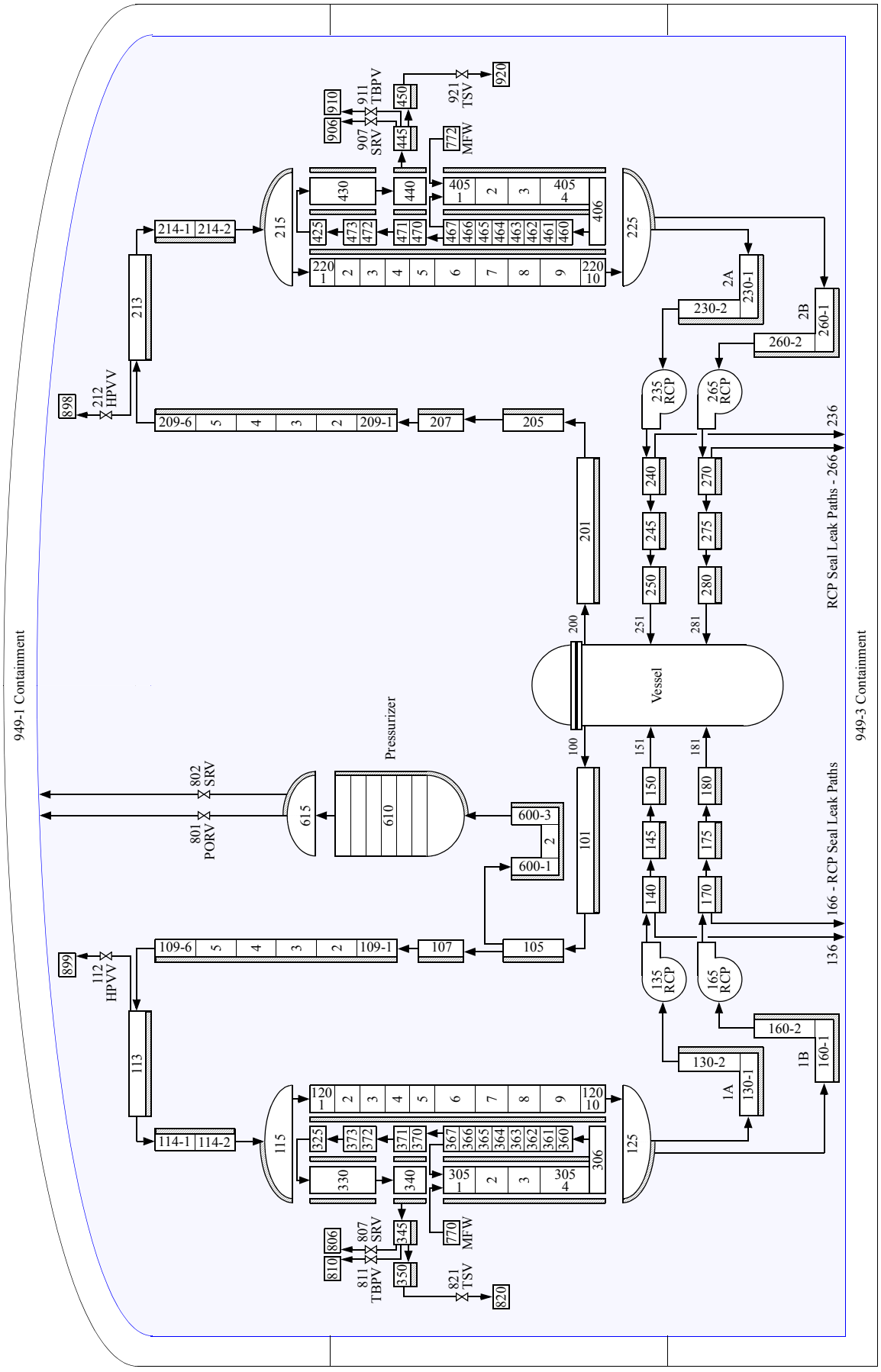

Figure 17. Oconee loop nodalization without provisions for hot leg countercurrent natural circulation.

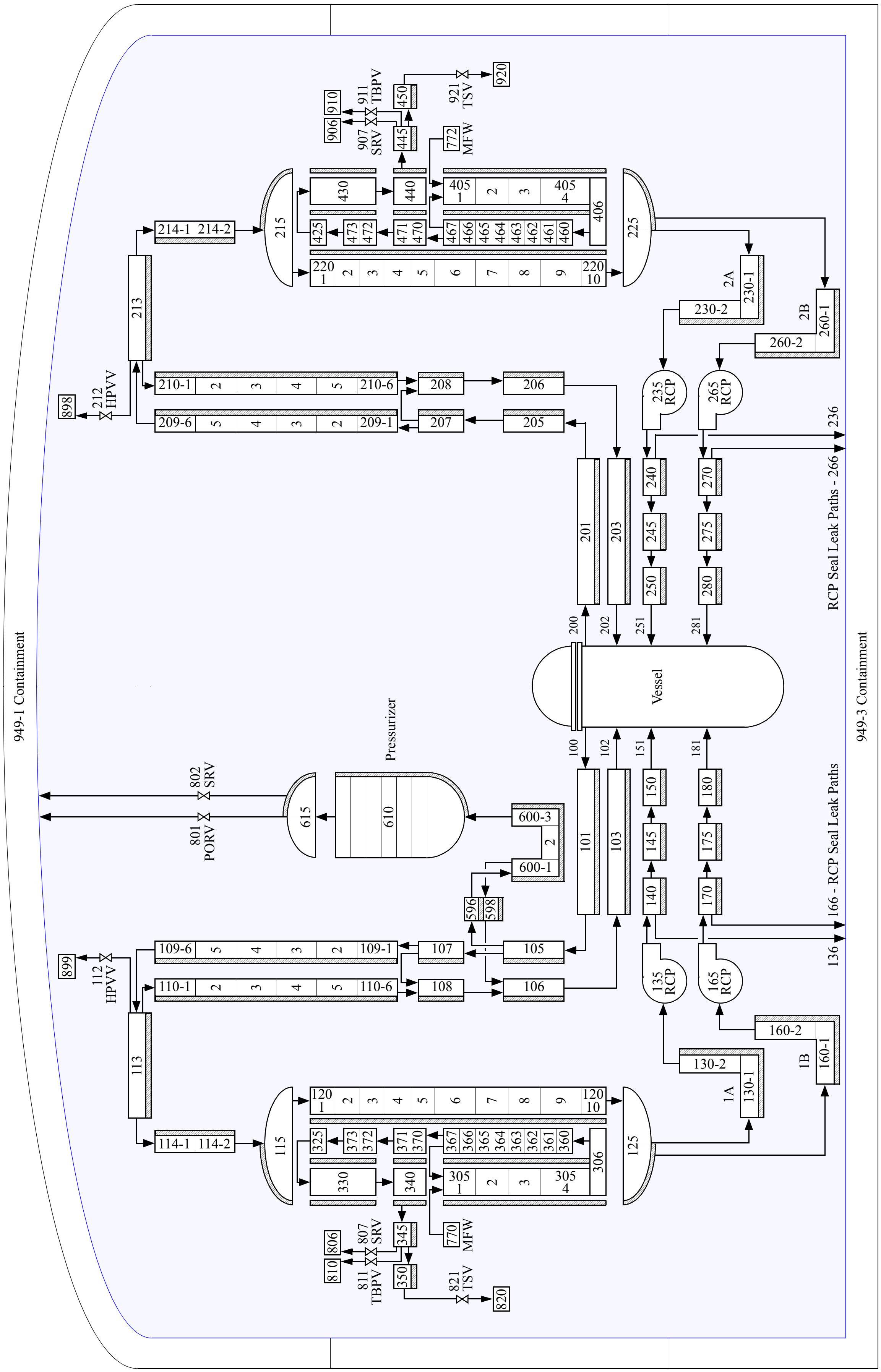

Figure 18. Oconee loop nodalization with provisions for hot leg countercurrent natural circulation.

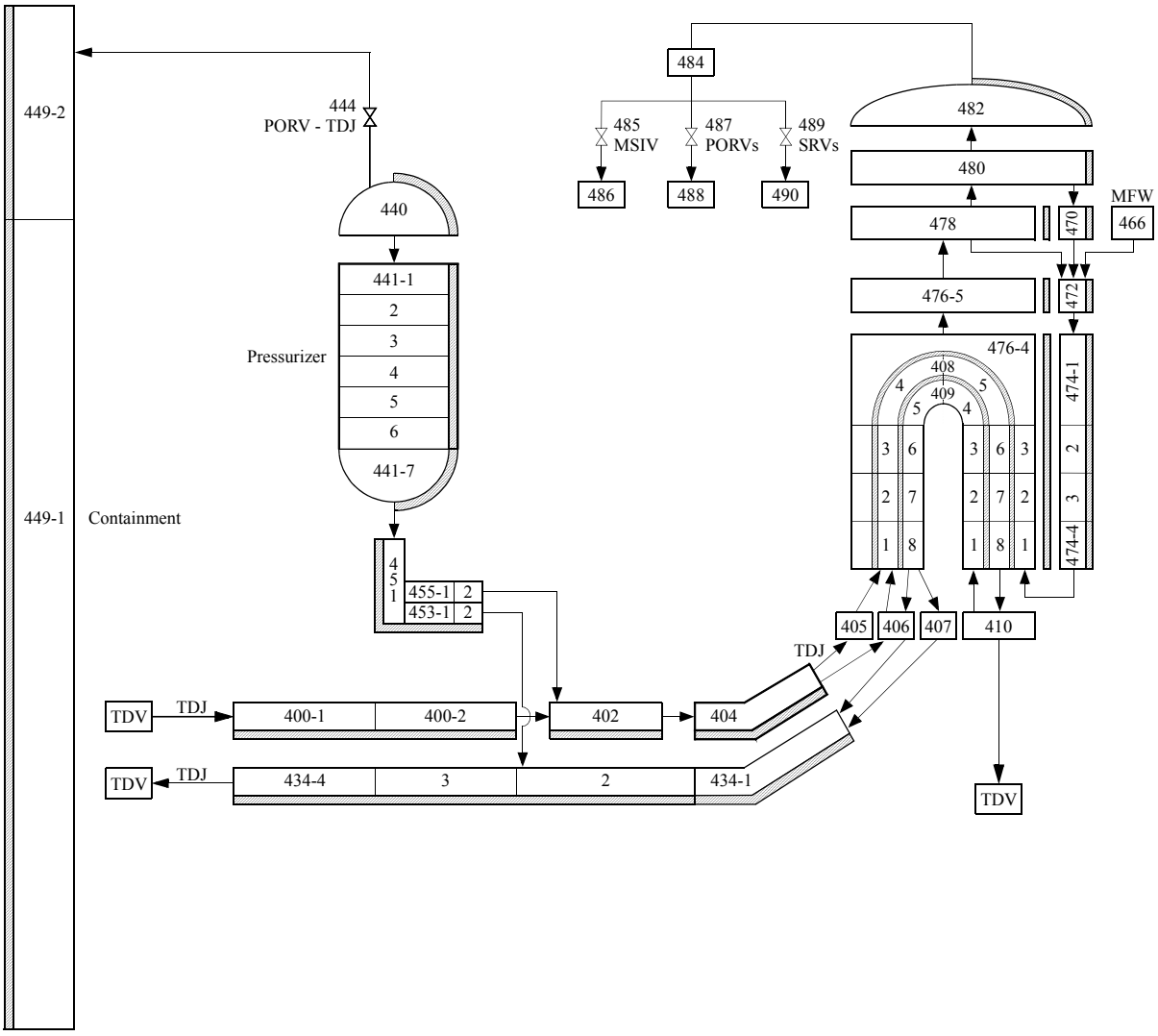

Figure 19. Nodalization used to complete the stand alone loop analyses.

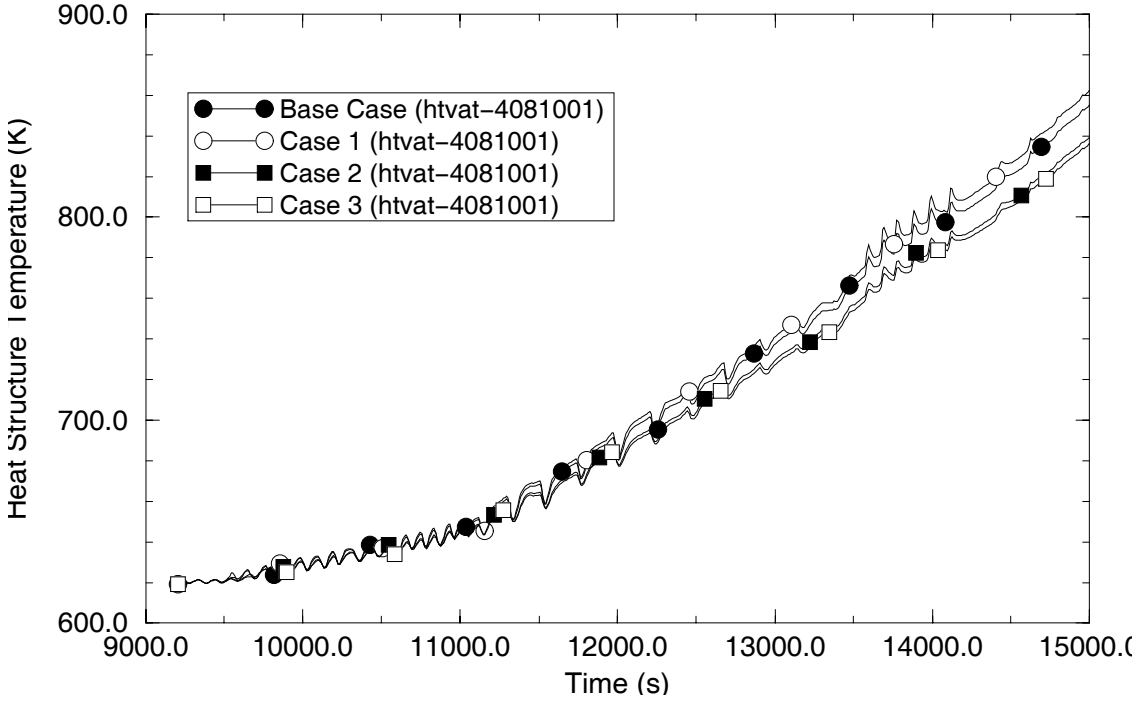

Figure 20. Volume-averaged SG U-tube temperatures at the tube bundle hot spot for the stand alone tube split sensitivity calculations.

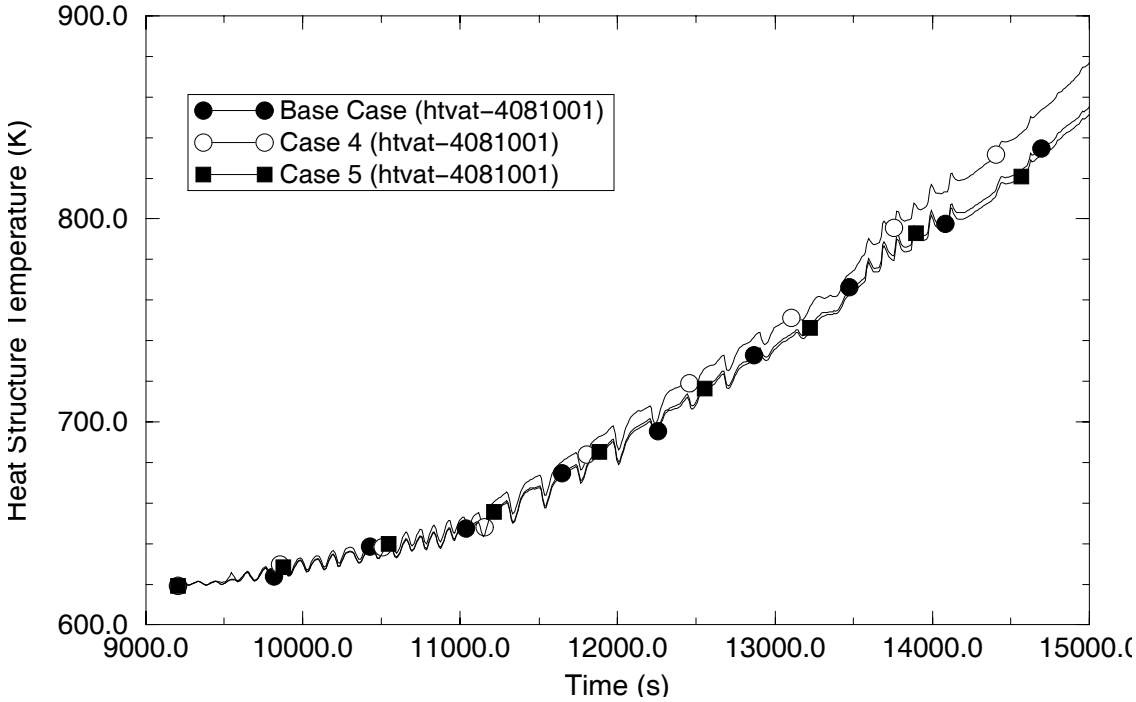

Figure 21. Volume-averaged SG U-tube temperatures at the tube bundle hot spot for the stand alone mixing fraction sensitivity calculations.

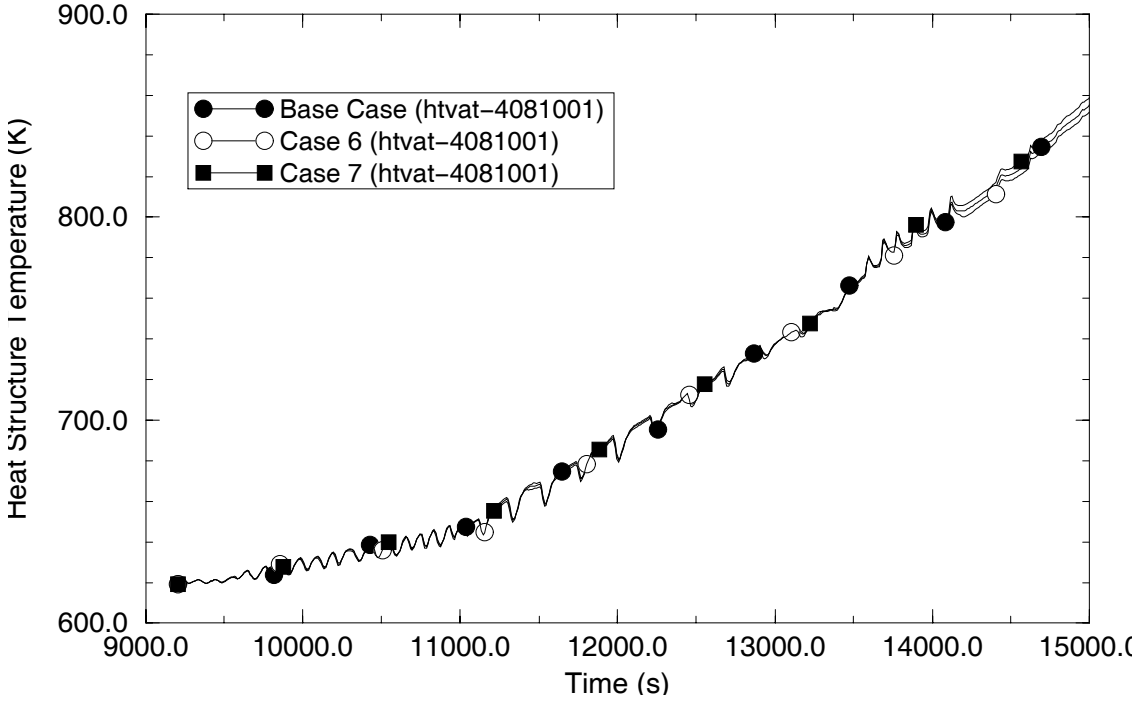

Figure 22. Volume-averaged SG U-tube temperatures at the tube bundle hot spot for the stand alone recirculation ratio sensitivity calculations.

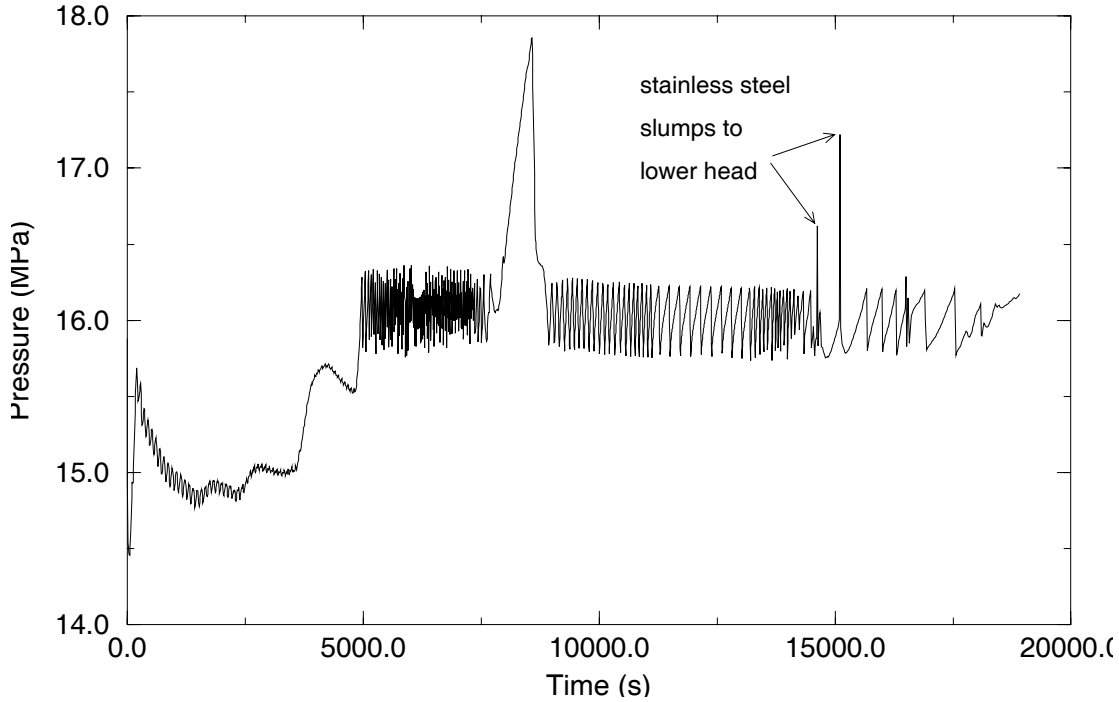

Figure 23. RCS pressure in the reactor vessel lower head for Surry Case SUR-01.

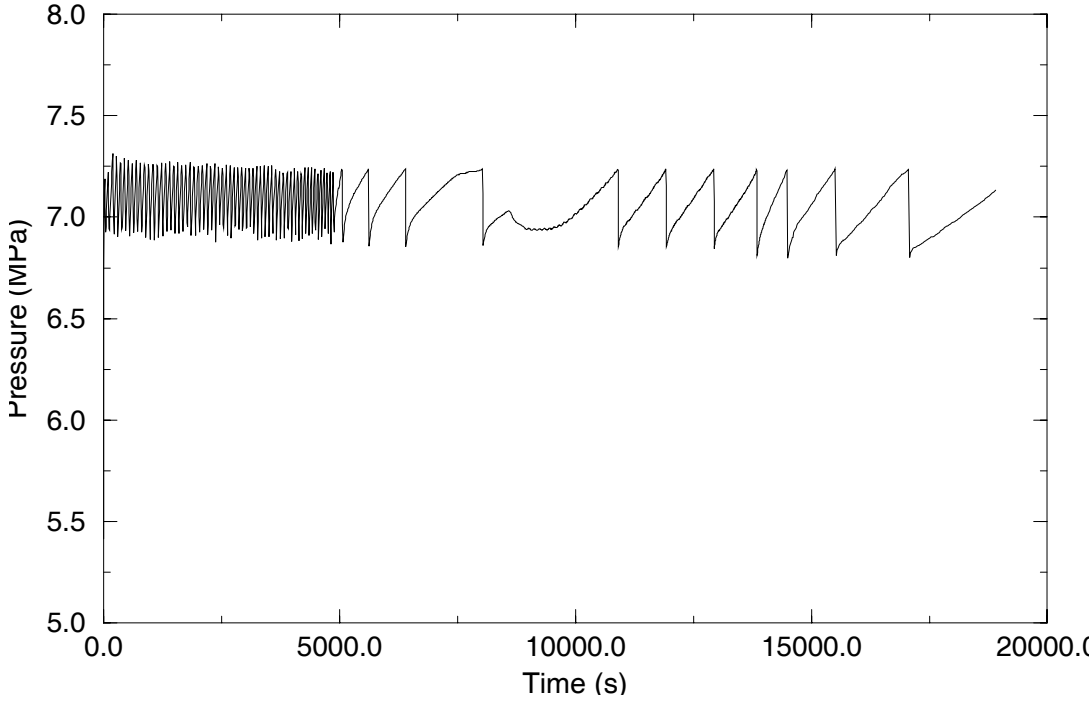

Figure 24. SG secondary pressure for Surry Case SUR-01.

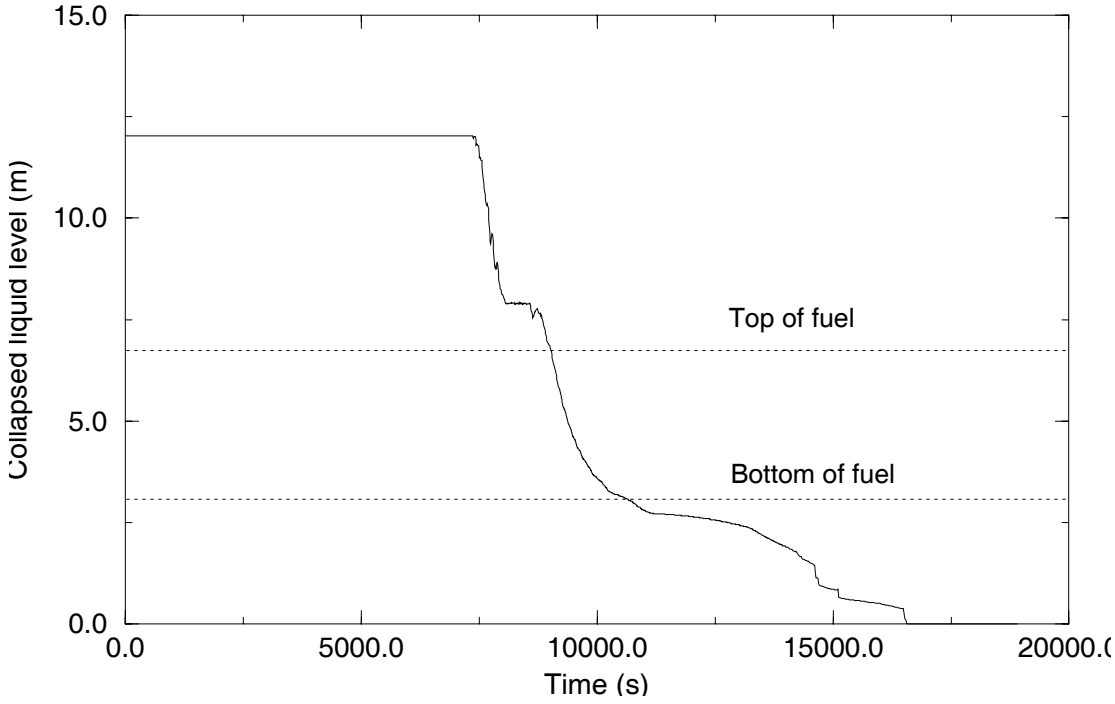

Figure 25. Reactor vessel collapsed liquid level for Surry Case SUR-01.

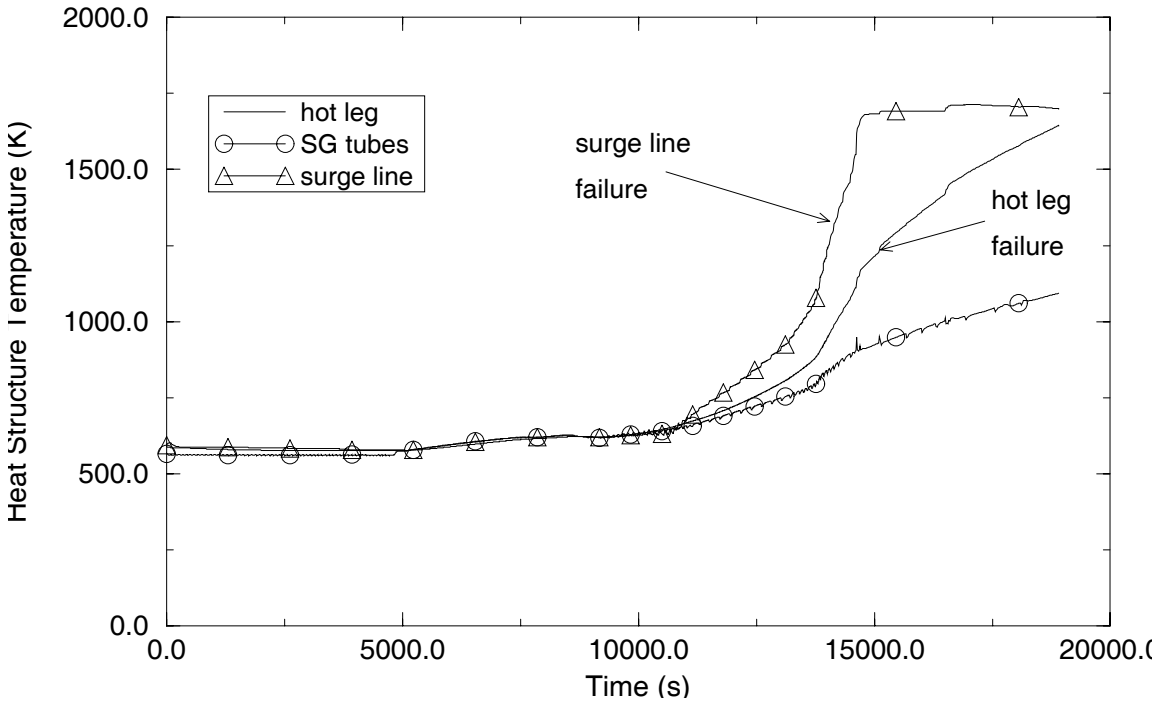

Figure 26. Volume-averaged temperatures of pressurizer loop piping for Surry Case SUR-01.

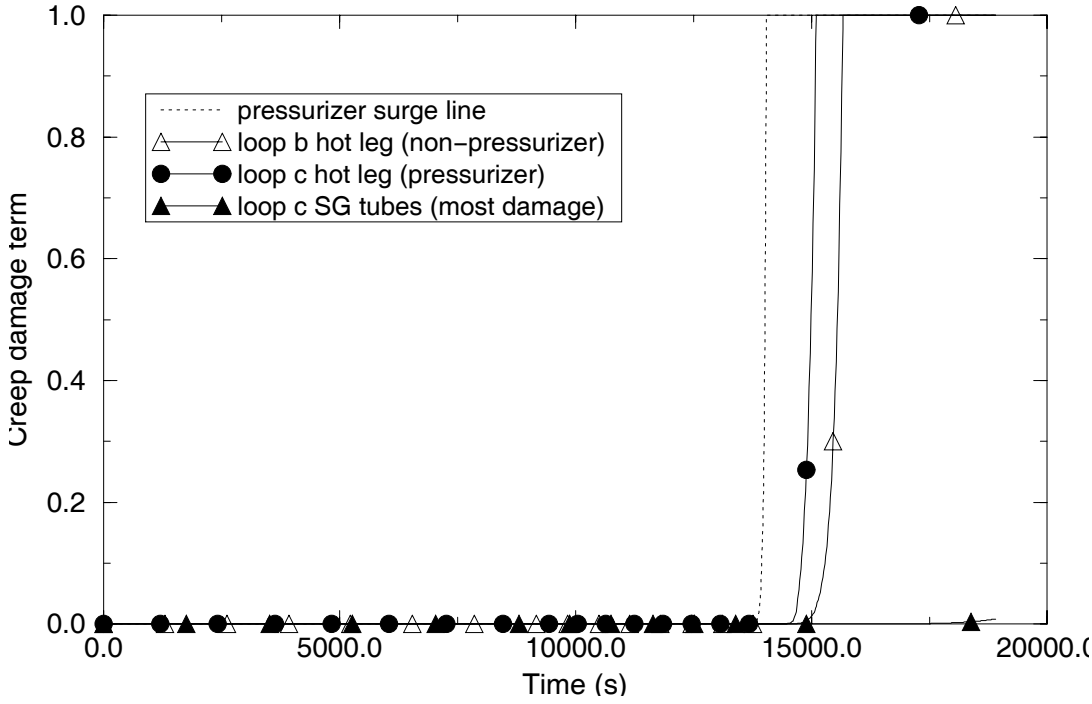

Figure 27. Creep damage terms for RCS piping in Surry Case SUR-01.

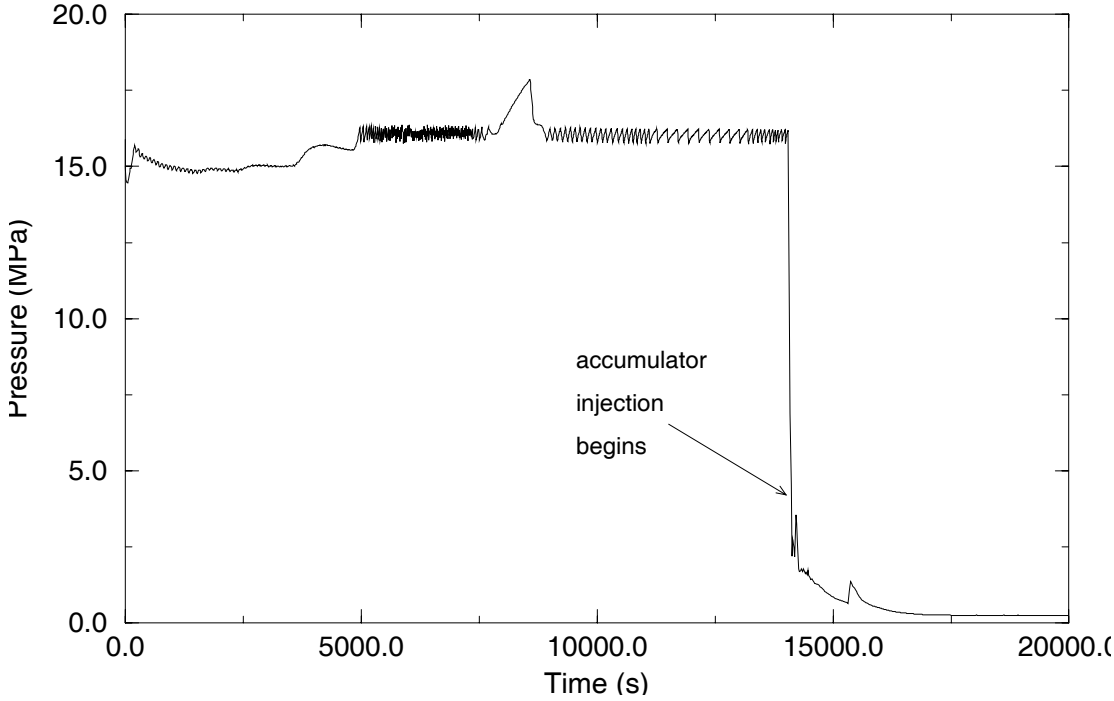

Figure 28. RCS pressure in the reactor vessel lower head for Surry Case SUR-02.

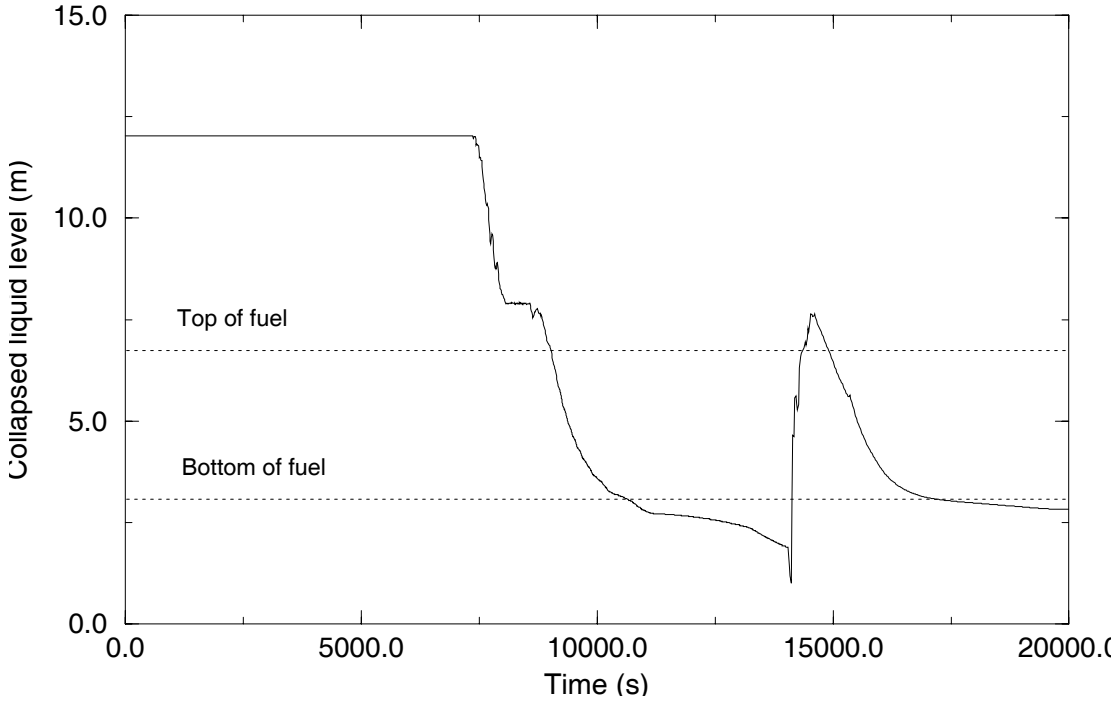

Figure 29. Reactor vessel collapsed liquid level for Surry Case SUR-02.

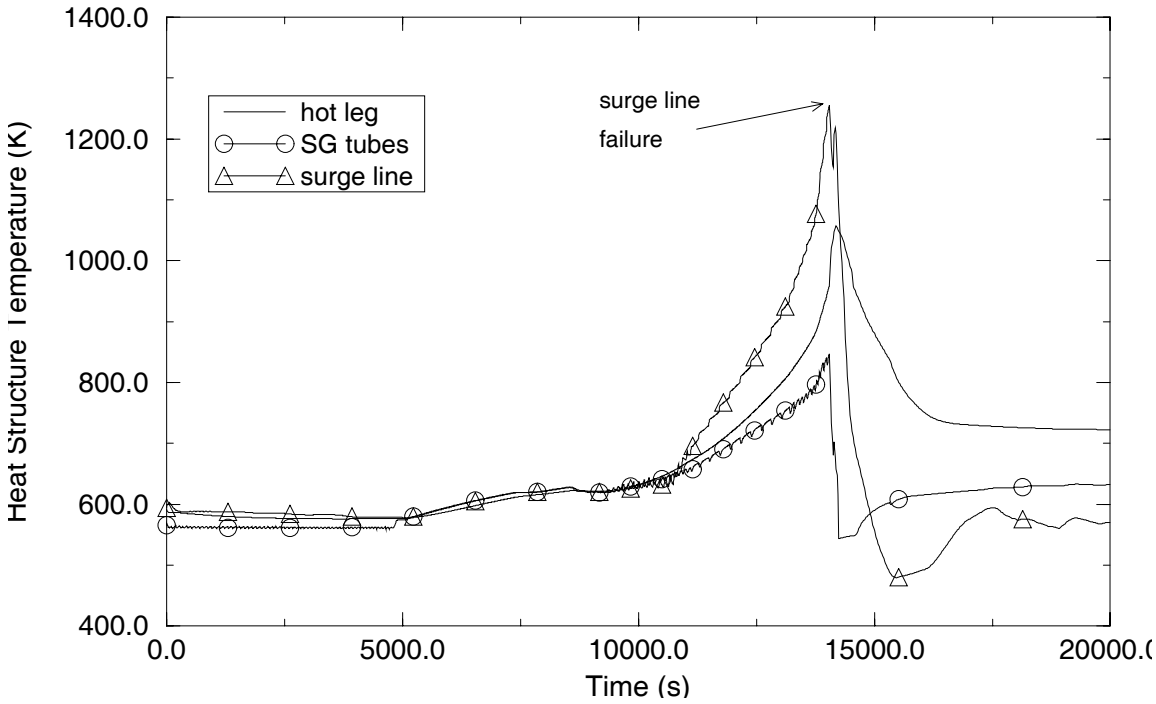

Figure 30. Volume-averaged temperatures of pressurizer loop piping for Surry Case SUR-02.

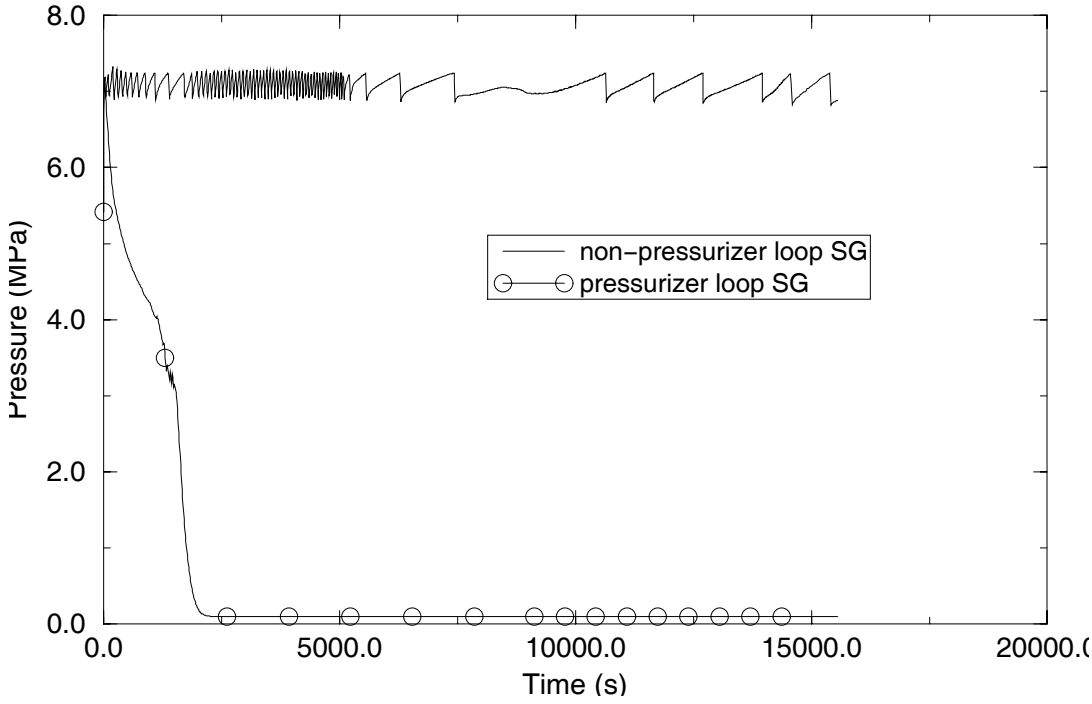

Figure 31. SG secondary pressures for Surry Case SUR-03.

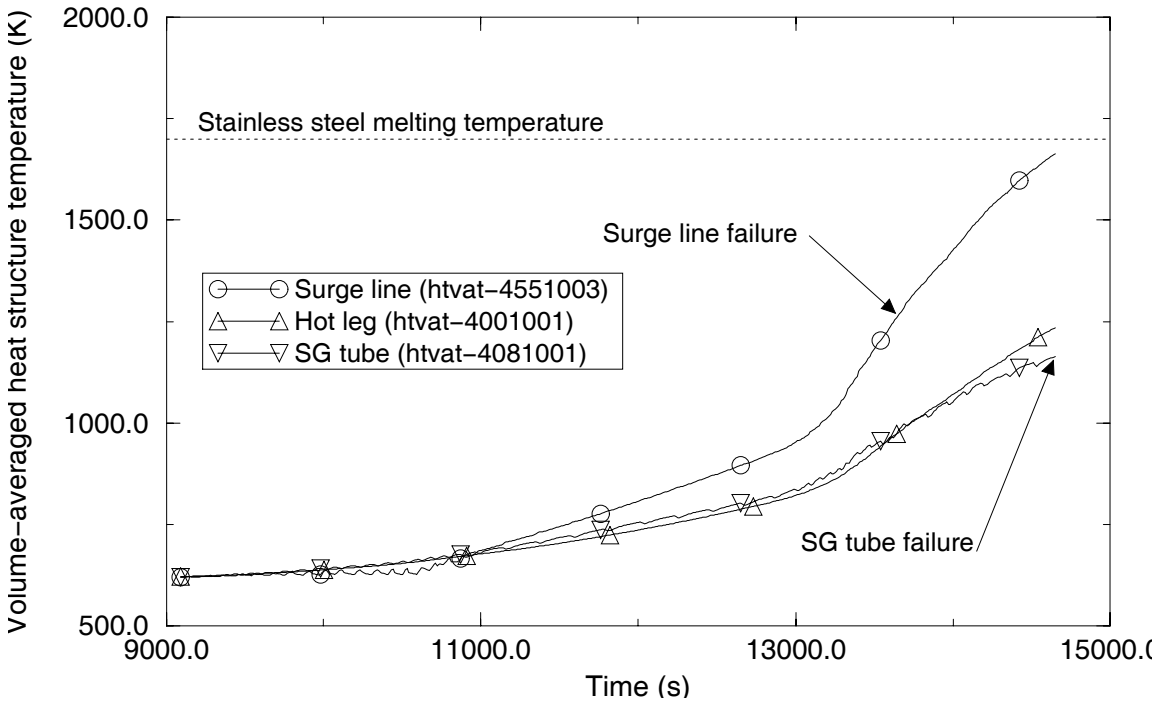

Figure 32. Volume-averaged temperatures of pressurizer loop piping for Surry Case SUR-03.

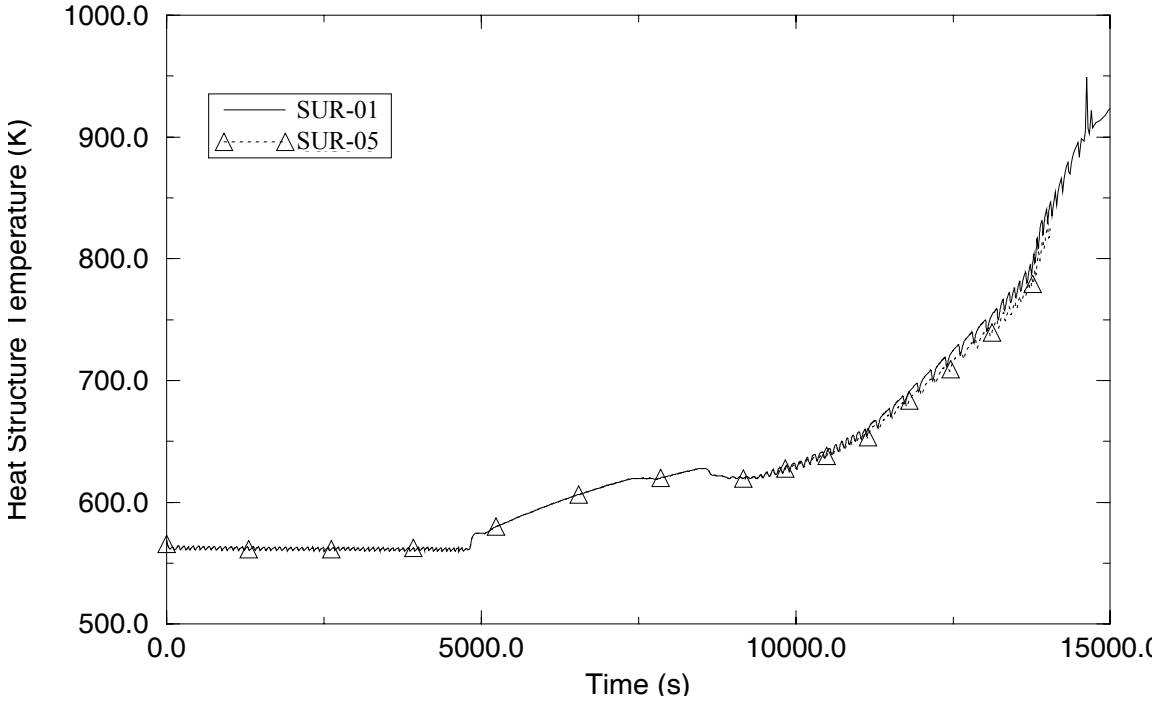

Figure 33. Comparison between volume-averaged temperatures of the pressurizer loop SG tubes for Surry Cases SUR-01 and SUR-05.

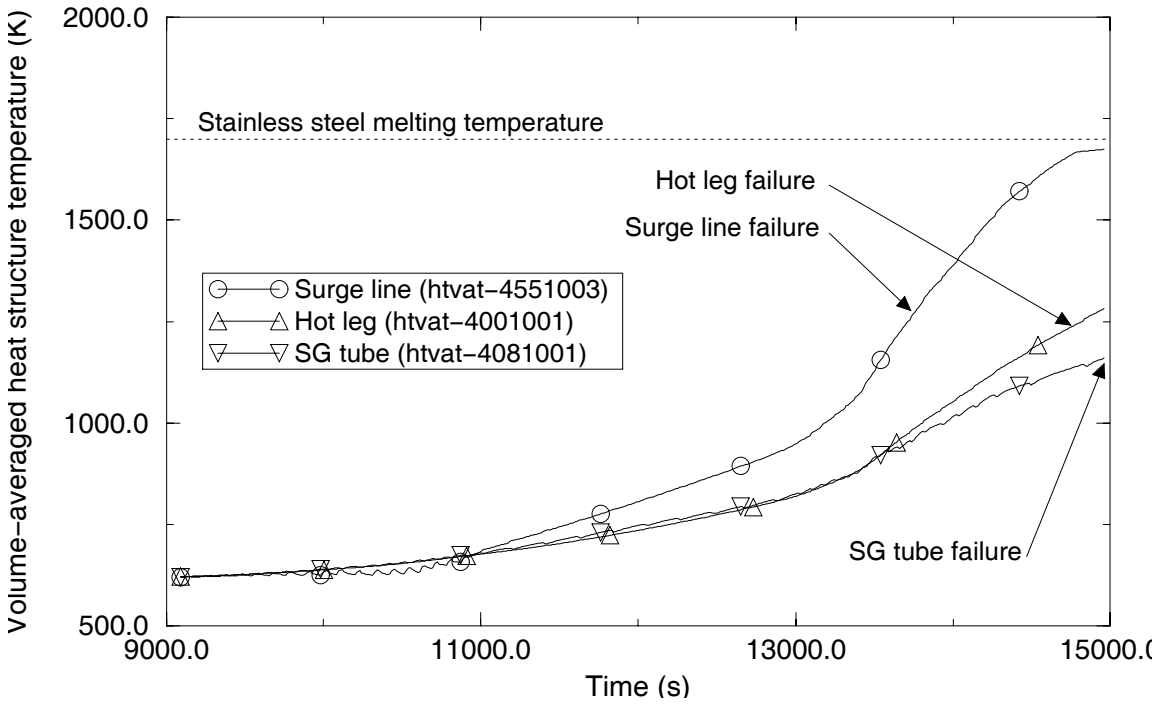

Figure 34. Volume-averaged temperatures of pressurizer loop piping for Surry Case SUR-06.

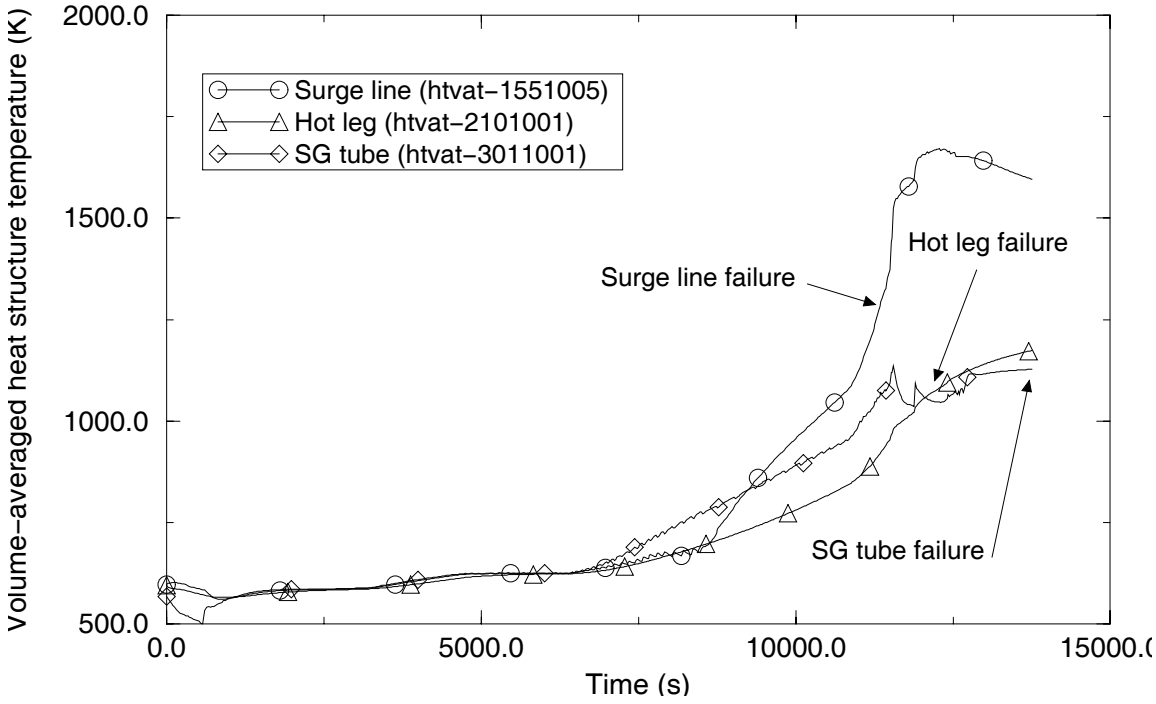

Figure 35. Volume-averaged temperatures of pressurizer loop piping for ANO2 Case ANO2-01.

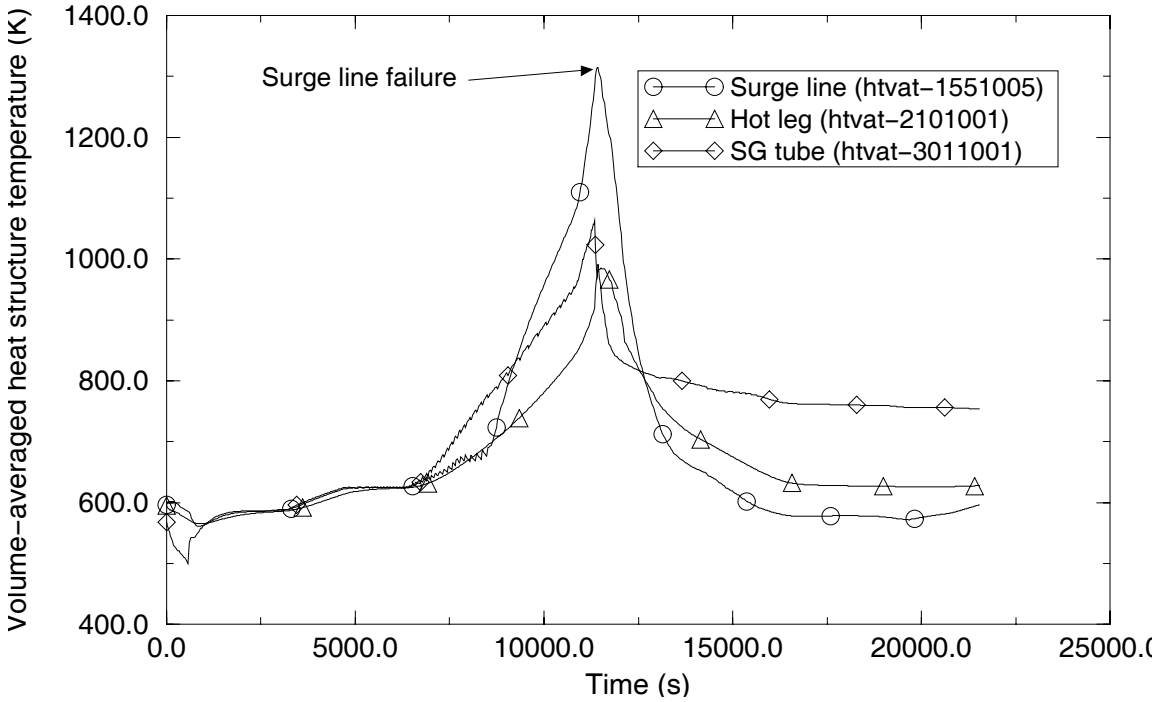

Figure 36. Volume-averaged temperatures of pressurizer loop piping for ANO2 Case ANO2-02.

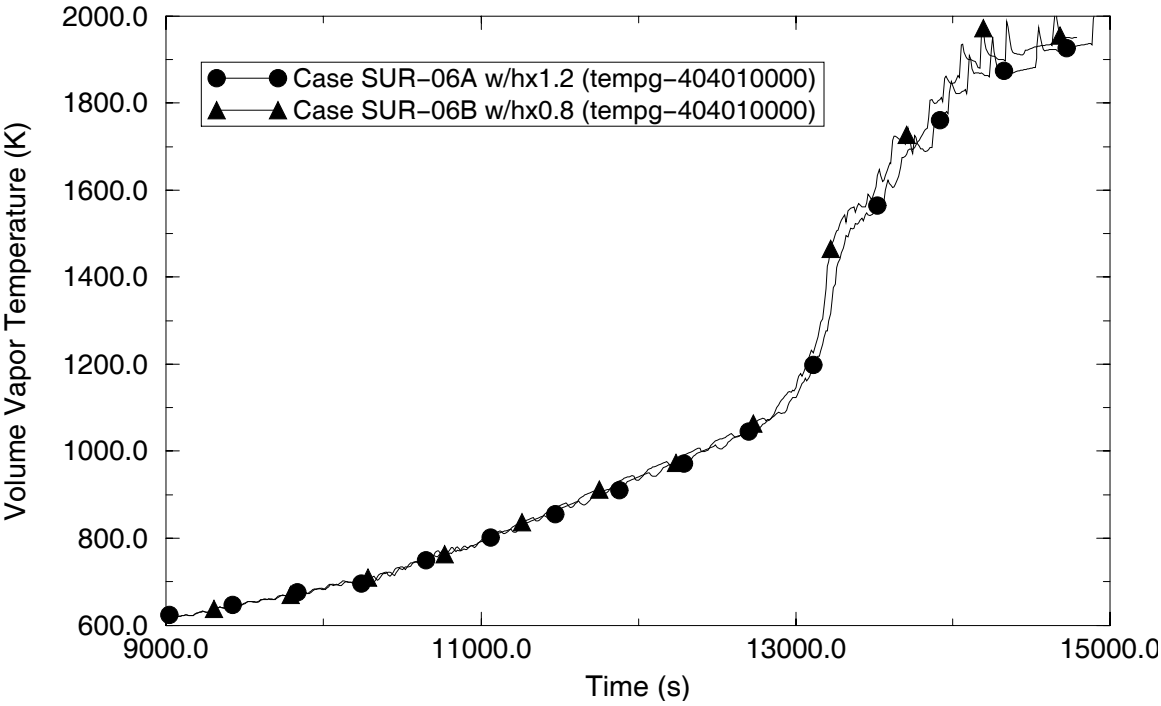

Figure 37. Pressurizer loop vapor temperatures upstream of the SGs for Surry Cases SUR-06A and SUR-06B.

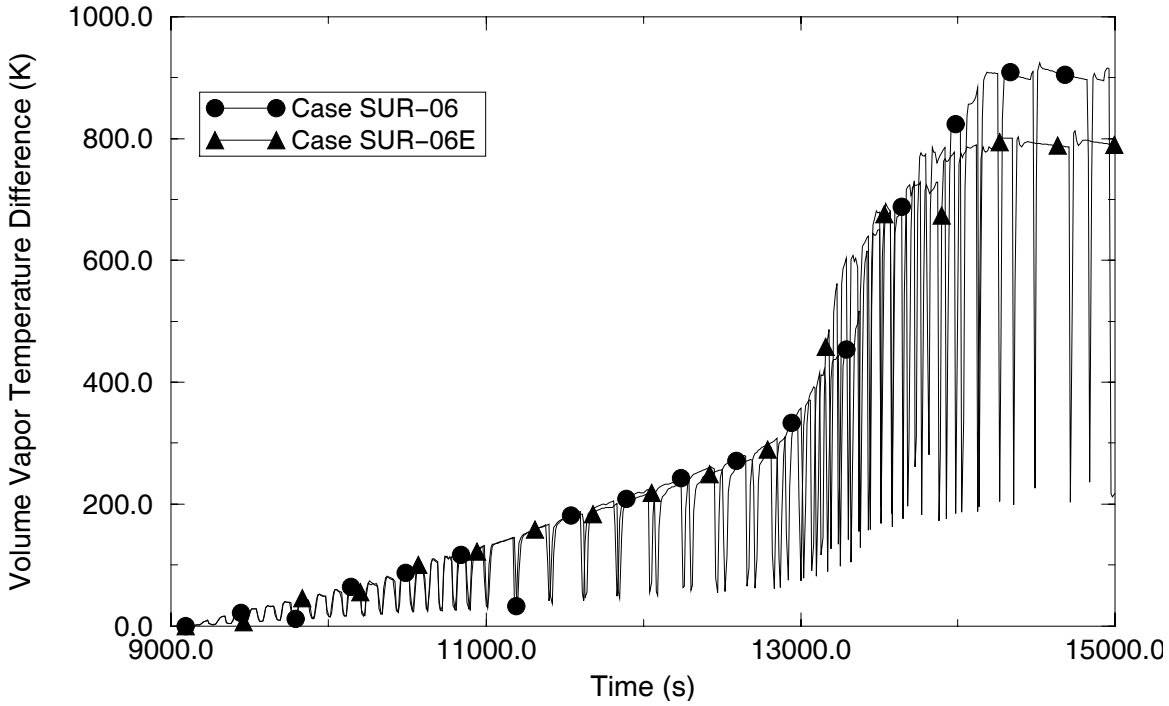

Figure 38. Pressurizer loop hot leg nozzle vapor temperature differences for Surry Cases SUR-06 and SUR-06E.

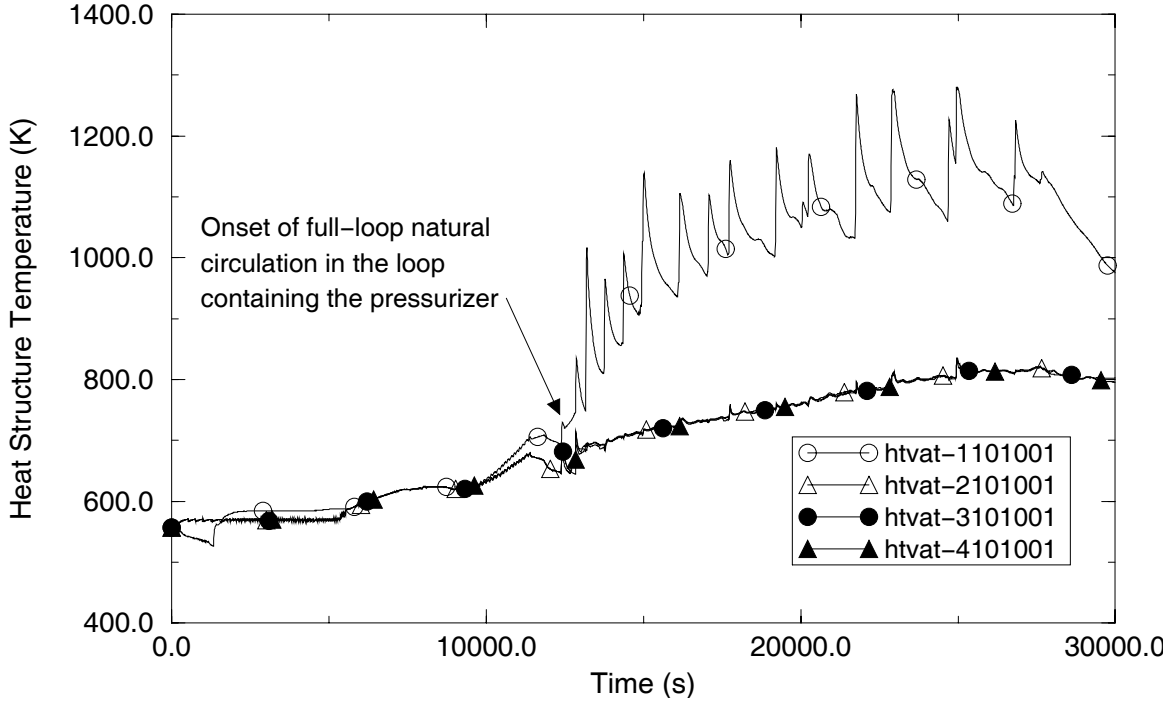

Figure 39. SG tube temperatures for Zion Case ZI-01.

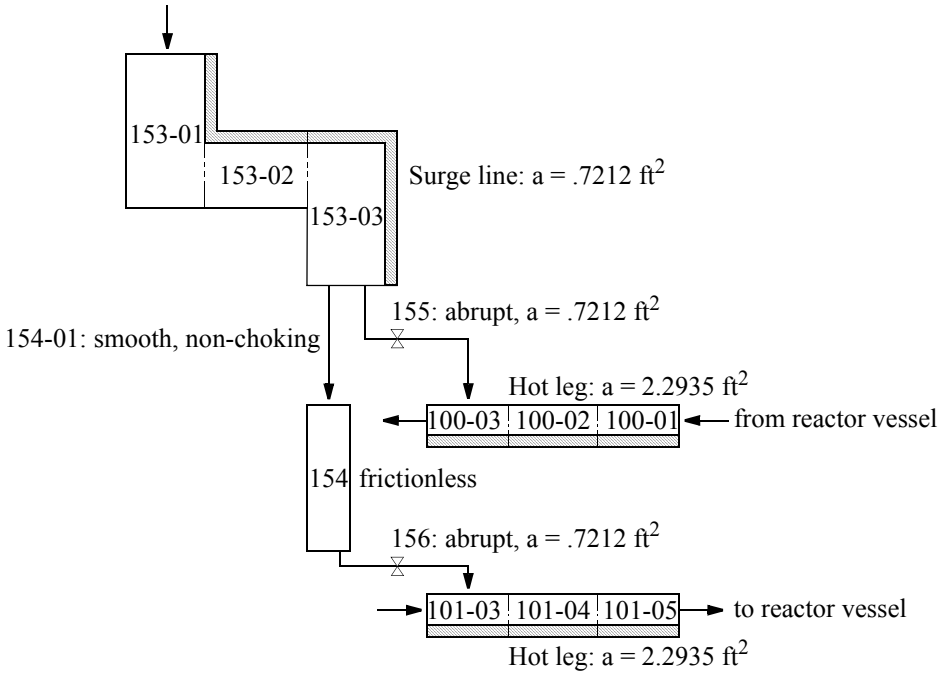

(a) Original hot leg/surge line connection

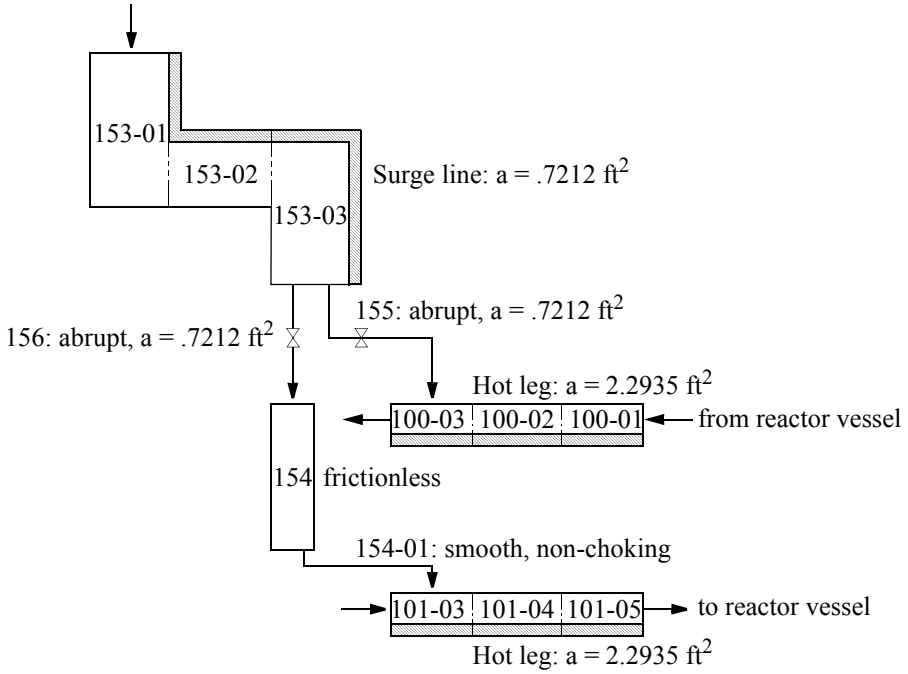

(b) Modified hot leg/surge line connection

Figure 40. Hot leg/surge line connections for the Zion PWR.

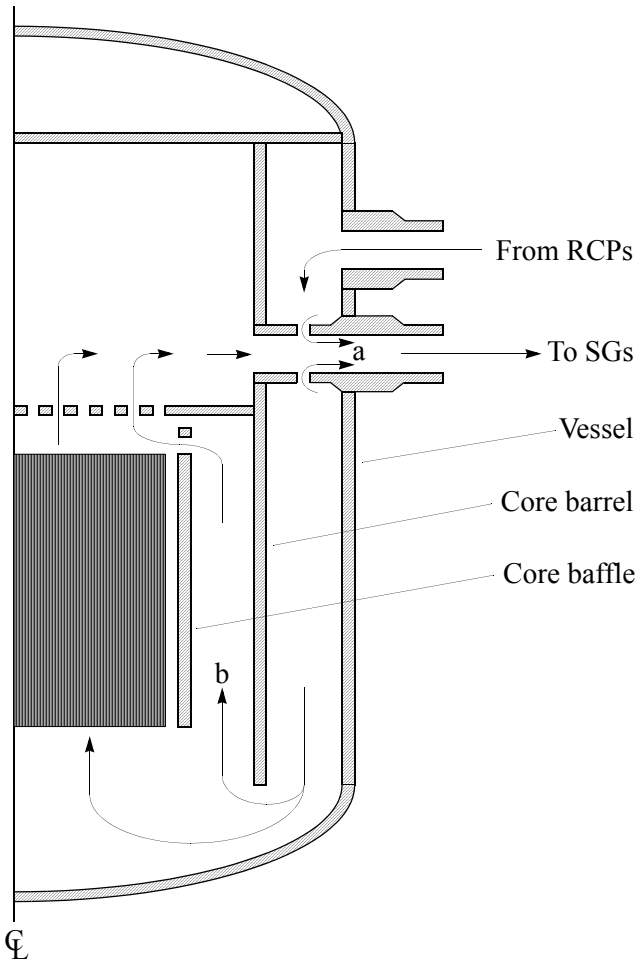

Figure 41. Normal circulation patterns in a PWR showing (a) DC-HL bypass and (b) core bypass flows.

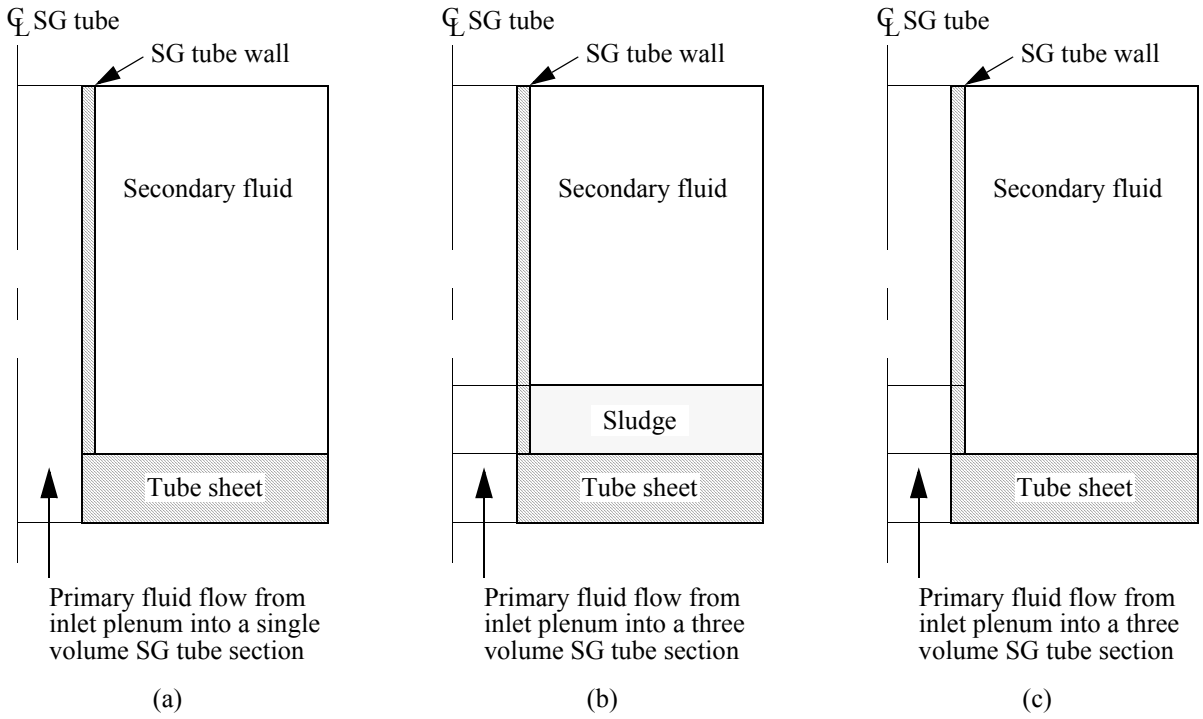

Figure 42. Details typical of regions near the SG tube sheet showing (a) conventional SCDAP/RELAP5 nodalization, (b) refined nodalization needed to calculate the thermal effects of SG sludge, and (c) nodalization needed for direct comparison of results without SG sludge.

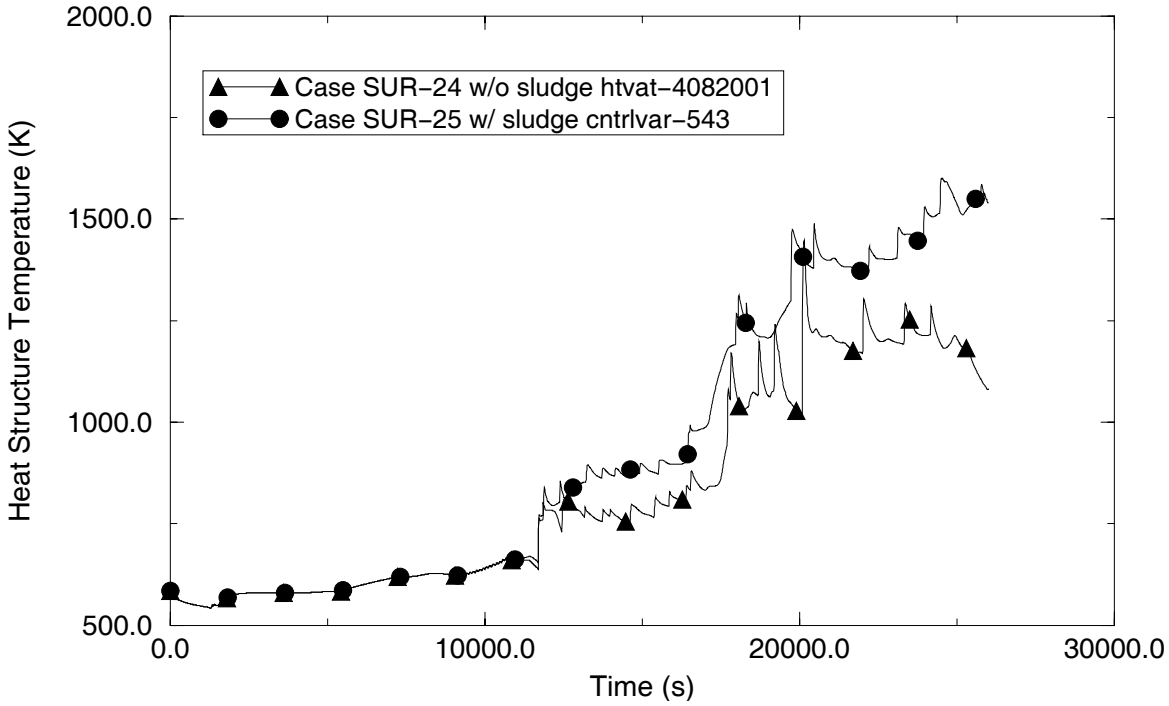

Figure 43. SG tube temperatures for Surry Cases SUR-24 (without SG sludge accumulation) and SUR-25 (with SG sludge accumulation).

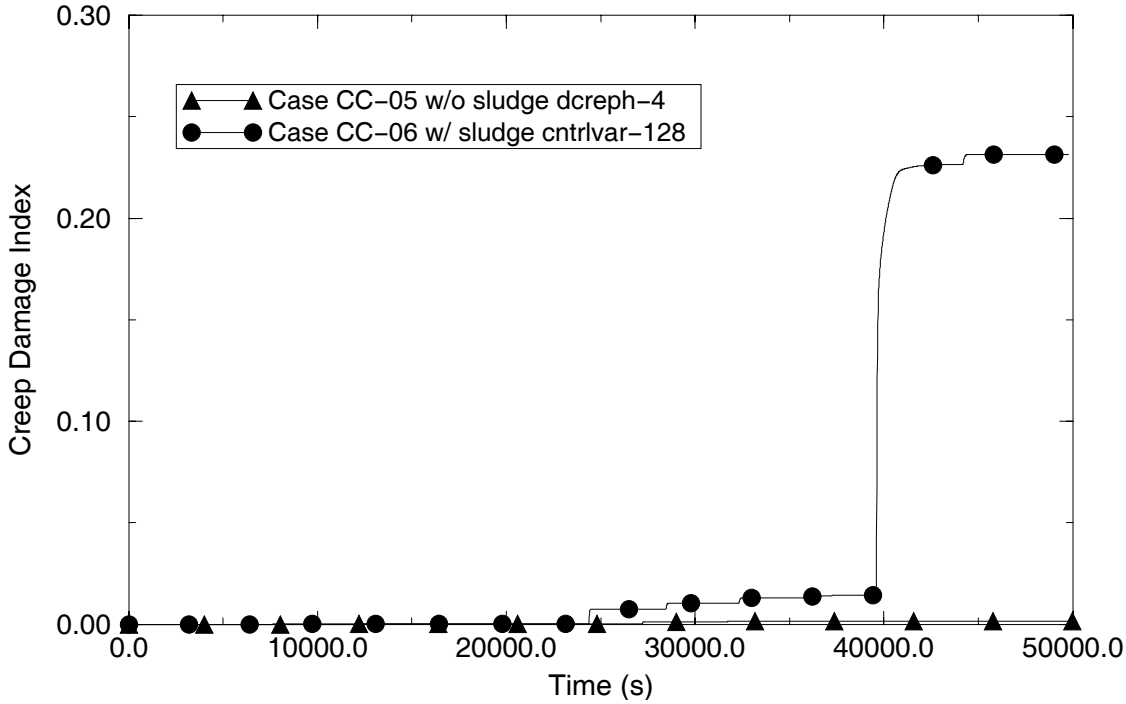

Figure 44. SG tube creep damage indices for Calvert Cliffs Cases CC-05 (without SG sludge accumulation) and CC-06 (with SG sludge accumulation).

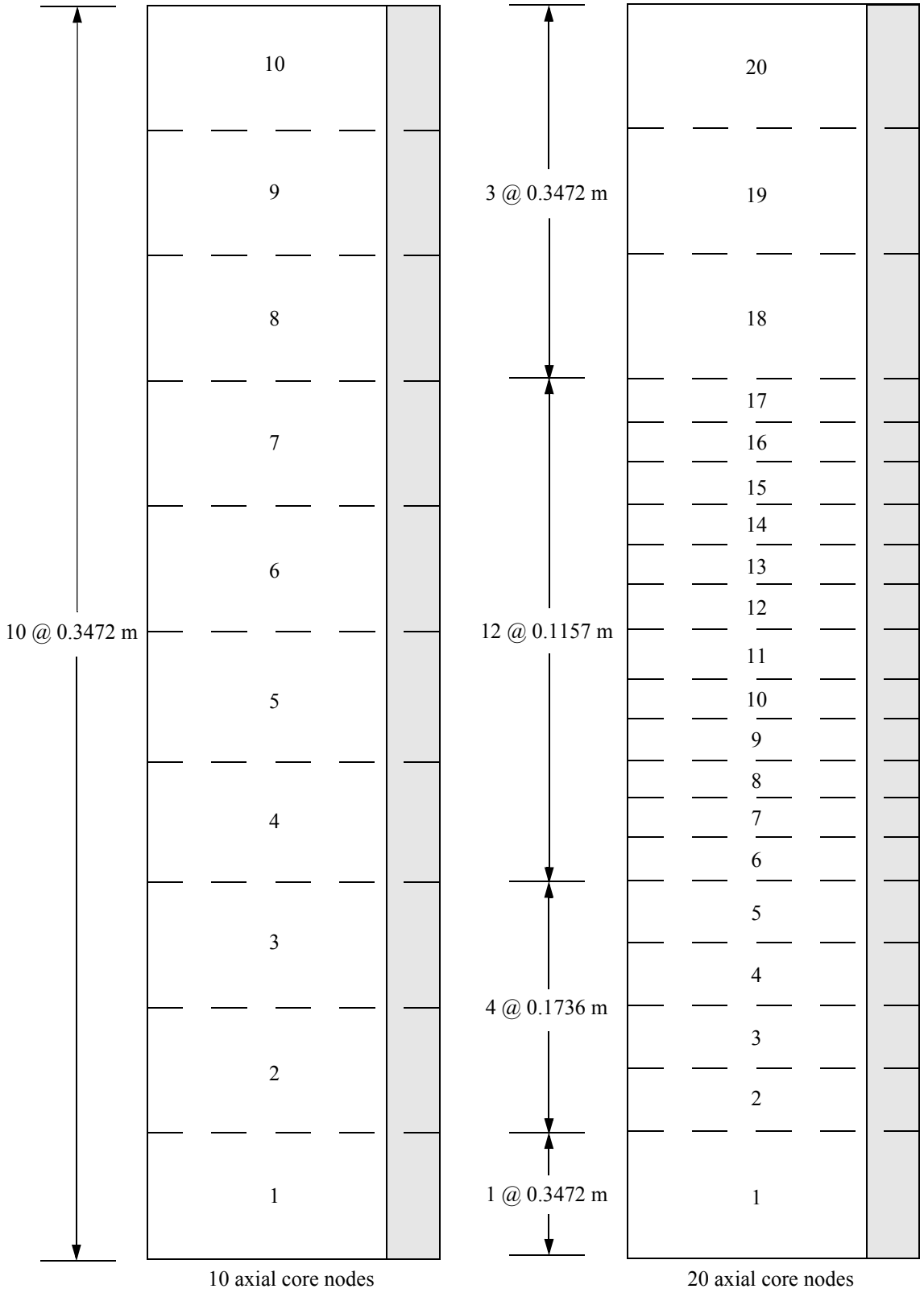

Figure 45. Calvert Cliffs nodalizations for core models with 10 and 20 axial nodes.

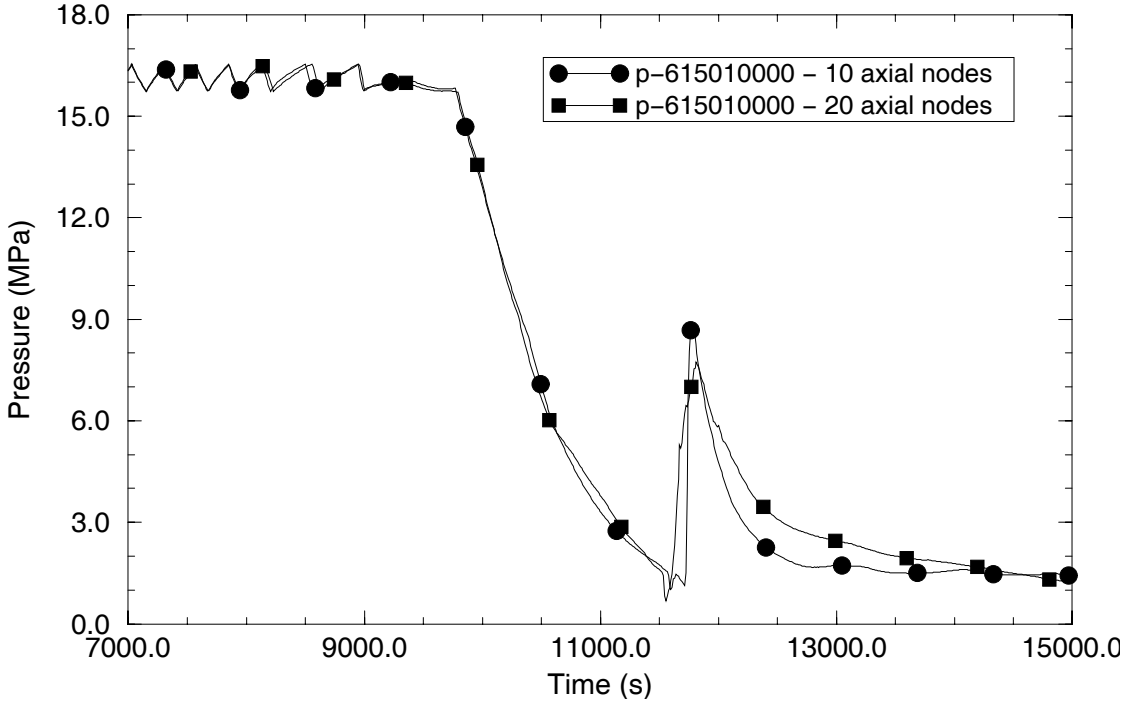

Figure 46. RCS pressure response for Calvert Cliffs using core models with 10 and 20 axial nodes.

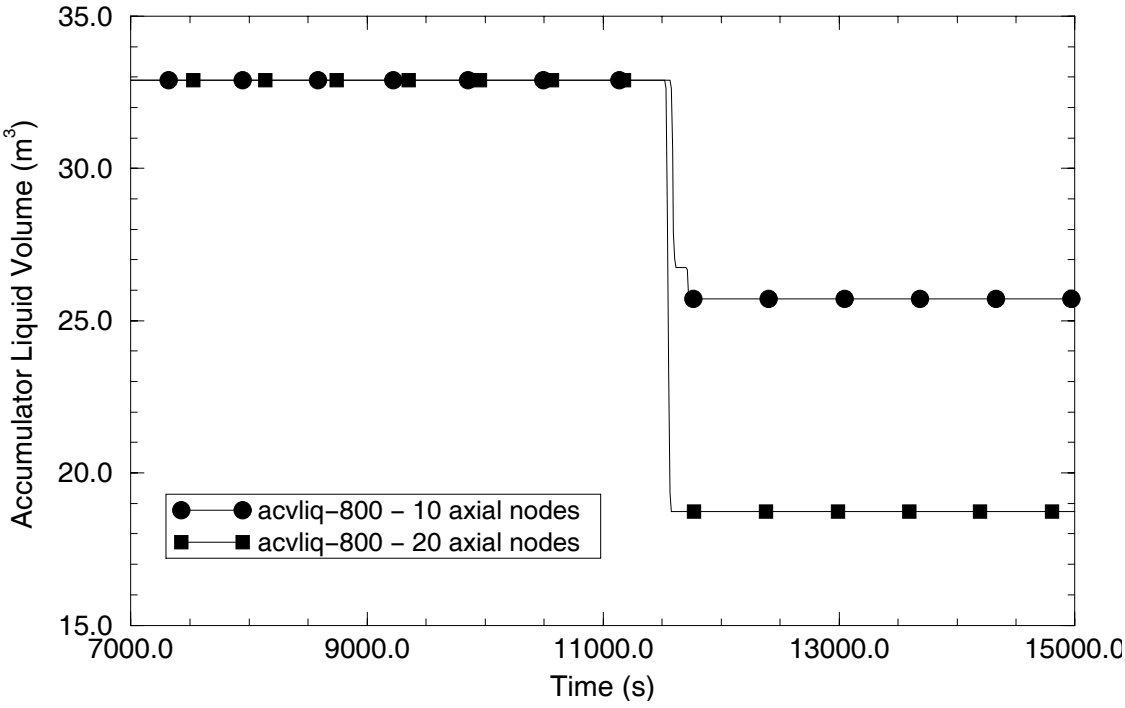

Figure 47. Accumulator liquid volumes for Calvert Cliffs using core models with 10 and 20 axial nodes.

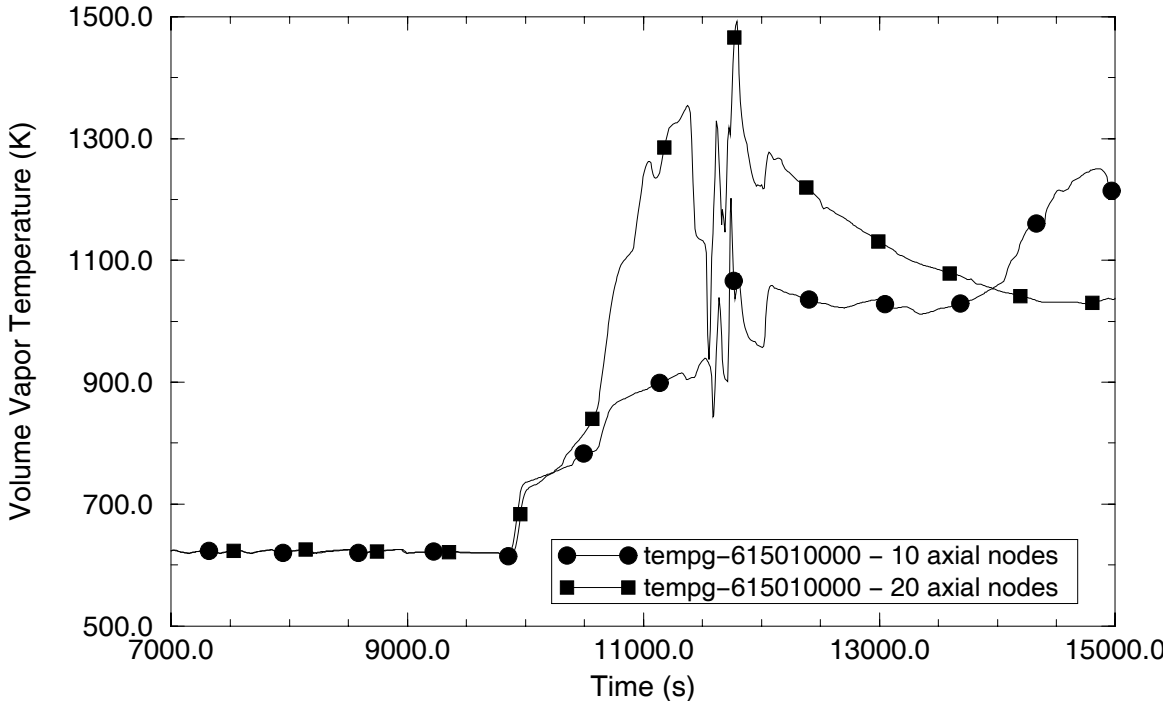

Figure 48. PORV inlet vapor temperatures for Calvert Cliffs using core models with 10 and 20 axial nodes.

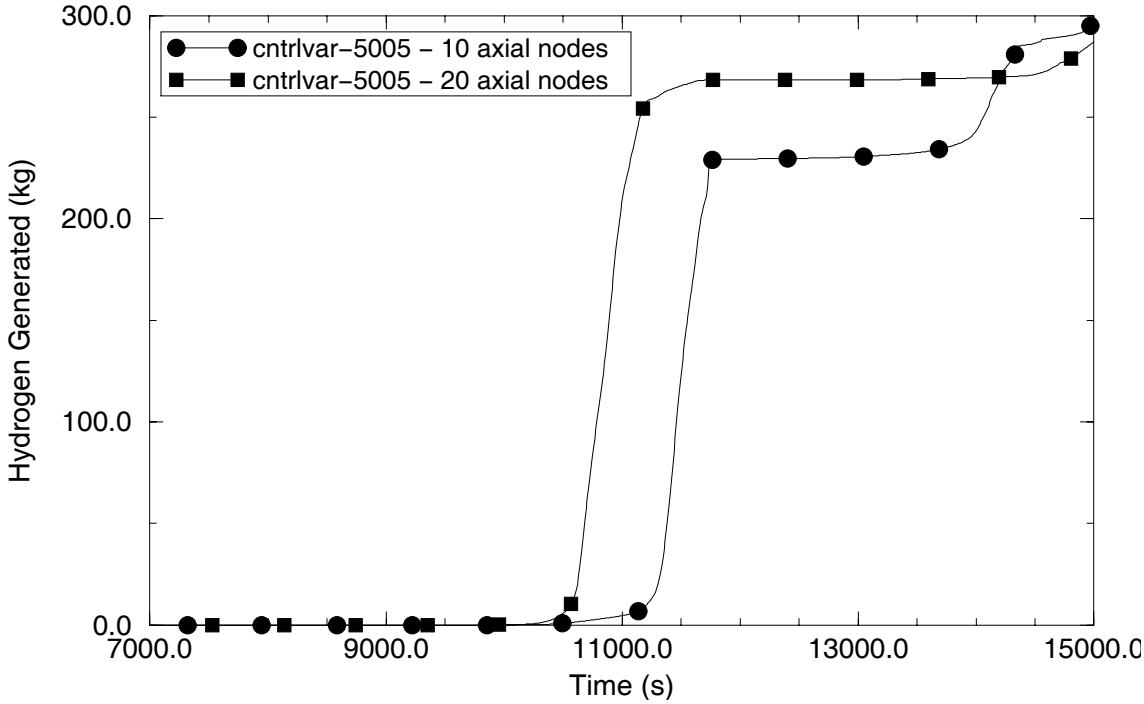

Figure 49. Total hydrogen generated for Calvert Cliffs using core models with 10 and 20 axial nodes.

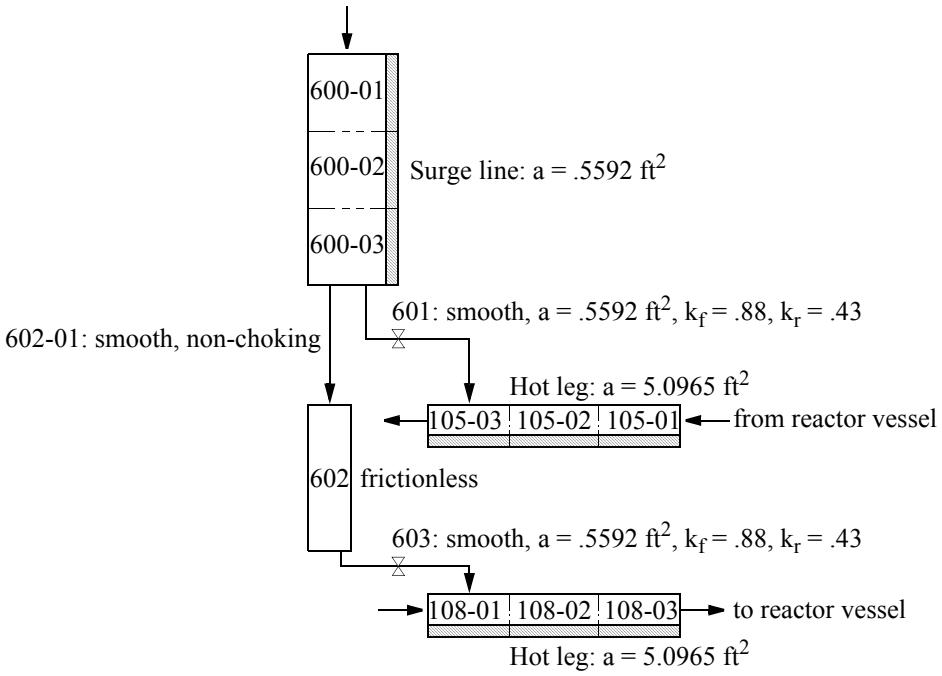

(a) Original hot leg/surge line connection

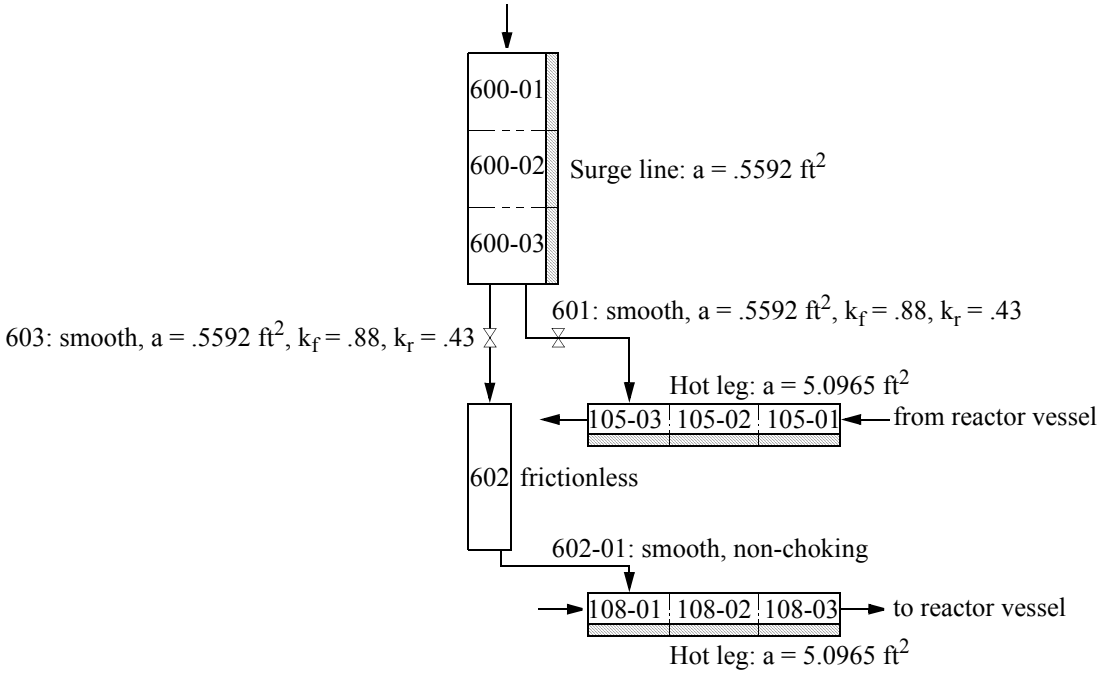

(b) Modified hot leg/surge line connection

Figure 50. Hot leg/surge line connections for the Calvert Cliffs PWR.

Table 1. Results from Westinghouse high pressure natural circulation experiments.[a]

Experiment[b]	Fraction of SG Tubes in Hot (Forward) Flow	Mixing Fraction[c]	Recirculation Ratio
SG-S1	0.35	0.87	2.18
SG-S2	0.29	0.89	1.78
SG-S3	0.35	0.85	2.01
SG-S4	0.29	0.85	1.69
SG-T1	0.55	0.78	1.88
SG-T2	0.51	0.83	2.39
SG-T3	0.61	0.76	2.28
SG-T4	0.47	0.86	2.10

a. See Reference 3.
b. Steady state tests include those with a '-Sx' designation while transient tests include those with a '-Tx' designation.
c. Hot and cold mixing fractions were assumed to be equal.

Table 2. Results from University of Maryland natural circulation experiments.[a]

Location	Temperature Rise (K)
Surge line	35.2
Hot leg 0.656 m above the surge line	17.5
Hot leg 1.75 m above the surge line	13.7
Hot leg 2.84 m above the surge line	11.1
Hot leg 5.03 m above the surge line	6.30
Hot leg 7.22 m above the surge line	3.60

a. See Reference 4.

Table 3. Variation of countercurrent flow parameters in SCDAP/RELAP5 stand alone loop analyses.[a]

Countercurrent Flow Parameter	Base Case	SG U-Tube Split Sensitivities			Mixing Fraction Sensitivities		Recirculation Ratio Sensitivities	
		Case 1	Case 2	Case 3	Case 4	Case 5	Case 6	Case 7
29% SG U-tubes in hot (forward) flow		x						
35% SG U-tubes in hot (forward) flow	x				x	x	x	x
53% SG U-tubes in hot (forward) flow			x					
61% SG U-tubes in hot (forward) flow				x				
Mixing fractions of 0.76					x			
Mixing fractions of 0.87	x	x	x	x			x	x
Mixing fractions of 0.89						x		
Recirculation ratio of 1.69							x	
Recirculation ratio of 1.92	x	x	x	x	x	x		
Recirculation ratio of 2.25								x

a. See Reference 22.

Table 4. SCDAP/RELAP5 analyses for operating PWRs.

Case	Description
SUR-01	Surry TMLB' without recovery; without operator actions; with quenching if upper plenum steel melts and relocates into lower head; without break initiation and associated depressurization following predicted RCS pressure boundary failures; without SG secondary depressurization; with natural circulation benchmarked at average steady state values (35%/65% hot/cold SG tube split, 0.87 mixing fraction, 1.9 recirculation ratio); with SG energy deposition above Reference 9 levels; without mixed convection code updates; without servo valve modeling refinement; also documented in Reference 23
SUR-02	Case SUR-01 with break initiation and associated depressurization following predicted RCS pressure boundary failure; also documented in Reference 23
SUR-03	Surry TMLB' without recovery; without operator actions; without quenching if upper plenum steel melts and relocates into lower head; without break initiation and associated depressurization following predicted RCS pressure boundary failures; with pressurizer loop SG secondary depressurization through failed relief valve; with natural circulation benchmarked at average steady state values (35%/65% hot/cold SG tube split, 0.87 mixing fraction, 1.9 recirculation ratio); with SG energy deposition above Reference 9 levels; with mixed convection code updates; without servo valve modeling refinement; also documented in Reference 23 with subsequent updates as documented in Reference 24
SUR-04	Case SUR-02 with pressurizer loop SG secondary depressurization through failed relief valve; also documented in Reference 23
SUR-05	Case SUR-01 with 53%/47% hot/cold SG tube split; also documented in Reference 23
SUR-06	Case SUR-03 with 53%/47% hot/cold SG tube split; also documented in Reference 23 with subsequent updates as documented in Reference 24
SUR-07	Case SUR-01 with depressurization of all SG secondaries through failed relief valves; also documented in Reference 23
SUR-08	Case SUR-03 with seal leaks of 250 gpm per RCP; with quenching if upper plenum steel melts and relocates into lower head; without mixed convection code updates; also documented in Reference 28
SUR-09	Case SUR-03 with seal leaks of 250 gpm per RCP; without mixed convection code updates; also documented in Reference 28
SUR-06A	Case SUR-06 with heat transfer coefficients multiplied by 1.2 in upper plenum, in hot legs, in surge line, and on inner and outer SG tube surfaces; also documented in Reference 24
SUR-06B	Case SUR-06 with heat transfer coefficients multiplied by 0.8 in upper plenum, in hot legs, in surge line, and on inner and outer SG tube surfaces; also documented in Reference 24
SUR-06C	Case SUR-06 with heat transfer coefficients multiplied by 1.3 in hot leg, surge line, and SG tube entrance volumes; also documented in Reference 24

Table 4. SCDAP/RELAP5 analyses for operating PWRs. (continued)

Case	Description
SUR-06D	Case SUR-06 with heat transfer coefficients multiplied by 1.3 in SG tube entrance volumes; also documented in Reference 24
SUR-06E	Case SUR-06 with hot leg fluid-to-fluid heat transfer and circumferential wall conduction; also documented in Reference 24
SUR-06F	Surry TMLB' without recovery; without operator actions; without quenching if upper plenum steel melts and relocates into lower head; without break initiation and associated depressurization following predicted RCS pressure boundary failures; with pressurizer loop SG secondary depressurization through failed relief valve; with natural circulation benchmarked at 5% transient data confidence values (43%/57% hot/cold SG tube split, 0.73 mixing fraction, 1.8 recirculation ratio); with SG energy deposition above Reference 9 levels; with mixed convection code updates; without servo valve modeling refinement; also documented in Reference 24
SUR-20	Surry TMLB' without recovery; without quenching if upper plenum steel melts and relocates into lower head; without break initiation and associated depressurization following predicted RCS pressure boundary failures; with pressurizer loop SG secondary depressurization through failed relief valve; with natural circulation benchmarked with 53%/47% hot/cold SG tube split, 0.87 mixing fraction, and 1.9 recirculation ratio; with Reference 9 SG energy deposition levels; with pressurizer PORVs latched open at a core exit temperature of 922 K; with mixed convection code updates; with servo valve modeling refinement; also documented in Reference 32
SUR-21	Case SUR-20 with seal leaks of 125 gpm per RCP; also documented in Reference 33
SUR-22	Case SUR-20 with seal leaks of 250 gpm per RCP; also documented in Reference 33
SUR-23	Case SUR-20 with downcomer-hot leg bypass closed when hot leg countercurrent nodalization was introduced; also documented in Reference 34
SUR-24	Case SUR-20 with renodalization of SG tube sheet when hot leg countercurrent nodalization was introduced; with correction of hot leg/surge line cross connecting valve trips; also documented in Reference 40
SUR-25	Case SUR-20 with renodalization of SG tube sheet and sludge accumulation to a depth of 12 in when hot leg countercurrent nodalization was introduced; with correction of hot leg/surge line cross connecting valve trips; also documented in Reference 40
ZI-01	Zion TMLB' without recovery; without quenching if upper plenum steel melts and relocates into lower head; without break initiation and associated depressurization following predicted RCS pressure boundary failures; with pressurizer loop SG secondary depressurization through failed relief valve; with natural circulation benchmarked with 53%/47% hot/cold SG tube split, 0.87 mixing fraction, and 1.9 recirculation ratio; with Reference 9 SG energy deposition levels; with pressurizer PORVs latched open at a core exit temperature of 922 K; with mixed convection code updates; with servo valve modeling refinement; also documented in Reference 32

Table 4. SCDAP/RELAP5 analyses for operating PWRs. (continued)

Case	Description
ZI-02	Case ZI-01 with seal leaks of 125 gpm per RCP; with corrected hot leg/surge line connection; also documented in Reference 33
ZI-03	Case ZI-01 with seal leaks of 250 gpm per RCP; with corrected hot leg/surge line connection; also documented in Reference 33
ZI-04	Case ZI-01 with downcomer-hot leg bypass closed when hot leg countercurrent nodalization was introduced; also documented in Reference 34
ZI-05	Case ZI-01 with renodalization of SG tube sheet when hot leg countercurrent nodalization was introduced; also documented in Reference 40
ZI-06	Case ZI-01 with renodalization of SG tube sheet and sludge accumulation to a depth of 12 in when hot leg countercurrent nodalization was introduced; also documented in Reference 40
CC-01	Calvert Cliffs TMLB' without recovery; without quenching if upper plenum steel melts and relocates into lower head; without break initiation and associated depressurization following predicted RCS pressure boundary failures; with pressurizer loop SG secondary depressurization through failed relief valve; with natural circulation benchmarked with 53%/47% hot/cold SG tube split, 0.87 mixing fraction, and 1.9 recirculation ratio; with Reference 9 SG energy deposition levels; with pressurizer PORVs latched open at a core exit temperature of 922 K; with mixed convection code updates; with servo valve modeling refinement; also documented in Reference 32
CC-02	Case CC-01 with seal leaks of 110 gpm per RCP; also documented in Reference 33
CC-03	Case CC-01 with seal leaks of 220 gpm per RCP; also documented in Reference 33
CC-04	Case CC-01 with downcomer-hot leg bypass closed when hot leg countercurrent nodalization was introduced; also documented in Reference 34
CC-05	Case CC-01 with renodalization of SG tube sheet when hot leg countercurrent nodalization was introduced; with modified hot leg/surge line connections; also documented in Reference 40
CC-06	Case CC-01 with renodalization of SG tube sheet and sludge accumulation to a depth of 12 in when hot leg countercurrent nodalization was introduced; with modified hot leg/surge line connections; also documented in Reference 40
CC-02CN	Case CC-02 with refined core nodalization (increased from 10 to 20 axial nodes)
CC-07	Case CC-05 with natural circulation re-benchmarked with 53%/47% hot/cold SG tube split, 0.87 mixing fraction, and 1.9 recirculation ratio
CC-07OSL	Case CC-07 without modified hot leg/surge line connections

Table 4. SCDAP/RELAP5 analyses for operating PWRs. (continued)

Case	Description
ANO2-01	ANO2 TMLB' without recovery; without operator actions; with quenching if upper plenum steel melts and relocates into lower head; without break initiation and associated depressurization following predicted RCS pressure boundary failures; with pressurizer loop SG secondary depressurization through failed relief valve; with natural circulation benchmarked at average steady state values (35%/65% hot/cold SG tube split, 0.87 mixing fraction, 1.9 recirculation ratio); with SG energy deposition above Reference 9 levels; without mixed convection code updates; without servo valve modeling refinement; also documented in Reference 30
ANO2-02	Case ANO2-01 with break initiation and associated depressurization following predicted RCS pressure boundary failure; also documented in Reference 30
ANO2-03	Case ANO2-01 with seal leaks of 220 gpm per RCP; also documented in Reference 30
ANO2-04	Case ANO2-03 without quenching if upper plenum steel melts and relocates into lower head; also documented in Reference 30
OC-01	Oconee TMLB' without recovery; without quenching if upper plenum steel melts and relocates into lower head; without break initiation and associated depressurization following predicted RCS pressure boundary failures; with pressurizer loop SG secondary depressurization through failed relief valve; with natural circulation benchmarked against University of Maryland experimental data listed in Table 2; with pressurizer PORVs latched open at a core exit temperature of 922 K; with mixed convection code updates; with servo valve modeling refinement; also documented in Reference 32
OC-02	Case OC-01 with seal leaks of 125 gpm per RCP; also documented in Reference 33
OC-03	Case OC-01 with seal leaks of 250 gpm per RCP; also documented in Reference 33
OC-04	Case OC-01 with downcomer-hot leg bypass closed when hot leg countercurrent nodalization was introduced; also documented in Reference 34

Table 5. Pressure boundary failure timing in the SCDAP/RELAP5 initial plant analyses.

Case	Failure Times (s)							First Tube Failure minus First Failure Timing Difference (s)	End of Calculation (s)
	Surge Line	Hot Legs			SG Tubes				
		A	B	C	A	B	C		
SUR-01[a]	14,050	15,670	15,670	15,110	nc[b]	nc	nc	nc	18,900
SUR-02	14,050	nc	nc	nc	nc	nc	nc	nc	21,000
SUR-03	13,640	nc	nc	nc	nc	nc	14,650	1010	14,650
SUR-04	14,460	nc	nc	nc	nc	nc	nc	nc	20,800
SUR-05	14,050	nc	nc	nc	nc	nc	nc	nc	14,050
SUR-06	13,730	nc	nc	14,750	nc	nc	14,960	1230	14,960
SUR-07	13,110	nc	nc	13,740	14,030	14,030	nc	1340	14,030
SUR-08	nc	nc	16,510	nc	nc	nc	nc	nc	16,510
SUR-09	nc	nc	16,130	nc	nc	nc	nc	nc	16,130
ANO2-01[c]	11,330	12,150	12,510	na[d]	13,750	nc	na	2420	13,750
ANO2-02	11,330	nc	nc	na	nc	nc	na	nc	21,550
ANO2-03	nc	nc	18,330	na	18,400	nc	na	70	18,400
ANO2-04	nc	24,530	21,400	na	nc	nc	na	nc	29,340

a. Surry has three primary coolant loops where hot leg C and SG tube C are part of the loop containing the pressurizer.
b. Not calculated.
c. ANO2 has two primary coolant loops where hot leg A and SG tube A are part of the loop containing the pressurizer.
d. Not applicable.

Table 6. Sequence of transient events in Surry Case SUR-01.

Event	Time (s)
TMLB' initiation	0
Onset of pressurizer PORV cycling	4980
Steam generators dry out (non-pressurizer/pressurizer loops)	5010/5040
End of full loop (liquid) natural circulation	7760
Collapsed liquid level falls below the top of the fuel rods	9030
Vapor in the core exit begins to superheat; hot leg countercurrent circulation begins	9205
Collapsed liquid level falls below the bottom of the fuel rods	10,670
Pressurizer drains; remains empty for duration of transient	11,180
Onset of fuel rod oxidation	11,460
Pressurizer surge line fails by creep rupture	14,050
Upper plenum stainless steel melts and relocates to the lower head	14,610
Upper plenum stainless steel melts and relocates to the lower head	14,680
Upper plenum stainless steel melts and relocates to the lower head	15,100
Pressurizer loop hot leg nozzle fails by creep rupture	15,110
Non-pressurizer loop hot leg nozzles fail by creep rupture	15,670
Upper plenum stainless steel melts and relocates to the lower head	16,490
End of calculation	18,900

Table 7. Sequence of transient events in Surry Case SUR-06.

Event	Time (s)
TMLB' initiation	0
Pressurizer loop SG RV opens and fails to close	< 20
Onset of pressurizer PORV cycling	1960
Steam generators dry out (pressurizer/non-pressurizer loops)	2020/5260
End of full loop (liquid) natural circulation	7690
Collapsed liquid level falls below the top of the fuel rods	8920
Vapor in the core exit begins to superheat; hot leg countercurrent circulation begins	9091
Collapsed liquid level falls below bottom of fuel rods	10,530
Pressurizer drains; remains empty for duration of transient	10,820
Onset of fuel rod oxidation	11,620
Pressurizer surge line fails by creep rupture	13,730
Upper plenum stainless steel melts and relocates to lower head	14,110
Upper plenum stainless steel melts and relocates to lower head	14,460
Pressurizer Loop C hot leg fails by creep rupture	14,750
Upper plenum stainless steel melts and relocates to lower head	14,930
Pressurizer Loop C SG tubes fail by creep rupture	14,960
End of calculation	14,960

Table 8. Results from selected SCDAP/RELAP5 plant sensitivity analyses.

Case	First SG Tube Failure minus First Failure Timing Difference	Pressurizer Loop SG Tube Temperature @ Surge Line Failure Time
SUR-06B ("h" x 0.8)	1180 s	964.4 K
SUR-06D ("h" x 1.3 in SG tube entrances)	1220 s	957.3 K
SUR-06 (nominal "h")	1230 s	956.8 K
SUR-06C ("h" x 1.3 in all entrances)	1250 s	944.2 K
SUR-06A ("h" x 1.2)	1310 s	937.6 K

Table 9. Pressure boundary failure timing in the SCDAP/RELAP5 plant sensitivity analyses.

Case	Failure Times (s)							First Tube Failure minus First Failure Timing Difference (s)	End of Calculation (s)
	Surge Line	Hot Legs			SG Tubes				
		A	B	C	A	B	C		
SUR-06	13,730	nc[a]	nc	14,750	nc	nc	14,960	1230	14,960
SUR-06A	13,590	14,760	14,760	14,440	nc	nc	14,900	1310	14,900
SUR-06B	13,610	nc	nc	nc	nc	nc	14,790	1180	14,790
SUR-06C	13,690	14,730	14,730	14,440	nc	nc	14,940	1250	14,940
SUR-06D	13,700	nc	nc	14,730	nc	nc	14,920	1220	14,920
SUR-06E	13,580	15,020	15,020	14,650	nc	nc	15,090	1510	15,090
SUR-06F	13,780	nc	nc	nc	nc	nc	14,580	800	14,580

a. Not calculated.

Table 10. Pressure boundary failure timing in SCDAP/RELAP5 intentional RCS depressurization analyses.

Case	Failure Times (s)									First Tube Failure minus First Failure Timing Difference (s)	End of Calculation (s)
	Surge Line	Hot Legs				SG Tubes					
		A	B	C	D	A	B	C	D		
SUR-20[a]	18,350	nc[b]	nc	25,200	na[c]	nc	nc	nc	na	nc	26,980
ZI-01[d]	13,440	20,330	nc	nc	nc	nc	nc	nc	nc	nc	30,000
CC-01[e]	22,000	27,430	nc	na	na	nc	nc	na	na	nc	50,000
OC-01[f]	8240	10,340	nc	na	na	nc	nc	na	na	nc	50,000

a. Surry has three primary coolant loops where hot leg C and SG tube C are part of the loop containing the pressurizer.
b. Not calculated.
c. Not applicable.
d. Zion has four primary coolant loops where hot leg A and SG tube A are part of the loop containing the pressurizer.
e. Calvert Cliffs has two primary coolant loops where hot leg A and SG tube A are part of the loop containing the pressurizer.
f. Oconee has two primary coolant loops where hot leg A and SG tube A are part of the loop containing the pressurizer.

Table 11. Pressure boundary failure timing in SCDAP/RELAP5 intentional RCS depressurization analyses with RCP seal leaks.

Case	Failure Times (s)									First Tube Failure minus First Failure Timing Difference (s)	End of Calculation (s)
	Surge Line	Hot Legs				SG Tubes					
		A	B	C	D	A	B	C	D		
SUR-21[a] (leaks of 125 gpm/RCP)	24,400	nc[b]	nc	nc	na[c]	nc	nc	nc	na	nc	31,130
SUR-22 (leaks of 250 gpm/RCP)	22,950	nc	nc	nc	na	nc	nc	nc	na	nc	35,480
ZI-02[d] (leaks of 125 gpm/RCP)	22,170	nc	nc	nc	nc	nc	nc	nc	nc	nc	23,690
ZI-03 (leaks of 250 gpm/RCP)	20,600	25,480	nc	nc	nc	nc	nc	nc	nc	nc	27,200
CC-02[e] (leaks of 110 gpm/RCP)	18,650	28,120	nc	na	na	nc	nc	na	na	nc	57,400
CC-03 (leaks of 220 gpm/RCP)	17,130	32,930	nc	na	na	nc	nc	na	na	nc	48,470
OC-02[f] (leaks of 125 gpm/RCP)	11,000	16,880	nc	na	na	nc	nc	na	na	nc	42,000
OC-03 (leaks of 250 gpm/RCP)	11,980	20,040	nc	na	na	nc	nc	na	na	nc	39,000

a. Surry has three primary coolant loops where hot leg C and SG tube C are part of the loop containing the pressurizer.
b. Not calculated.
c. Not applicable.
d. Zion has four primary coolant loops where hot leg A and SG tube A are part of the loop containing the pressurizer.
e. Calvert Cliffs has two primary coolant loops where hot leg A and SG tube A are part of the loop containing the pressurizer.
f. Oconee has two primary coolant loops where hot leg A and SG tube A are part of the loop containing the pressurizer.

Table 12. Pressure boundary failure timing in SCDAP/RELAP5 intentional RCS depressurization analyses with and without DC-HL bypass flows.

Case	Failure Times (s)									First Tube Failure minus First Failure Timing Difference (s)	End of Calculation (s)
	Surge Line	Hot Legs				SG Tubes					
		A	B	C	D	A	B	C	D		
SUR-20[a] (with bypass flows)	18,350	nc[b]	nc	25,200	na[c]	nc	nc	nc	na	nc	26,980
SUR-23 (without bypass flows)	22,600	nc	nc	nc	na	nc	nc	nc	na	nc	26,530
ZI-01[d] (with bypass flows)	13,440	20,330	nc	nc	nc	nc	nc	nc	nc	nc	30,000
ZI-04 (without bypass flows)	16,070	19,760	nc	nc	nc	nc	nc	nc	nc	nc	30,000
CC-01[e] (with bypass flows)	22,000	27,430	nc	na	na	nc	nc	na	na	nc	50,000
CC-04 (without bypass flows)	35,200	32,950	nc	na	na	nc	nc	na	na	nc	48,030
OC-01[f] (with bypass flows)	8240	10,340	nc	na	na	nc	nc	na	na	nc	50,000
OC-04 (without bypass flows)	8800	10,710	nc	na	na	nc	nc	na	na	nc	50,000

a. Surry has three primary coolant loops where hot leg C and SG tube C are part of the loop containing the pressurizer.
b. Not calculated.
c. Not applicable.
d. Zion has four primary coolant loops where hot leg A and SG tube A are part of the loop containing the pressurizer.
e. Calvert Cliffs has two primary coolant loops where hot leg A and SG tube A are part of the loop containing the pressurizer.
f. Oconee has two primary coolant loops where hot leg A and SG tube A are part of the loop containing the pressurizer.

Table 13. Thermal properties of steam generator sludge constituents based an Indian Point III analysis.

Constituent	Weight Percent	Specific Gravity (at ambient conditions)	Volume Percent	k (W/m-K)[a]		c_p (J/kg-K)[a]		
				400 K	1500 K	400 K	1000 K	1500 K[b]
Cu	27	8.96	6.1	392	330[c]	398	502[c]	502
Fe	24	7.87	6.1	69.4	31.8	502	1680	670
Zn	2.7	2.20	2.5	116	7.30[d]	398	461	461[e]
Ni	2.2	8.90	0.5	80.1	82.5	670	628	628
Mn	1.4	7.33	0.4	7.80[f]	7.80[f]	502	670	670
SiO_2	1	1.82	1.1	1.5	6.20[g]	879	1260	1260
C	0.45	2.10	0.4	2.2	3.5	837	1800	1800
H_2O	41.25 (liquid)	1 (steam 0.00055)	82.9	0.03 (steam)	0.1 (steam)	2000 (steam)	2600 (steam)	2600 (steam)

a. All thermal properties, except those for silicon dioxide and water, were taken from References 38 and 39. Silicon dioxide and water properties were taken from Reference 37.
b. With the exception of iron, all heat capacities at 1500 K were essentially identical to heat capacities at 1000 K.
c. Data is for solid copper at 1356 K. Copper melts at 1356 K.
d. Data is an estimate at 1100 K. Zinc melts at 693 K.
e. Data is for solid zinc at 693 K. Zinc melts at 693 K.
f. Data is an estimate at 300 K.
g. Data is an estimate at 1400 K.

Table 14. Thermal properties of steam generator sludge used in the SCDAP/RELAP5 analyses.

Temperature (K)	Thermal Conductivity (W/m-K)	Heat Capacity (J/kg-K)
400	3.1	272
1000	2.7	586
1500	2.4	343

Table 15. Pressure boundary failure timing in SCDAP/RELAP5 intentional RCS depressurization analyses with and without SG sludge accumulation.

Case	Failure Times (s)									First Tube Failure minus First Failure Timing Difference (s)	End of Calculation (s)
	Surge Line	Hot Legs				SG Tubes					
		A	B	C	D	A	B	C	D		
SUR-25[a] (with sludge)	19,460	nc[b]	nc	24,070	na[c]	nc	nc	24,790	na	5330	26,000
SUR-24 (without sludge)	19,550	nc	nc	nc	na	nc	nc	nc	na	nc	26,000
ZI-06[d] (with sludge)	17,460	20,810	nc	nc	nc	20,930	nc	nc	nc	3470	30,000
ZI-05 (without sludge)	17,460	19,780	nc	nc	nc	nc	nc	nc	nc	nc	29,740
CC-06[e] (with sludge)	17,280	26,370	nc	na	na	nc	nc	na	na	nc	49,780
CC-05 (without sludge)	16,230	26,570	nc	na	na	nc	nc	na	na	nc	50,000

a. Surry has three primary coolant loops where hot leg C and SG tube C are part of the loop containing the pressurizer.
b. Not calculated.
c. Not applicable.
d. Zion has four primary coolant loops where hot leg A and SG tube A are part of the loop containing the pressurizer.
e. Calvert Cliffs has two primary coolant loops where hot leg A and SG tube A are part of the loop containing the pressurizer.

Table 16. Timing of surge line failures in selected Calvert Cliffs SCDAP/RELAP5 analyses relative to selected differences in nodalization.

Case	Hot Leg/Surge Line Connection		SG Sludge Nodalization	Surge Line Failure Times (s)
	Original	Modified		
CC-01	x		no	22,000
CC-05		x	yes	16,230
CC-07		x	yes	16,350
CC-07OSL	x		yes	21,850